

UNIVERSITY OF SÃO PAULO

FACULTY OF PHARMACEUTICAL SCIENCES

Post-Graduation Program in Biochemical-Pharmaceutical Technology

**Exploring the role of a glycosylated L-asparaginase expressed
by a recombinant *Pichia pastoris* as an antileukemic
biopharmaceutical**

**Explorando o papel de uma L-asparaginase glicosilada
expressa por *Pichia pastoris* recombinante como um
biofármaco antileucêmico**

Eduardo Krebs Kleingesinds

Thesis presented for the Degree of Doctor
in Sciences.

Advisor:
Prof. Dr. Adalberto Pessoa Junior

São Paulo

2021

UNIVERSITY OF SÃO PAULO

FACULTY OF PHARMACEUTICAL SCIENCES

Post-Graduation Program in Biochemical-Pharmaceutical Technology

**Exploring the role of a glycosylated L-asparaginase expressed
by a recombinant *Pichia pastoris* as an antileukemic
biopharmaceutical**

**Explorando o papel de uma L-asparaginase glicosilada
expressa por *Pichia pastoris* recombinante como um
biofármaco antileucêmico**

Eduardo Krebs Kleingesinds

Original version

Thesis presented for the Degree of Doctor
in Sciences.

Advisor:

Prof. Dr. Adalberto Pessoa Junior

São Paulo

2021

Autorizo a reprodução e divulgação total ou parcial deste trabalho, por qualquer meio convencional ou eletrônico, para fins de estudo e pesquisa, desde que citada a fonte.

Ficha Catalográfica elaborada eletronicamente pelo autor, utilizando o programa desenvolvido pela Seção Técnica de Informática do ICMC/USP e adaptado para a Divisão de Biblioteca e Documentação do Conjunto das Químicas da USP

Bibliotecária responsável pela orientação de catalogação da publicação:
Marlene Aparecida Vieira - CRB - 8/5562

K64e Kleingesinds, Eduardo Krebs
Exploring the role of a glycosylated
L asparaginase expressed by a recombinant *Pichia
pastoris* as an antileukemic biopharmaceutical /
Eduardo Krebs Kleingesinds. – São Paulo, 2021.
120 p.

Tese (doutorado) – Faculdade de Ciências
Farmacêuticas da Universidade de São Paulo.
Departamento de Tecnologia Bioquímico-Farmacêutica –
Programa de Pós-Graduação em Tecnologia Bioquímico-
Farmacêutica.
Orientador: Pessoa, Adalberto

1. Leukemia. 2. Bioprocess. 3. Recombinant
proteins. 4. Tumor microenvironment. 5. Co-culture.
I. T. II. Pessoa, Adalberto, orientador.

Eduardo Krebs Kleingesinds

Exploring the role of a glycosylated L-asparaginase expressed by a recombinant *Pichia pastoris* as an antileukemic biopharmaceutical

Commission of Thesis for Degree of Doctor in Sciences

Prof. Dr. Adalberto Pessoa Junior
Advisor/President

1st Examiner

2nd Examiner

3rd Examiner

São Paulo, _____, 2021.

INSCRIPTION

This thesis is dedicated to my parents, Aron and Renate, for all their efforts to educate their children.

I would like to express my gratitude to...

FAPESP, Fundação de Amparo à Pesquisa do Estado de São Paulo (Grant Numbers 2017/20384-9 and 2019/06919-2) for all financial support.

My advisor, Professor Adalberto Pessoa Junior, who always listened to me and advised me through the most different situations. I am grateful for having welcomed me into his research group and for having opened the doors of the world to me. It was four years of many lessons that I will take in my professional and personal life to be a better scientist, lecturer and human. Thank you for your friendship and for all the many opportunities you gave me.

Professors Carlota Yagui for all collaboration and academic support during my PhD and for your kindness and friendship along those years.

Professor Gisele Monteiro who gently gave us the yeast for this work. Without any doubt, your collaboration was extremely important for the development of this work and I am grateful to you.

Professor Paul Long for having received me at King's College London for 14 months and for having invited me twice to teach a course of protein purification for master's students at KCL.

Professor Yolanda Calle-Patino who opened the doors of her lab for me during my time in London. I am also grateful to you for all your many lessons about cell culture and your extremely important collaboration for the final steps of this work. I will never forget what you have done for me. Big problems, big solutions!

Professor Volker Behrends and Maria Teresa Esposito for all their support at Roehampton University.

My uncle Hermano for all his wise advices.

My dearest friend Tomislav who is one of the best persons I have ever met in my life. Thank you for your friendship, for all your English corrections, and for all the pleasant and unforgettable moments we have had. I will never forget when we were at the airport opening my luggages because they were overweight, and you were there for me to help me think and to say goodbye.

My friends Jean-Nicola and Matic for all friday vegan friendly dinners and boardgames we had during my time in London. You were really kind to have welcomed me in your place.

My dearest friend, Letícia Parizzoto, for your friendship, your kindness and for all our unforgettable memories we had in the lab and especially in Brussels.

My dear friend Livia Seno for listening to me and supporting me with your wise and encouraging advice when I needed it.

My friends Rodolfo Ferreira, Anna Carolina Piazzentin, Viviane Borges, Sabrina Sabo, André Moreni, Alexsandra Apolinário, Thiago Fiorenzano, Sergio Andrade, Maria Laura for their friendship.

My labmates from Pharmaceutical Biotechnology Lab Flaviana, Renata, Vanessa, Larissa, Letícia, Francisco and Rodrigo for all the good coffee times we had and for the surprise parties.

The labmates from Nanobiolab and Labinbin for all the good times we had together.

All other Professors from the Faculty of Pharmaceutical Sciences.

All workers from the Faculty of Pharmaceutical Sciences specially the lab technician Larissa Bentim for all your supportive work and Rose from academic support.

And finally, for all those who near or far cheered me up.

Thank you very much!

*“It is said that even before a river falls into the ocean,
it trembles with fear.*

*It looks back at the whole journey, the peaks of the mountains,
the long winding path through the forests,
through the people, and it sees in front of it such a vast ocean that
entering into it is nothing but disappearing forever.*

But there is no other way.

The river cannot go back. No one can go back.

*Going back is impossible in existence,
you can only go forward.*

The river must take the risk and go into the ocean.

*And only when it enters the ocean will the fear disappear,
because only then will the river know that it is not disappearing
into the ocean, rather, it is becoming the ocean.*

*It is a disappearance from one side, and it is a tremendous resurrection on
the other side”.*

The River and the Ocean, Osho

ABSTRACT

KLEINGESINDS, E. K. **Exploring the role of a glycosylated L-asparaginase expressed by a recombinant *Pichia pastoris* as an antileukemic biopharmaceutical.** 2021. PhD thesis – Faculty of Pharmaceutical Sciences, University of Sao Paulo, 2021.

According to the World Health Organization (WHO), in 2020, 474 519 new cases of leukemia were reported around the world, and 311 594 new deaths were reported. The importance of L-asparaginase (L-ASNase) as a biopharmaceutical to treat Acute Lymphoblastic Leukemia (ALL) is recognized worldwide. This work describes the bioprocessing of L-ASNase from *Erwinia chrysanthemi* expressed extracellularly by *Pichia pastoris* with a human-like glycosylation pattern. Firstly, it was optimized the upstream conditions in the orbital shaker flask. Then, it was scaled up using a 3L benchtop bioreactor at batch mode under 35 °C and 1.5% methanol as an inductor for L-ASNase production. The downstream processing was evaluated using crossflow ultrafiltration with different cut-offs (10-100 kDa) followed by cation exchange chromatography and size exclusion chromatography. It was possible to reach a final yield of 54.93% with a purification factor of 70.93 fold and the proteomics data confirmed the attainment of an extremely pure enzyme. At pH 8.0 and 50 °C, the enzyme showed its optimum activity. Kinetic parameters, k_M and V_{max} , were found to be 76.4 μM and 0.065 $\mu mol\ min^{-1}$, respectively. The thermodynamic study showed that the enzyme irreversible deactivation is well described by first-order kinetics. Finally, using a high throughput fluorescent-based *in vitro* experimental platform, it was investigated the concomitant impact of this recombinant L-ASNase on enhanced green fluorescent protein (eGFP)-labeled tumor cell lines (SEMK2, HB119, REH, and MV411) when co-cultured with the mCherry-labelled bone marrow fibroblastic stroma cells HS5. The outcomes of this research suggest that the eGFP-Hb11-9 strain was the most sensitive strain when treated with the glycosylated L-ASNase, in contrast with the eGFP-REH that was the most resistant lineage. It was also observed lower effectiveness of the drug when tumor cells were co-cultured with stromal cells than when tumor cells were cultured on their own. Hence, this work paves the way for production, scale-up, and pre-clinical trials of this promising novel biopharmaceutical, which may help improve the remission rates and quality of life for many cancer patients around the world.

Keywords: Leukemia. Bioprocess. Recombinant proteins. Tumor microenvironment. Co-culture.

RESUMO

KLEINGESINDS, E. K. **Explorando o papel de uma L-asparaginase glicosilada expressa por *Pichia pastoris* recombinante como potencial biofármaco anti-leucêmico.** Tese de Doutorado – Faculdade de Ciências Farmacêuticas, Universidade de São Paulo, 2021.

Segundo a Organização Mundial da Saúde (OMS), em 2020, foram notificados 474 519 novos casos de leucemia em todo o mundo e 311 594 novos óbitos. A importância da L-asparaginase (L-ASNase) como biofármaco para o tratamento da Leucemia Linfoblástica Aguda (LLA) é reconhecida mundialmente. Neste trabalho, descreve-se o bioprocesso da L-ASNase de *Erwinia chrysanthemi* expressa extracelularmente por *Pichia pastoris* com um padrão de glicosilação semelhante ao humano. Inicialmente, foram otimizadas as condições de cultivo em agitador orbital. Em seguida, o processo foi escalonado utilizando um biorreator de bancada de 3L a 35 °C e 1,5% de metanol como um indutor para a produção de L-ASNase. A purificação foi avaliada utilizando ultrafiltração tangencial com cartuchos de diferentes tamanhos de poro (10-100 kDa) seguido por cromatografia de troca catiônica e de exclusão molecular. Foi possível atingir um rendimento final de 54,93% com fator de purificação de 70,93 vezes e os dados obtidos pelo ensaio de proteômica confirmaram a obtenção de uma enzima extremamente pura. Em pH 8,0 e 50 °C, a enzima mostrou sua atividade ótima. Os parâmetros cinéticos, K_M e V_{max} , foram de 76,4 μM e 0,065 $\mu mol\ min^{-1}$, respectivamente. Finalmente, foi investigado o impacto concomitante desta L-ASNase recombinante em linhagens de células tumorais marcadas com proteína fluorescente verde (eGFP) (SEMK2, HB119, REH e MV411) quando co-cultivadas com células do fibroblasto da medula óssea (HS5) marcadas com mCherry. Os resultados desta pesquisa sugerem que a linhagem eGFP-Hb11-9 foi a mais sensível quando tratada com a L-ASNase glicosilada, em contraste com eGFP-REH que foi a linhagem mais resistente. Também foi observada menor eficácia da droga quando as células tumorais foram co-cultivadas com células HS5 do que quando as células tumorais foram cultivadas sozinhas. Portanto, este trabalho abre o caminho para a produção, escalonamento e ensaios pré-clínicos deste promissor novo biofármaco, que pode ajudar a melhorar as taxas de remissão e a qualidade de vida de muitos pacientes com câncer em todo o mundo.

Palavras-chave: Leucemia. Bioprocesso. Proteínas recombinantes. Microambiente tumoral. Co-cultura.

LIST OF FIGURES

Chapter 1

Figure 1. Stem cell differentiation from the bone marrow.....	24
Figure 2. A comparison of the number of cases of leukaemia reported in 1990 and in 2017 per a) sex b) age c) leukaemia subtype.....	27
Figure 3. a) Number of new cases of leukaemia around the world b) Number of related deaths around the world.....	28
Figure 4. The tetramer of L-ASNase.....	29
Figure 5. Reaction mechanism of L-asparagine catalysis by L-asparaginase.....	31
Figure 6. Manufacturing processes for biopharmaceuticals. The output from the bioreactor goes through different units manufacturing steps called “Downstream” to purify the biotherapeutic.....	35
Figure 7. Comparative analysis of the three main host system for manufacturing biopharmaceuticals.....	37

Chapter 2

Graphical abstract. Schematic representation of the methodology used to produce and purify the glycosylated L-ASNase.....	47
Figure 1. Response surface analysis of the L-ASNase activity as a function of cultivation temperature (°C) and MeOH concentration (%) plotted using plotly in R (https://cran.r-project.org/web/packages/plotly/citation.html).....	59
Figure 2. (a) L-ASNase activity along 96 hours of batch cultivation. (b) Profile of variation in pH and oxygen consumption by <i>Pichia pastoris</i> during glycosylated L-ASNase production under optimized cultivation conditions by batch mode c) Cell growth and substrate consumption	60
Figure 3. Chromatograms of glycosylated L-ASNase after: (a) cationic exchange chromatography (b) size exclusion chromatography.....	61
Figure 4. SDS-PAGE of glycosylated L-ASNase from each purification step: Extracellular Medium (EM); Crossflow filtration (CF); Cationic Exchange chromatography (CE); Size exclusion chromatography (SE).....	62
Figure 5. Cell viability of ALL cell lines treated with glycosylated L-ASNase. Cytotoxicity was evaluated by the MTT reduction test. The cells were incubated with 6 concentrations (0.01, 0.05, 0.1, 0.3, 0.6 and 1 U/mL) of ASNase at 37 °C for 72 h (MOLT-4 and JURKAT cell lines) and analysed spectrophotometrically after MTT reduction...	68

Chapter 3

Figure 1. Evaluation of optimum a) pH and b) temperature of the glycosylated L-ASNase.....	76
Figure 2. Determination of specific activity of the glycosylated L-ASNase for a) L-asparagine b) L-glutamine.....	77
Figure 3. Enzymatic kinetics of the glycosylated L-ASNase on a) L-asparagine and b) L-glutamine substrates.....	77
Figure 4. Arrhenius-type plots of relative activity of glycosylated L-ASNase.....	78
Figure 5. Semi-log plots of the residual enzymatic activity of glycosylated L-ASNase along the time.....	79
Figure 6. Semi-log plots of the first-order denaturation constant (kd) vs. the reciprocal temperature (1/T). The slopes of the resulting straight lines were used to estimate the activation energie (Ed*) of irreversible inactivation (denaturation).....	80

Chapter 4

Graphical abstract. Schematic representation of the methodology used for image acquisition of ALL/AML cell cultures.....	85
Figure 1. Evaluation of cytotoxicity of glycosylated L-ASNase using co-culture models with eGFP-ALL and eGFP-AML cell lines cultured by their own and co-cultured with BM mCherry HS5 cells.....	89
Figure 2. Glycosylated L-ASNase blocks proliferation of the ALL cell line SEMK2 in the presence of BM stromal cells. Evaluation of A) tumor cell proliferation and B) cell apoptosis of eGFP-SEMK2 lineage after 72 hours of treatment with glycosylated L-ASNase in the range of 0.1-1.0 IU cultured alone or co-cultured with mCherry HS5 BM stroma cells. Micrographs showing the presence of GFP-ALL cells acquired using a 10X magnification lens. Glycosylated L-ASNase inhibited proliferation of SEMK2 cells cultured alone or in the presence of the BM stromal cell line HS5.....	92
Figure 3. Glycosylated L-ASNase blocks proliferation of the ALL cell line Hb11-9 in the presence of BM stromal cells. Evaluation of: A) tumor cell proliferation and B) cell apoptosis of eGFP-Hb11-9 lineage after 72 hours of treatment with glycosylated L-ASNase in the range of 0.1-1.0 IU cultured alone or co-cultured with mCherry HS5 BM stroma cells. Micrographs showing the presence of GFP-ALL cells acquired using a 10X magnification lens. Glycosylated L-ASNase inhibited proliferation of Hb11-9 cells cultured alone or in the presence of the BM stromal cell line HS5.....	95
Figure 4. Glycosylated L-ASNase blocks proliferation of the ALL cell line REH in the presence of BM stromal cells. Evaluation of: A) tumor cell proliferation and B) cell apoptosis of eGFP-REH lineage after 72 hours of treatment with glycosylated L-ASNase in the range of 0.1-1.0 IU cultured alone or co-cultured with mCherry HS5 BM stroma cells. Micrographs showing the presence of eGFP-ALL cells acquired using a 10X	

magnification lens. Glycosylated L-ASNase inhibited proliferation of REH cells cultured alone or in the presence of the BM stromal cell line HS5..... 98

Figure 5. Glycosylated L-ASNase blocks proliferation of the AML cell line MV4-11 in the presence of BM stromal cells. Evaluation of: A) tumor cell proliferation and B) cell apoptosis of eGFP-MV4-11 lineage after 72 hours of treatment with glycosylated L-ASNase in the range of 0.1-1.0 IU cultured alone or co-cultured with mCherry HS5 BM stroma cells. Micrographs showing the presence of GFP-AML cells acquired using a 10X magnification lens. Glycosylated L-ASNase inhibited proliferation of MV4-11 cells cultured alone or in the presence of the BM stromal cell line HS5.....101

Figure 6. Percentage of cell apoptosis of tumor lineages after 72 hours of treatment with glycosylated L-ASNase in the range of 0.1-1.0 IU cultured alone or co-cultured with mCherry HS5 BM stromal cells. A) eGFP-SEMK2 B) eGFP-Hb119 C) eGFP-REH D) eGFP-MV411..... 103

Figure 7. Glycosylated L-ASNase depletes asparagine when tumor cells are culture on their own, however, in the presence of BM stromal cells it is possible to detect asparagine even after 24 hours of the treatment suggesting that the tumor microenvironment influences the response to chemotherapy. L-ASNase concentration: 0.3 IU. The following leukemic lineages were evaluated A) Hb119 B) REH and C) MV411..... 105

LIST OF TABLES

Introduction

Table 1. Values of ASNase biopharmaceuticals presented in the bidding carried out by the Ministry of Health in 2017. It is estimated that 61,300 doses were purchased..... 20

Chapter 1

Table 1. Leukemic cell lines according to type, morphology, and age. Data collected from Expasy (<https://web.expasy.org/cgi-bin/cellosaurus/search>)..... 28

Table 2. ASNase biopharmaceuticals that are currently approved for the treatment of ALL..... 32

Chapter 2

Table 1. (a) 2^{4-1} Fractional factorial design with triplicate at the central point for L-ASNase production. Variables studied: temperature (X_1 , °C); initial inoculum (X_2 , X_0); inductor concentration (MeOH, X_3); periodicity of induction (Δt induction, X_4). **(b)** Experimental design for optimizing L-ASNase production. Variables studied: temperature (X_1 , °C) and inductor concentration (MeOH, X_2)..... 51

Table 2. Analysis of variance (ANOVA) of the fractional factorial design 2^{4-1} used for screening the statistically significant variables for the production of L-ASNase in shaker flasks considering (a) first-order effects of the 4 variables tested and (b) only the first-order effect of temperature..... 58

Table 3. Analysis of variance (ANOVA) of the experimental design used for optimizing the cultivation temperature (°C) and MeOH concentration (%) for the production of L-ASNase in shaker flasks..... 59

Table 4. Proteins identified by LC-MS/MS analyses from L-ASNase with human-like glycosylation pattern expressed extracellularly by recombinant *Pichia pastoris* after protein purification..... 63

Table 5. (a) Purification process of L-ASNase with human-like glycosylation pattern expressed extracellularly by recombinant *Pichia pastoris* using a 10 kDa cassette during crossflow filtration (strategy 1) **(b)** Purification process of L-ASNase with human-like glycosylation pattern expressed extracellularly by recombinant *Pichia pastoris* using a 300 kDa cassette before the 10 kDa cassette during crossflow filtration (strategy 2)..... 64

Table 6. Evaluation of purification fold and final yield of the downstream process from the glycosylated L-ASNase through crossflow filtration using cassettes with variable cut-off sizes..... 66

Table 7. Final yield and specific activity of different recombinant L-ASNase reported in the literature..... 67

Chapter 3

Table 1. Kinetic parameters of the glycosylated L-ASNase..... 77

Table 2. Thermodynamic and kinetic parameters of the irreversible thermal deactivation (denaturation) of glycosylated L-ASNase..... 79

ABBREVIATIONS

L-ASNase	L-Asparaginase
BMGY	Buffered Glycerol Complex Medium
OD ₆₀₀	Optical Density at 600 nm wavelength
k _M	Michaelis Constant (μM)
ALL	Acute Lymphoblastic Leukemia
AML	Acute Myeloid Leukemia
CLL	Chronic Lymphocytic Leukemia
CML	Chronic Myeloid Leukemia
SDS-PAGE	Sodium Dodecyl Sulfate – Polyacrylamide Gel
PTM	Post-Translational Modification
TEAB	Triethylammonium Bicarbonate Buffer
BM	Bone Marrow
CTSB	Cathepsin B
LSC	Leukemic Stem Cells
Asn	Asparagine
Gln	Glutamine
MTT	3-(4,5-Dimethylthiazol-2-yl)-2,5-diphenyltetrazolium bromide

SUMMARY

Presentation	19
Introduction and Justification	20
Chapter 1. Literature Review.....	24
1.1. Leukemia.....	24
1.2. L-Asparaginase	29
1.3. Modern trends in biopharmaceuticals	34
1.4. <i>Pichia pastoris</i> and glycosylation	37
1.5. Downstream process	39
Chapter 2	46
Upstream and downstream processing of L-asparaginase with human-like glycosylation pattern expressed by recombinant <i>Pichia pastoris</i>	46
Abstract.....	46
1. Introduction	47
2. Material and methods	49
2.1. Upstream	49
2.1.1. Expression system.....	49
2.1.2. Determination of <i>Pichia pastoris</i> cell concentration	50
2.1.3. Experimental design for shake flask cultivation	50
2.1.4. Measurement of L-asparaginase activity	53
2.1.5. Production of L-ASNase with human-like glycosylation pattern in a bench bioreactor	53
2.2. Downstream	53
2.2.1. Crossflow filtration	53
2.2.2. Cationic exchange chromatography	54
2.2.3. Size-exclusion chromatography	54
2.2.4. Determination of L-ASNase activity	55
2.2.5. Polyacrylamide gel electrophoresis (SDS-PAGE).....	55
2.2.6. Total protein assay	55
2.2.7. Proteomics analysis by LC-MS/MS.....	56
2.2.8. Cell culture and cytotoxicity assay	56
3. Results and Discussion.....	57
4. Conclusion.....	68
References	69

Chapter 3	71
Biochemical, kinetical and thermodynamics characterization of the glycosylated L-ASNase	71
Abstract.....	71
1. Introduction	72
2. Material and Methods	73
2.1. Optimum pH and temperature	73
2.2. Kinetic parameters	73
2.3. Thermodynamic study	74
3. Results and Discussion	76
3.1. Optimum pH and temperature	76
3.2. Kinetic parameters	76
3.3. Thermodynamic properties	78
3.4. Thermostability and half-life	79
4. Conclusion	81
References	81
Chapter 4	84
Evaluation of the concomitant impact of a recombinant glycosylated L-asparaginase on ALL and AML cancer cells and the bone marrow tumour microenvironment using a high throughput fluorescent-based <i>in vitro</i> experimental platform	84
Abstract.....	84
1. Introduction	85
2. Materials and Methods	87
2.1. Enzyme production and purification	87
2.2. Enzymatic activity assay	87
2.3. Cell culture	88
2.4. Determination of cell proliferation and viability of tumor cells in co-culture with m-Cherry HS5 cells.....	88
2.5. Fluorescent Microscopy	89
2.6. Flow cytometry analysis	89
2.7. Intracellular amino acid quantification	89
3. Results and Discussion	90
4. Conclusions	106
References	106

Final Remarks.....	109
List of Publications.....	110
Additional Files	111

Presentation

This thesis is organized in form of scientific articles (published, submitted, or to be submitted for publication), and is divided in the following chapters:

Chapter 1: “Literature Review”. This chapter intends to provide the reader with the fundamental concepts that guided this research through the state of the art of topics such as leukemia, L-asparaginase, expression of recombinant proteins, glycosylation, and downstream processes.

Chapter 2: “Upstream and downstream processing of L-asparaginase with human-like glycosylation pattern expressed by recombinant *Pichia pastoris*”. This chapter discloses the optimization of cultivation of *Pichia pastoris* to improve the production of L-ASNase. Subsequently, it presents the outcomes of the downstream process of this L-ASNase with an extremely high purity fold. Finally, it shows the L-ASNase cytotoxicity against two leukemic cell lines using the MTT methodology. This manuscript is submitted to Process Biochemistry Journal, and the authors are followed listed. Eduardo Krebs Kleingesinds, Brian Effer, Letícia de Almeida Parizotto, Francisco Vitor Santos da Silva, Yolanda Calle, Steven Lynham, Paul F. Long, Jorge G. Farías, Gisele Monteiro, Adalberto Pessoa-Jr.

Chapter 3: “Biochemical, kinetical and thermodynamics characterization of the glycosylated L-ASNase”. This chapter discloses the biochemical, kinetical, and thermodynamical characterization of the glycosylated L-asparaginase. The biochemical and kinetical data are already published in collaboration in the following manuscript “*Glycosylation of Erwinase results in active protein less recognized by antibodies*” and the thermodynamics study will be submitted in collaboration.

Chapter 4: “Evaluation of the concomitant impact of a recombinant glycosylated L-asparaginase on ALL and AML cancer cells and the bone marrow tumour microenvironment using a high throughput fluorescent-based in vitro experimental platform”. This chapter discloses the outcomes obtained during my internship in London with the BEPE scholarship (FAPESP process: 2019/06919-2). This study aimed to evaluate the cytotoxicity of the L-ASNase against ALL and AML cell lines when co-cultured with bone marrow cells.

Introduction and Justification

Since 2011, the continued supply of drugs used in oncology, especially onco-haematology, has been a cause of great concern in Brazil, since the supply chain of some drugs has been interrupted, causing great concern in the entire onco-haematological patient care system.

Until 2013, the biopharmaceutical L-Asparaginase (L-ASNase) used in therapy against Acute Lymphoid Leukaemia (ALL) was from American and German laboratories (Merck-Sharp & Dohme and Lundbeck INC and OSO Biopharmaceutical) and distributed by the Argentine laboratory Bagó that held the registration in Brazil of L-ASNase with the trade name Elspar®. However, production was discontinued and the disruption in the supply of the biopharmaceutical caused serious inconvenience to patients and forced the government to find emergency alternatives, such as the importation of more expensive medication (Aginasa®).

In 2013, the Ministry of Health acquired Leuginase® from the Chinese laboratory Beijing SL Pharmaceutical, which was distributed by the company Xetley SA for approximately four times less than the other competitors (Ministério Público, 2017). Table 1 shows the values of the drugs in this bid.

Table 1. Values of ASNase biopharmaceuticals presented in the bidding carried out by the Ministry of Health in 2017. It is estimated that 61,300 doses were purchased.

Commercial name	Source	Price per dose (USD)
Leuginase®	<i>Escherichia coli</i> wild type	38
Oncaspar®	<i>E. coli</i> PEGylated version	1619,10
Spectrila®	Recombinant <i>E. coli</i>	582,17

(Ministério da Saúde, 2017).

According to tests carried out by the American laboratory MSBioworks and the Brazilian National Laboratory of Biosciences (LNBio), Leuginase contains a high degree of impurities in comparison to the references produced in Japan and Germany. Additionally, in a recent publication by the journal Lancet Oncology (2018), Cecconello and collaborators demonstrated that Leuginase® has a lower half-time life than the reference and claim that the medicine imported by Brazil has low quality. These changes have caused controversy regarding the questionable quality of L-ASNases used in the treatment of ALL.

According to the Brazilian Ministry of Health, approximately 51% of the available budget for the SUS (Unified Health System) for the purchase of medicines is intended for distribution of biological medicines, which represent only 4% of the total quantity purchased (Brasil, 2017). This dependence on imported biopharmaceuticals is worrisome not only for the economic perspective, but also for the risk of discontinuity of supply.

Another very current example of this dependence of pharmaceutical raw material from other countries is the IFAS to produce the COVID-19 vaccine. During 2021 we watched many stoppages in the production of vaccines due to this dependence on the foreign market. Therefore, it is extremely important to promote the development of a national technology to produce biopharmaceuticals like L-ASNase, in order to create conditions of dominance over the production process and quality control in Brazil, in addition to reducing dependence on the foreign market for this biopharmaceutical.

Hence, in order to assist in supplying the national demand for biopharmaceuticals, Professor Adalberto had proposed a FAPESP's thematic project entitled “Production of extracellular L-asparaginase: from bioprospecting to engineering an antileukemic biopharmaceutical” (process 13/08617/7), whose main goal was to obtain, on an industrial scale, the enzyme L asparaginase (ASNase) which is used in the treatment of Acute Lymphoblastic Leukemia. Currently, our group proposes to develop innovative forms of ASNase with the potential to become biopharmaceuticals. We currently have four forms of ASNase in development, three produced in recombinant strains from *Escherichia coli* and one from *Pichia pastoris*, which is the object of study of this doctorate.

This *P. pastoris* has as a differential the ability to produce recombinant ASNase of *Erwinia chrysanthemi* with human-like N-glycosylation pattern. Post-translational modification such as glycosylation improves solubility, correct protein folding and body tolerance by reducing aggregation and immunogenicity (Wang; Lomino, 2012; Nadeem et al., 2018). Because of these attributes, about 70% of approved biopharmaceuticals for treatment are glycosylated (Nadeem et al., 2018). Additionally, there are already approved biopharmaceuticals produced by *P. pastoris* since 2009 (RCT, 2009). Therefore, it is believed that this strain is suitable for the production of this antileukemic therapeutic.

References

- BRASIL, P. Indústria nacional prioriza fabricação de 52 remédios. Disponível em: <http://www.brasil.gov.br/saude/2017/01/industria-nacional-prioriza-fabricacao-de-52-remedios>.
- Cecconello DK, Werlang ICR, Alegretti AP, et al. Monitoring asparaginase activity in middle-income countries. *The Lancet. Oncology*. 19(9):1149-1150. 2018. doi: 10.1016/s1470-2045(18)30584-9.
- MINISTÉRIO PÚBLICO. EXTRATO DE CONTRATO No 11/2017 - UASG 250005. Diário oficial da União- Seção 3 Issn 1677-7069, 2017. Disponível em: <http://pesquisa.in.gov.br/imprensa/servlet/INPDFViewer?jornal=3&pagina=87&data=26/01/2017&capt=chafield=&firstAccess>
- Nadeem T, Khan MA, Ijaz B, Ahmed N, Rahman ZU, Latif MS, Ali Q, Rana MA. Glycosylation of Recombinant Anticancer Therapeutics in Different Expression Systems with Emerging Technologies. *Cancer Res*. 1;78(11):2787-2798. 2018. doi: 10.1158/0008-5472.CAN-18-0032.
- RCT. FDA grants first approval for a product derived from *Pichia pastoris*. FDA grants first approval for a product derived from *Pichia pastoris*. Research Corporation Technologies Research Corporation Technologies (rctech.com).
- Wang LX, Lomino JV. Emerging technologies for making glycan-defined glycoproteins. *ACS Chem Biol*. 7(1):110-122. 2012. doi:10.1021/cb200429n

OBJECTIVE

General

This work aimed to produce and purify a glycosylated L-Asparaginase expressed by a recombinant *Pichia pastoris* in reproducible conditions and enough amount to characterize and evaluate its cytotoxicity against leukemic cell lineages.

Specifics

- ✚ Establish a reproducible methodology for the glycosylated L-ASNase production in a benchtop bioreactor using a recombinant *Pichia pastoris*;
- ✚ Increase the downstream outcomes such as the purity and the yield through crossflow ultrafiltration strategies and high-resolution chromatography techniques;
- ✚ Establish the biochemical, kinetical and thermodynamics parameters of the glycosylated L-ASNase;
- ✚ Evaluate the concomitant impact of this recombinant glycosylated L-ASNase on ALL and AML cancer cells and the bone marrow tumour microenvironment using a high throughput fluorescent-based *in vitro* experimental platform.

Chapter 1.

Literature Review

1.1. Leukemia

The hematopoietic system is essential for the maintenance of life. The balance between the production and apoptosis of blood cells and the immune system, as well as the composition of the plasma, is vital for the process of oxygenation and nutrition of tissues and the body's homeostasis processes.

In normal haematopoiesis, the hematopoietic stem cell gives rise to multipotent precursor cells that give rise to lymphoid and myeloid precursors (Figure 1). The lymphoid precursor is responsible for the production and renewal of B and T lymphocytes and natural killer (NK) cells (Figure 1). The myeloid precursor is responsible for the production and renewal of red blood cells, platelets, basophils, mast cells, eosinophils, neutrophils, macrophages, erythrocytes, thrombocytes, leukocytes (granulocytes and monocytes) and dendritic cells (Figure 1). However, haematopoiesis can be compromised by the sequential accumulation of multiple genetic and epigenetic events that trigger the dysregulation of white blood cell production and function in a process known as leukemogenesis.

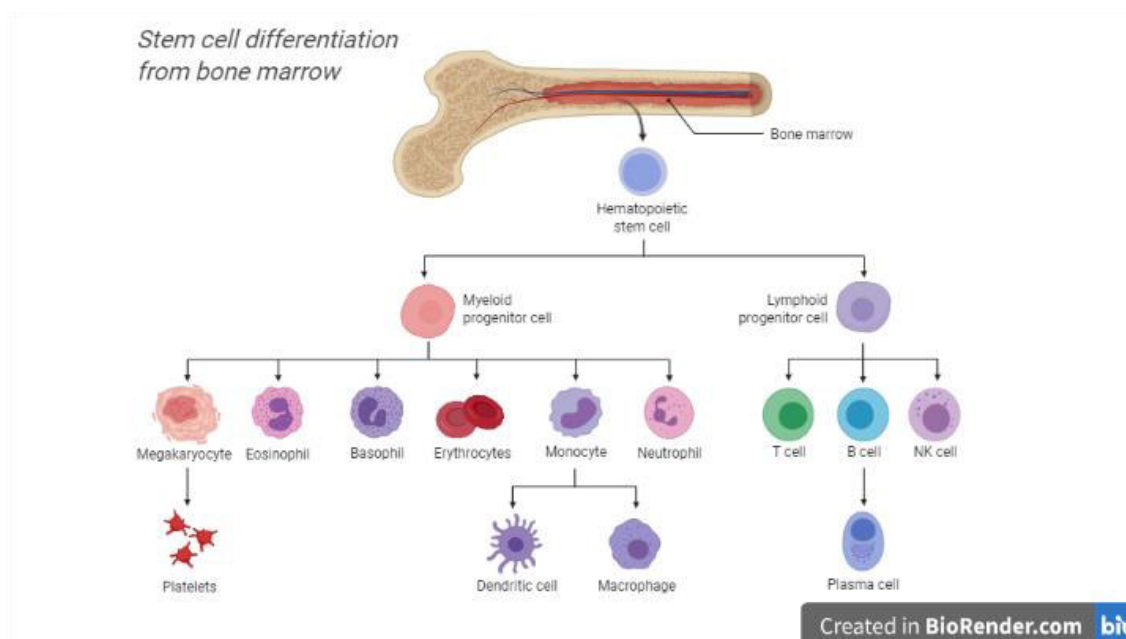


Figure 1. Stem cell differentiation from the bone marrow.

Leukaemia refers to cancer of the blood or bone marrow in which cells lose their ability to differentiate, resulting in the accumulation of immature cells called blasts with abnormal cell function and proliferation. Leukemic stem cells are a heterogeneous group of cells, with stemness properties, which hijack the normal hematopoietic niche initiating and maintaining the disease, giving rise to more differentiated blasts (Michelozzi et al, 2019).

The general classification of leukaemia is divided into chronic (slow growing) and acute (fast growing), which can be further divided into myelocytic and lymphocytic subtypes (Kaser et al, 2021). According to this division, myeloid subtype begins in early myeloid cells, and lymphoid leukaemia affect lymphoid cells.

Acute lymphoblastic leukaemia (ALL) is an aggressive malignancy, accounting for 90% of all childhood leukaemia (its incidence peaks in children aged 2–5 years old) and 20% of adult leukaemia (Kaser et al, 2021; Chew et al, 2020). The implementation of multi-agent chemotherapy agents has offered cure rates of 90% in pediatric patients, however this outcome was not achieved in adults with ALL (Chew et al, 2020).

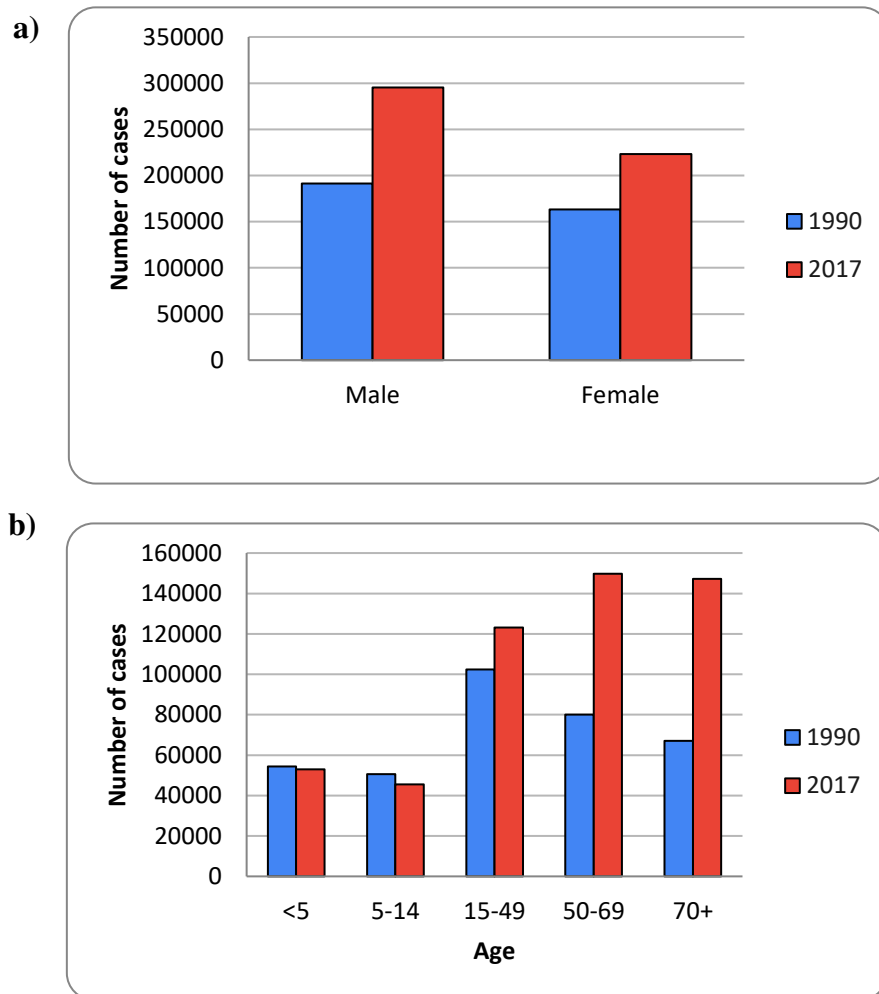
Acute myeloid leukaemia (AML) is a heterogeneous blood cancer most frequently diagnosed in adults (25%) and accounts for 15–20% cases in children (Michelozzi et al, 2019). In AML, an oncogenic transformation occurs in a myeloid precursor blood cell which loses its ability to differentiate properly resulting in an uncontrollable division of the cells (Kaser et al, 2021). This leads to accumulation of blast cells (immature blood cells) in the bone marrow and they spread to the blood, and then travel to other parts of the body such as the lymph nodes, liver, spleen, and central nervous system (Kaser et al, 2021).

The chronic leukaemia occurs more frequently in elderly people and have a more indolent growth pattern compared to acute leukaemia (Kaser et al, 2021). In Chronic Lymphocytic Leukaemia (CLL), lymphocyte maturation is arrested, and the accumulation of these cells results in increased susceptibility to infection, which is a critical part of CLL disease progression (Kaser et al, 2021).

According to Dong and collaborators (2020), in 1990, 354 500 cases of leukaemia were reported around the world, being that 191 300 were male and 163 100 females (Figure 2a). These data had suffered tremendous changes and, in 2017, 518 500 new cases were reported being 295 400 in males and 223 100 in females (Figure 2a).

Another interesting data evaluated by this study revealed that the number of new cases in children and adolescents remained stable between 1990 and 2017, however, the number of cases for elderly people had significantly risen (Figure 2b) (Dong et al, 2020).

From Figure 2c we can observe that AML is the type of leukaemia with high prevalence (more than 100 000 new cases were reported) followed by ALL with more than 60 000 new cases reported around the world. CLL dramatically increased between 1990 and 2017 and CML remains at the same level (Figure 2c) (Dong et al, 2020). This can be explained by the increased life expectancy and that this kind of leukaemia affects more often elderly people.



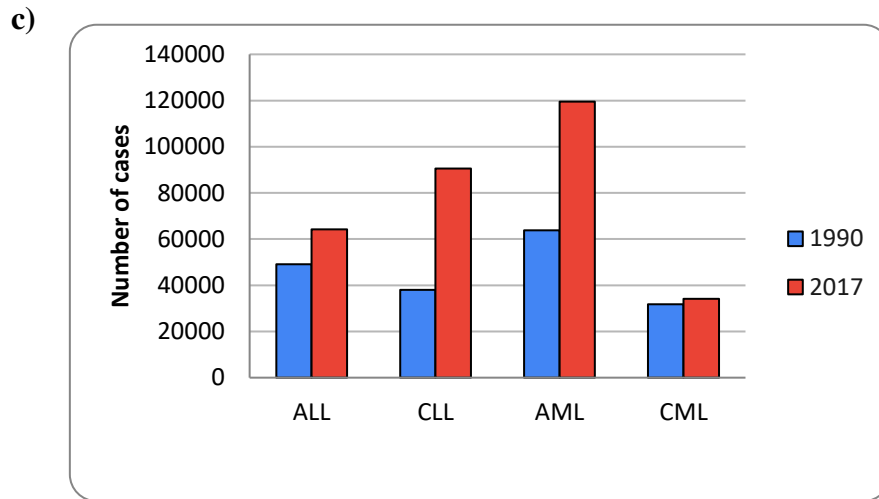
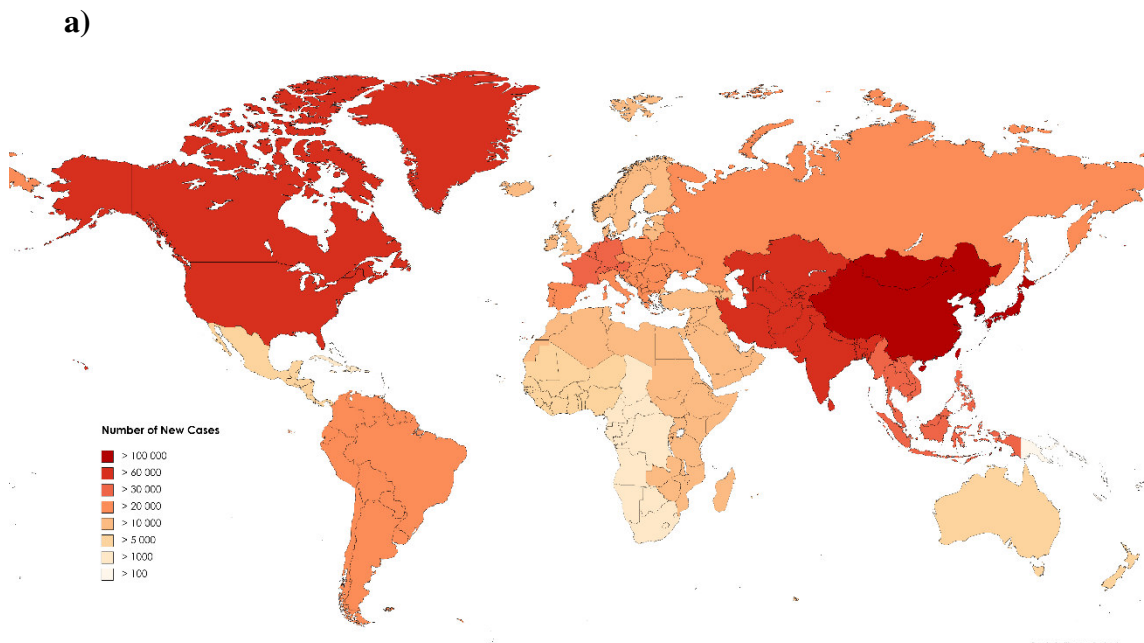


Figure 2. A comparison of the number of cases of leukaemia reported in 1990 and in 2017 per a) sex b) age c) leukaemia subtype.

According to the World Health Organization (WHO), in 2020, 474 519 new cases of leukaemia were reported around the world and 311 594 new deaths were reported (Globocan, 2020). This data suggests that leukaemia occupies the 15th place in rank of most common cancers around the world and the 10th most lethal. From Figure 3 we can observe the countries with high incidence and mortality caused by leukaemia.



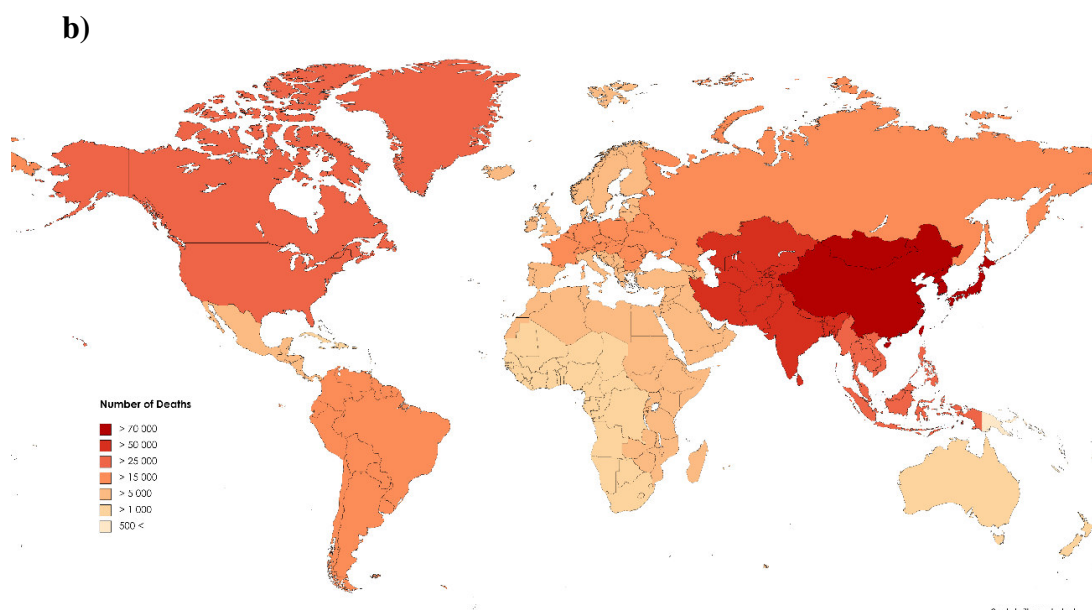


Figure 3. a) Number of new cases of leukaemia around the world b) Number of related deaths around the world.

Among the leukemia types, we have different cell lines with different genotypes and phenotypes which respond differently to protocol treatments. Table 1 shows some cell lines that were studied in this thesis.

Table 1. Leukemic cell lines according to type, morphology, and age. Data collected from Expsy (<https://web.expasy.org/cgi-bin/cellosaurus/search>).

Name of cell line	Organism, Ethnicity	Age/Gender	Tissue/Primary Tumour	Morphology
MOLT-4	Homo sapiens/Caucasian	19/Male	Peripheral blood/ ALL	Precursor T-Lymphoblast
MV4-11	Homo sapiens/Caucasian	10/Male	Peripheral blood/ AML	Round cells
REH	Homo sapiens/Caucasian	Female	Peripheral blood/ ALL	Precursor B-Lymphoblast
THP-1	Homo sapiens/Caucasian	1/Male	Peripheral blood/ AML	Monocytic cells
Jurkat	Homo sapiens/Caucasian	Male	Peripheral blood/ ALL	T-Lymphoblast
SEMK2	Homo sapiens/Caucasian	5/Female	Peripheral blood/ ALL	Precursor B-Lymphoblast

The exact cause of leukaemia is not completely understood. Genetic mutations were reported in most cases. Patients who received alkylating chemotherapy or radiation as part of a prior cancer treatment, genetic disorders such as Down Syndrome, and increasing age can be considered as risk factors for developing leukaemia (Kaser et al, 2021). Clinical symptoms due to blast cells accumulating in the bone marrow include fatigue, easier bleeding, increased number of infections and bone tenderness (Kaser et al, 2021).

According to the importance of leukemic stem cells in leukemia pathogenesis, therapeutic approaches are necessary to eradicate these cells, thus preventing their further evolution and consequent relapse (Michelozzi et al, 2019).

1.2. L-Asparaginase

Among the main therapeutic agents used in the protocols treatments of leukemia, such as ALL, is L-Asparaginase (EC 3.5.1.1, L-asparaginaamidohydrolase). This protein is a deamidating enzyme that catalyses the hydrolysis of L-asparagine into aspartic acid and ammonia, causing L-asparagine depletion in the blood and bone marrow (Michelozzi et al, 2019; Steiner et al, 2012; Tong et al, 2013). It also shows L-glutamine activity resulting in L-glutamine reduction (Steiner et al, 2012). With a tetrameric structure (Figure 4), it has around 330 amino acid residues and a molar mass between 140-160 kDa, is responsible for the catalysis of the hydrolysis reaction of asparagine. Its component monomers are arranged in 14 β -sheets and 8 α -helices. The isoelectric point (pI) for the proteoform from *E. coli* is 4.5 while the pI of the ASNase from *E. chrysanthemi* is 8.6 and under human physiological conditions (37°C and pH 7.2) it has optimal activity (Pourhossein; Korbekandi, 2014; Zhang et al., 2004).

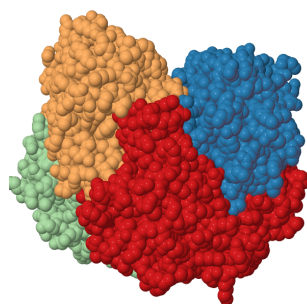


Figure 4. The tetramer of L-ASNase.

In 1948, Farber and collaborators reported the temporary remission of acute leukemia in five children treated with a synthetic compound, aminopterin, starting chemotherapy for this disease. In 1962, Pinkel and coworkers started a treatment program for childhood leukemia that aimed to achieve complete remission of the disease. Between 1962 and 1965, all four of the then known effective antileukemic agents that are still at the core of current ALL treatments were introduced simultaneously (AUR et al., 1971).

In 1953, Kidd (1953) noted that guinea pig serum induced regression of lymphomas. Just eight years later, Broome (1961) identified that ASNase is the agent responsible for this action. In addition, the author explained the mechanism of action, noting that tumor cells need exogenous asparagine (Broome; Schwartz, 1967). In the same year, Campbell and collaborators (1967) found two types of ASNase, type I and II, with activity for L-asparagine and L-glutamine, however, type II is more specific for L-asparagine and has an antitumor function (Batoool et al., 2016).

Other clinical trials were conducted, and a key study in the 1970s showed that the use of high doses of ASNase combined with other chemotherapeutic protocols were effective in the remission of leukemic lymphoblasts in about 93% of children with ALL (Ortega et al., 1977).

The amino acids asparagine (L-asparagine, Asn or N) and glutamine (L-glutamine, Gln, or Q) are not recognized as essential in the diet, as many healthy cells can synthesize them, however, they are essential for the surveillance of cancer cells, serving as a source of carbon and nitrogen, in addition to its use in protein synthesis under conditions of high cell proliferation. Leukemic lymphoblasts have a deficiency in the expression levels of the gene asparagine synthetase (ASNS) causing, therefore, insufficiency in the synthesis of L-asparagine (Asn). Thus, neoplastic cells become dependent on asparagine from the bloodstream.

Protocols using ASNase are also applicable in other hematological and solid cancers since they also show low levels of ASNS and, therefore, should be Asn auxotrophs and ASNase sensitive (Chiu et al., 2020). Manifestations such as non-Hodgkin lymphoma, myelocytic leukemia subtypes and chronic lymphoblastic leukemia, sarcomas, ovarian cancer and brain cancer (Song et al., 2015) and even in animals (Saba et al., 2009; Vimal; Kumar, 2018). Furthermore, there is great potential as an anti-tumor for breast cancer (Shiromizu et al., 2018) and as an inhibitory agent of the evolution of this cancer to metastasis (Knott et al., 2018). Other clinical applications are in infectious and autoimmune diseases (Baruch et al., 2014; Vimal; Kumar, 2018).

As it is an amidohydrolase, when injected into the patient, the action of L-ASNase consists in the depletion of circulating asparagine in the blood through the catalysis of this amino acid, leading to the formation of L-aspartate and ammonia products through the nucleophilic attack promoted by a threonine residue (Figure 5) (VERMA et al., 2014).

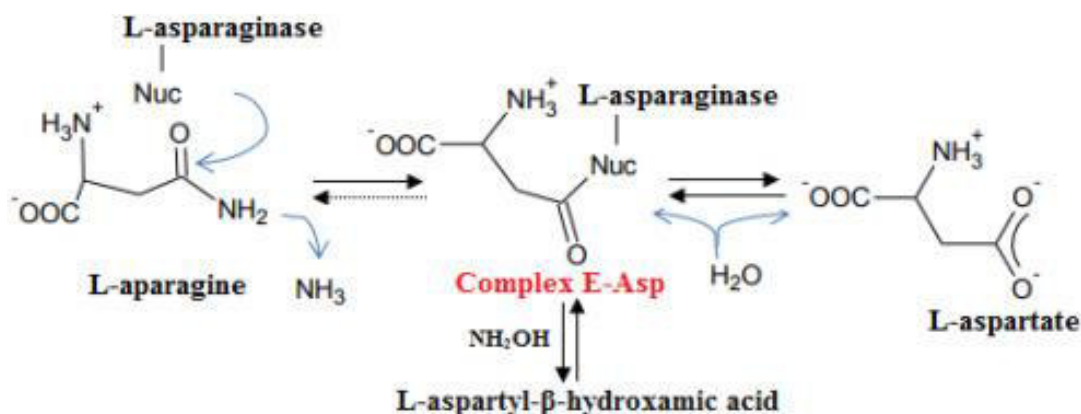


Figure 5. Reaction mechanism of L-ASNase. L-Asparagine is depleted into L-aspartate and ammonia (Costa-Silva et al., 2020).

Under conditions deprived of these amino acids, it leads to inhibition of the synthesis of constitutive proteins, in addition to fundamental regulatory proteins such as those of the cell cycle (cyclin-dependent kinases (cdKs) and cyclins) and anti-apoptotic proteins, resulting in leukemic cell death (Avramis, 2012; Nomme et al., 2012). Healthy cells, on the other hand, as they have the asparagine synthetase gene, are self-sufficient in the production of this amino acid and are not affected by the action of L-ASNase (Brumano et al., 2019).

It is noteworthy that ASNase toxicity is intrinsically related to its mechanism of action. This is due to the peculiarity of the enzyme that also possesses glutamine activity, being able to catalyze the glutamine hydrolysis reaction into glutamate and ammonia, but with lower affinity. This reaction is clinically manifested in the patient with the appearance of adverse reactions such as hepatotoxicity, pancreatitis and immunosuppression (Effer et al., 2020). However, some authors claim that without glutamine activity, ASNase would have no effect on the Asn substrate.

Currently, the three forms of ASNases therapeutically used in the treatment of ALL source from bacterial strains and are shown in Table 2.

Table 2. ASNase biopharmaceuticals that are currently approved for the treatment of ALL.

Commercial name/Laboratory	Source	Approved by
Kidrolase® e Leunase® (Kyowa); Aginasa® (Medac/Kyowa); Elspar® (Merck); Leuginase® (Beijing SL Pharmaceutical)	<i>Escherichia coli</i> wild type	1978 (FDA)
Oncaspar® (Sigma Tau)	<i>E. coli</i> PEGylated	1994 (FDA)
Erwinase® (Jazz Pharmaceuticals Inc.)	<i>Erwinia chrysanthemi</i>	2011 (FDA)
Spectrila® (Medac)	Recombinant <i>E. coli</i>	2016 (EMA)

All types have the same mechanism of action, but differ in their pharmacokinetic properties (Rizzari et al., 2013). Asparaginases from these microorganisms are less humanized when compared to asparaginases from animal sources. As a result, the administration of exogenous proteins can induce an immune response, producing anti-asparaginase antibodies, thus limiting its use (Rizzari et al., 2013). These are the main causes of drug resistance resulting in reduced activity. Resistance to ASNase can be symptomatic, with signs of clinical hypersensitivity such as allergic dermatological reactions, gastrointestinal disorders, hemorrhages (Brumano et al., 2019), or asymptomatic, when neutralizing antibodies are produced resulting in attenuation of enzymatic activity, an effect known as silent inactivation (Covini et al., 2012). Furthermore, the aforementioned drugs have short half-life times, making more frequent applications necessary. Due to the side effects caused during the treatment of ALL with bacterial ASNases, the use of the human enzyme could be a therapeutic alternative (Sugimoto et al., 1998; Nomme et al., 2012). However, the therapeutic potential of human ASNases is questionable, since it has a k_M value in the millimolar range, unsuitable for use as an injectable biopharmaceutical (Nomme et al., 2012).

Although bacterial ASNases are therapeutic products of great importance, their main limitations lie in their low stability in serum, due to the degrading action of plasma proteases, and in the immunogenic response of patients, leading to the need for injection of several doses during the treatment of leukemia. Some studies suggest that the resistance to L-ASNase is due to the L-Asn and L-Gln secreted by mesenchymal stromal cells and adipocytes surrounding blasts in bone marrow (Michelozzi et al, 2019; Iwamoto et al, 2007; Ehsanipour et al, 2013). Other mechanisms proposed that L-ASNase can be inactivated by cellular lysosomal cysteine proteases (Patel et al, 2009) and by cathepsin

B (CTSB) produced by macrophages (van der Meer et al, 2017) causing therapy failure. This results in the inactivation of circulating ASNase and exposure of enzyme epitopes which are related to the patient's immune system response (Patel et al., 2009; Offman et al., 2011). Albeit the addition of L-ASNase has improved outcome in pediatric ALL, its use remains limited in adult ALL due to its toxicities (Chew et al, 2020).

In order to reduce the adverse reaction caused by chemotherapy, alternative formulations of ASNase have been reported, with emphasis on the PEGylated form (PEGASNase) in which the PEG conjugation strategy aims to limit immunogenicity, as this polymer can mask immunogenic epitopes and decrease the susceptibility to the action of plasma proteases (Pasut; Veronese, 2012; Nomme et al., 2012). The pegylated form, marketed as Oncaspar® (Enzon Pharmaceuticals, Inc.), was approved by the Food and Drug Administration (FDA) in February 1994 as an alternative treatment for patients sensitized by native *E. coli* ASNase (Pieters et al., 2011) and in Brazil on June 12, 2017. This formulation reduces the excretion of the biomolecule in the urine and optimizes its immune profile by attenuating the formation of anti-asparaginase antibodies (Lopes et al., 2015). It also has the advantage of having a longer biological half-life than native ASNase (Pieters et al., 2011). However, the existence of a cross-reaction between antibodies developed in patients previously treated with native ASNase and PEG-ASNase turns unfeasible the change from one treatment to the other.

Chrisantaspase, approved in 2011 by the FDA, emerged as an alternative for patients who present reactions to any of the *E. coli* formulations (Figueiredo et al., 2016). Although crisantaspase does not cross-react with the other two types of ASNase, one third of patients still suffer from side effects (Pieters et al., 2011; Rizzari et al., 2013). In addition, it has a shorter half-life and greater neurotoxicity than asparaginases from *E. coli* (Brumano et al., 2019). The neurotoxic effects are related to the activity of L-ASNase by glutamine, which is approximately 2% for *E. coli* and 10% for *E. chrysanthemi* (Pieters et al., 2011; Avramis, 2012).

ASNase is used in the first phase and its dosage varies on the range between 80,000-100,000 U/m² of the patient's body area (INCA, 2001). Treatment protocols are selected according to the patient's degree of risk, which depends on the number of blasts and the size of the liver and spleen, and differ in terms of dosage and treatment time (INCA, 2001). There is a tendency to customize the treatment protocol, such as adjusting the dosage according to the phenotype and genotype of leukemic cells (Pui and Evans, 2013) and pharmacogenomics (Pui et al, 2008). It is believed that, in the future, each

patient will have a unique treatment in order to minimize the relapse rates caused by the mechanisms of resistance and sensitivity to drugs (Scherf et al., 2000; Holleman et al., 2004). However, while the costs of genomic analysis prevent its scalability, especially in non-developed countries, research is justified by the development of drugs that reduce side effects (Pui; Evans, 2013) and improve the patient's quality of life.

1.3. Modern trends in biopharmaceuticals

There is an ongoing global shift in pharmaceutical industry from small molecule drugs to biologics. Biopharmaceuticals are inherently biological in nature and manufactured by living organisms involving bioprocessing techniques for the prevention, treatment and diagnosis of diseases (Evans et al, 2021). The biopharmaceuticals market was valued at €214 billion in 2018, mostly reflecting the manufacture of recombinant proteins, monoclonal antibodies (mABs) and is driven to the development of vaccines (Evans et al, 2021; Huebbers et al, 2021).

The manufacturing processes for biopharmaceuticals is fundamentally different from the chemical manufacturing processes because biologics are much larger and more complex molecules compared with well-defined chemically synthesized drugs, such as aspirin (Lin-Gibson and Srinivasan, 2021). Manufacturing predominantly relies on fermentation-based production platforms with a series of process steps calls unit manufacturing (Figure 6). Each of these steps is usually carried out in a “batch” mode and the output from the bioreactor (upstream) is the input for the purifying steps (downstream) (Lin-Gibson and Srinivasan, 2021). During the upstream, nutrients are added into the bioreactor to promote cell growth and prevent nutrient depletion. In the manufacturing of biopharmaceuticals, this operation mode is called fed-batch process and it works well for producing large batches of therapeutic proteins (Lin-Gibson and Srinivasan, 2021).

As the biopharmaceutical industry works according to the current healthcare necessities, it faces some manufacturing challenges. The production rate of some biopharmaceuticals may have to be scaled-up rapidly during a pandemic and scaled-down after it gone. Thus, is strongly desirable a flexibility in the production (Lin-Gibson and Srinivasan, 2021).

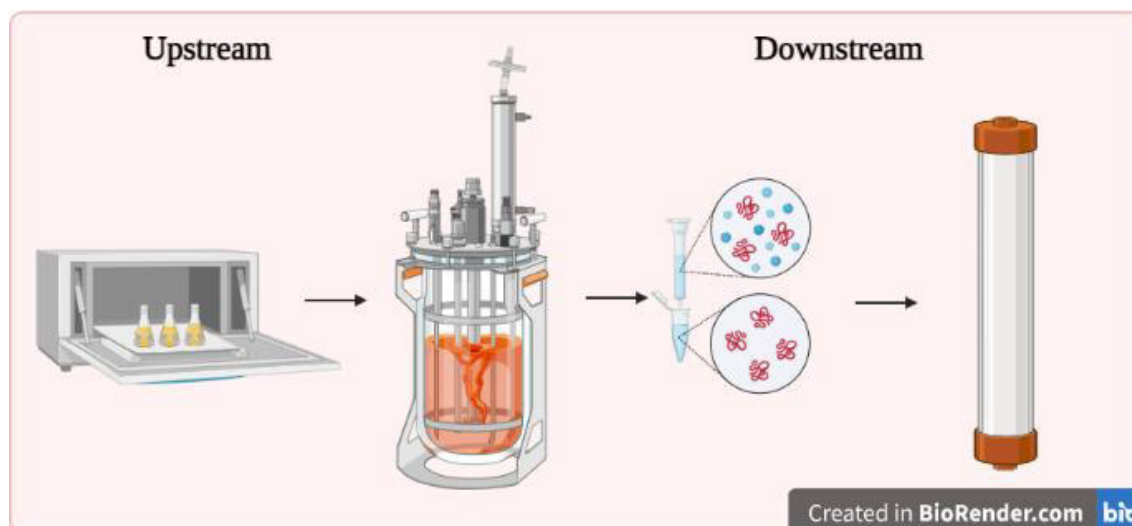


Figure 6. Manufacturing processes for biopharmaceuticals. The output from the bioreactor goes through different units manufacturing steps called “Downstream” to purify the biotherapeutic.

One alternative to minimize the cost is to produce biosimilars, which according to the FDA there is no clinically meaningful differences from the originator drugs that had the patent protection. The unique mandatory requirement for biopharmaceutical manufacturing is the rigorous product testing necessary to ensure patient safety and product quality (Lin-Gibson and Srinivasan, 2021).

Currently, there are many prokaryotic and eukaryotic hosts available for the expression of biopharmaceuticals at industrial scale. These expression platforms can be mainly grouped into mammalian, bacteria, yeast, plant and insect systems (Amann et al., 2019).

The crescent demand for recombinant biopharmaceuticals turns necessary the discovery of more molecules with post-translational modifications (PTMs), such as monoclonal antibodies (mAbs) and blood factors (Amann et al., 2019). Correct PTMs, in particular N-glycosylation, can be essential for *in vivo* function and may provides a higher plasma half-life and may prevents immunological reactions by masking immunogenic epitopes (Amann et al., 2019; Effer et al., 2020). While non-glycosylated drugs are mostly produced in bacteria and yeast, glycosylated proteins, for another hand, require expression in mammalian cell lines. Thus, the number of approved biotherapeutics produced in mammalian expression systems, such as Chinese Hamster Ovary (CHO), aligns with the trend for proper PTMs and other quality parameters (Amann et al., 2019). Since sufficient protein modulation, folding and secretion can be achieved in mammalian cells, they are the most appropriated choice for the production of complex biopharmaceuticals (Amann et al., 2019). However, the use of mammalian cells for

upstream production attracts high costs due to the expensive media (Huebbers et al., 2021).

Hence, to provide alternative sources for express proteins with human-like glycosylation pattern, many cell platforms were therefore reengineered (Amann et al., 2019). In addition to correct post-translational modification of the desired bioproduct, when it comes to choose the best-suited expression platform, several requirements to meet the needs of bioprocessing must to be fulfilled. Among them, genomic stability, a functional secretory machinery, high rates of growth and productivity, easy bioprocess handling, scalability, and easy downstream purification, plays an important role from a holistic point of view (Amann et al., 2019).

Bacterial expression systems, such as *Escherichia coli* (*E. coli*), are widely used for the production of smaller drugs, including hormones, and growth factors (Amann et al., 2019). However, contrary from what is found in mammalian cells, bacterias can not perform most PTMs, including glycosylation, which are essential for the production of active biopharmaceuticals (Amann et al., 2019). Using an appropriate signal sequence, the bioproduct of interest can be directed to the periplasm where a reducing environment allows protein oxidation for disulfide bond formation, thus enabling protein folding (Amann et al., 2019). Although bacteria presents some benefits of manufacturing in bioprocessing such its high expression levels, rapid cell division, less expensive, less complex bioprocessing and its easy handling for scale-up (Figure 7), this microorganism express some endotoxins that must be removed during the downstream process, turning this step more costly (Amann et al., 2019; Brumano et al., 2019).

Yeasts platform such as *Pichia pastoris* (*P. pastoris*) and *Saccharomyces cerevisiae* (*S. cerevisiae*) are capable to perform correct protein folding and also shows the ability to perform PTMs including N-glycosylation and O-linked glycosylation, phosphorylation, sulfation and ubiquitination (Irani et al., 2016). However, in contrast to N-glycosylation in mammalian cells, yeast perform hypermannosylation (Vervecken et al., 2004). Because of this they are mainly used for the manufacturing of smaller proteins, hormones and vaccines (Amann et al., 2019; Mattanovich et al., 2012). The advantages in manufacturing recombinant proteins in this system lie in its cost-efficient and the absence of endotoxins, as seen in bacteria, turns the downstream processing less costly. Population doubling times within hours, simple medium compositions, high recombinant

protein yields, and its easy handling for scale-up (Figure 7) are features that enable these hosts attractive for biomanufacturing (Amann et al., 2019).

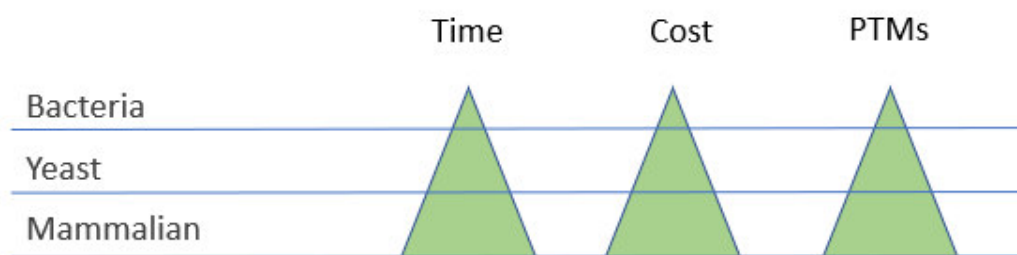


Figure 7. Comparative analysis of the three main host system for manufacturing biopharmaceuticals.

1.4. *Pichia pastoris* and glycosylation

Yeasts stand out in the production of L-ASNase since they are eukaryotic organisms and are capable to perform post-translational modifications. Such modifications are related to greater protein stability and the masking of immunogenic sites. This characteristic tends to reduce adverse reactions such as those observed with the use of bacterial asparaginase enzymes. Among yeasts, the best known is *S. cerevisiae* which, similarly to *E. coli*, expresses the two isoforms of asparaginase (Lopes et al., 2015). However, the ASNase secretion capacity by *S. cerevisiae* is inferior when compared to other yeasts, such as, for example, *Pichia pastoris*, which in an industrial context can hinder the production of the biopharmaceutical of interest. Thus, an ideal strain with superior production must be selected, to meet the industrial demand (Lopes et al., 2015).

One advantage in using the machinery of *Pichia pastoris* instead of *Saccharomyces cerevisiae*, in the production of heterologous proteins, lies in its ability to grow on both glucose or glycerol and methanol, providing high cell density cultures (more than 50 g_{dry biomass}/L). Another advantage of its use is because its gene expression system is regulated by methanol, through the enzyme alcohol oxidase, facilitating the manipulation of genes in obtaining heterologous proteins. Furthermore, this expression system is not pathogenic (Kurtzman, 2009).

The cultivation of *P. pastoris* is carried out in two stages. In the first, aimed at cell growth, the culture medium contains glycerol as a carbon source. In the second step, methanol feeding begins in order to induce the production of the recombinant protein of

interest. Thus, two operational strategies are adopted. Firstly, aiming the cell growth, the batch is feed with glycerol. Subsequently, a methanol feeding begins. The second strategy consists of feeding methanol at the same time as glycerol, thus reducing the cellular adaptation time to substrate change (Kastilan et al., 2017).

The importance of methanol for the production of recombinant proteins has been reported in many studies (Damasceno et al., 2004; Zhang et al., 2005; Cos et al., 2006; Potvin et al., 2012). The methanol concentration must be sufficient for the induction of AOX genes, however, insufficient to cause cell growth inhibition. The concentration range between 2.0 and 3.5 g/L of methanol is considered optimal (Potvin et al., 2012).

Glycosylation is a post-translational modification that frequently occurs in secretion proteins or those associated with membranes and synthesized in eukaryotes. It resides in the addition of oligosaccharides to proteins in an analogous way to pegylation, providing stability to the protein and its folding and can influence both its cellular activity and its biological function (Vervecken et al., 2004).

The advantage of glycosylation rather than pegylation is due to glycosylation be a biological process, whereas PEGylation is a synthetic chemical process. Oligosaccharides can be added to asparagine (Asn) residues and form N-glycans (most frequent), or to threonine or serine residues, forming O-glycans (Skropeta., 2009).

Yeast and mammalian N-glycosylation has a common partially glycosylated intermediate with eight mannose and two N-acetylglucosamine residues, Man₈GlcNAc₂ (Man₈). When this polypeptide is transferred to the Golgi complex, differentiation of this pathway begins. In yeast, mannose residues are added to the chain resulting in a hypermannosylated (immunogenic) structure. In mammals, Man₈ is processed up to Man₅GlcNAc₂ and the chain can be extended to hybrid structures, or complexes, with residues of N-acetyl-glucosamine, fucose, galactose, and sialic acid (Vervecken et al., 2004).

The humanization of the glycosylation pattern in *Pichia pastoris* involves two steps. First, hyper-mannosylation is eliminated by disruption of α -1,6-Mannosyltransferases (OCH1), *alg3* and *alg11* (De Pourcq et al., 2012; Jacobs et al., 2009), followed by the introduction of genes encoding the production of human glycosyltransferases and glycosidases (MnsI, GnTI, GnTII, SiaT) (Davidson et al., 2004).

Currently, the company Biogrammmatics Inc. offers a genetically modified *Pichia pastoris* strain called GlycoSwitch[®]. This strain can express proteins with N-

glycosylation with a human-like pattern which stands as an alternative approach for therapeutic purposes (Effer et al., 2020).

1.5. Downstream process

In the search for mitigation of immunogenic complications, increased half-life in order to reduce the frequency of administration, and preservation of high enzymatic activity, several strategies have been developed to improve the performance of proteins with therapeutic applications. As they decompose under acidic conditions of the stomach, therapeutic agents of a protein character should not be administered orally, requiring their injection directly into the bloodstream and, therefore, requiring a high degree of purity (Pacheco et al., 2012).

Several techniques have been widely used for enzyme purification. Among them, we can mention pre-purification techniques, such as fractional precipitation, liquid-liquid extraction and tangential filtration, which normally allow concentrating the biomolecule of interest with low efficiency in the purification process, removing protein character impurities, in addition to nucleic acids and lipids (Hesse and Wagner, 2000; Soares et al., 2012).

Among the processes that provide a higher degree of purity are the chromatographic techniques, such as affinity chromatography, ion exchange and gel filtration, which aim to recover and purify biomolecules with high degrees of purity. From an economic and technological point of view, the steps involving the isolation and purification of proteins correspond to 70-90% of the total production costs (Brumano et al., 2019). To consolidate a technological process and make it economically viable, it is desirable to reduce the number of steps intrinsic to the process and increase its yield. Therefore, the best efficiency can be achieved through the synergism between different unit operations (Kilikian and Pessoa, 2020).

Liquid chromatography is the main process for protein purification in the pharmaceutical industry. It includes different techniques with their own characteristics that allow the separation of enzymes of interest from other compounds present in solution. These characteristics are based on its size, charge, hydrophobicity and its specific biological activity. Selecting a technique, or combinations of techniques, that can be scaled in an industrial context, is highly desirable (Kilikian and Pessoa, 2020).

Ion exchange chromatography is a widely used efficient purification method that consists of modulating the ionic strength between the buffer, the protein and the ion exchange resin. Protein charge varies with pH and bonding occurs when the protein and exchanger have opposite charges. The protein adsorbs onto the resin and initially the column is eluted with a low ionic strength buffer. At pH values close to the isoelectric point (pI), proteins bind tightly to resins and are not eluted with low ionic strength buffers. The protein desorption process from resins begins when the pH of the medium is 0.5-1.0 above its isoelectric point. Thus, column elution is in the ionic strength gradient mode in order to separate components as a function of the charges exchanged between solute and resin (Kilikian and Pessoa, 2020). In the case of L-ASNase, knowing the isoelectric point of this protein, it is possible to proceed with its elution in a gradient mode so that the enzyme adsorbs onto the resin and is eluted according to the variation in the ionic strength of the eluent.

The size exclusion chromatography technique separates biomolecules according to their different sizes. The stationary phase consists of insoluble, hydrophilic and porous particles packed in a column. Small molecules can penetrate the pores, while the larger ones interact less with the pores and are, therefore, the first to be eluted (Kilikian and Pessoa, 2020). L-ASNase, being a tetrameric protein with 160 kDa, shows less interaction with the resin pores, being eluted before smaller proteins and other impurities. In the pharmaceutical industry this technique is applied in the purification of hyaluronic acid (Sousa, 2009) and in the separation of α -Lactalbumin and β -Lactalbumin (Naqvi et al., 2010).

It is noteworthy that purification by just one chromatographic technique may not be sufficient, especially for injectable pharmaceutical products, and that is why a multi-step system is proposed, in order to combine the different chromatographic techniques in their modes of operation, in which obtain the desired level of purification.

References

- Amann T, Schmieder V, Fastrup Kildegaard H, Borth N, Andersen MR. Genetic engineering approaches to improve posttranslational modification of biopharmaceuticals in different production platforms. *Biotechnol Bioeng*. 116(10):2778-2796. 2019. doi: 10.1002/bit.27101.
- Aur RJA, Simone J, Hustu HO, Walters T, Borella L, Pratt C, Donald P. Central Nervous System Therapy and Combination Chemotherapy of Childhood Lymphocytic Leukemia. *Blood Journal*. v. 37. p. 272–281. 1971. <https://doi.org/10.1182/blood.V37.3.272.272>
- Avramis VI. Asparaginases: biochemical pharmacology and modes of drug resistance. *Anticancer Res*. 32(7):2423-37. 2012.
- Baruch M, Belotserkovsky I, Hertzog BB, Ravins M, Dov E, Mciver KS, Le Breton YS, Zhou Y, Chen CY, Hanski E. An extracellular bacterial pathogen modulates host metabolism to regulate its own sensing and proliferation. *Cell*. v. 156. n. 1–2. p. 97–108. 2014. <http://dx.doi.org/10.1016/j.cell.2013.12.007>.
- Batool T, Makky EA, Jalal M, Yusoff MM. A Comprehensive Review on L-Asparaginase and Its Applications. *Appl Biochem Biotechnol*. 178(5):900-23. 2016. doi: 10.1007/s12010-015-1917-3.
- Broome JD, Schwartz JH. Differences in the production of L-asparagine in asparaginase-sensitive and resistant lymphoma cells. *Biochim Biophys Acta*. 30;138(3):637-9. 1967. doi: 10.1016/0005-2787(67)90569-2.
- Brumano LP, da Silva F, Costa-Silva TA, Apolinário AC, Santos J, Kleingesinds EK, Monteiro G, Rangel-Yagui CO, Benyahia B, Junior AP. Development of L-Asparaginase Biobetters: Current Research Status and Review of the Desirable Quality Profiles. *Frontiers in bioengineering and biotechnology*. 6, 212. 2019. <https://doi.org/10.3389/fbioe.2018.00212>.
- Campbell HA, Mashburn LT, Boyse EA, Old LJ. Two L-asparaginases from *Escherichia coli* B. Their separation, purification, and antitumor activity. *Biochemistry*. 6(3):721-30. 1967. doi: 10.1021/bi00855a011.
- Chew S, Jammal N, Kantarjian H, Jabbour E. Monoclonal antibodies in frontline acute lymphoblastic leukemia. *Best Practice & Research Clinical Haematology*. Volume 33, 101226, Issue 4, 2020. <https://doi.org/10.1016/j.beha.2020.101226>.
- Chiu M, Taurino G, Bianchi MG, Kilberg MS, Bussolati O. Asparagine Synthetase in Cancer: Beyond Acute Lymphoblastic Leukemia. *Frontiers in oncology*, 9, 1480. 2020. <https://doi.org/10.3389/fonc.2019.01480>.
- Cos O, Ramon R, Montesinos JL, Valero F. A simple model-based control for *Pichia pastoris* allows a more efficient heterologous protein production bioprocess. *Biotechnol Bioeng*. 5;95(1):145-54. 2006. doi: 10.1002/bit.21005.
- Costa-Silva TA, Costa IM, Biasoto HP, Lima GM, Silva C, Pessoa A, Monteiro G. Critical overview of the main features and techniques used for the evaluation of the clinical applicability of L-asparaginase as a biopharmaceutical to treat blood cancer. *Blood Reviews*. 43, 100651. 2020. <https://doi.org/10.1016/j.blre.2020.100651>.
- Covini D, Tardito S, Bussolati O, Chiarelli LR, Pasquetto MV, Digilio R, Valentini G, Scotti C. Expanding targets for a metabolic therapy of cancer: L-asparaginase. *Recent Pat Anticancer Drug Discov*. 7(1):4-13. 2012. doi: 10.2174/157489212798358001.
- Damasceno LM, Pla I, Chang HJ, Cohen L, Ritter G, Old LJ, Batt CA. An optimized fermentation process for high-level production of a single-chain Fv antibody fragment in *Pichia pastoris*. *Protein Expr Purif*. 37(1):18-26. 2004. doi: 10.1016/j.pep.2004.03.019.
- Davidson RC, Nett JH, Renfer E, Li H, Stadheim TA, Miller BJ, Miele RG, Hamilton SR, Choi BK, Mitchell TI, Wildt S. Functional analysis of the ALG3 gene encoding the Dol-P-Man: Man5GlcNAc2-PP-Dol mannosyltransferase enzyme of *P. pastoris*. *Glycobiology*. 14(5):399-407. 2004. doi: 10.1093/glycob/cwh023.
- De Pourcq K, Tiels P, Van Hecke A, Geysens S, Vervecken W, Callewaert N. Engineering *Yarrowia lipolytica* to produce glycoproteins homogeneously modified with the universal Man3GlcNAc2 N-glycan core. *PLoS One*. 7(6):e39976. 2012. doi: 10.1371/journal.pone.0039976.

- Dong Y, Shi O, Zeng Q. Leukemia incidence trends at the global, regional, and national level between 1990 and 2017. *Exp Hematol Oncol*. 2020. <https://doi.org/10.1186/s40164-020-00170-6>.
- Effer B, Kleingesinds EK, Lima GM, Costa IM, Sánchez-Moguel I, Pessoa A, Santiago VF, Palmisano G, Farias JG, Monteiro G. Glycosylation of Erwinase results in active protein less recognized by antibodies. *Biochemical Engineering Journal*. 163, 107750. 2020. <https://doi.org/10.1016/j.bej.2020.107750>.
- Evans SE, Harrington T, Rivero MCR, Rognin E, Tuladhar T, Daly R. 2D and 3D inkjet printing of biopharmaceuticals – A review of trends and future perspectives in research and manufacturing. *International Journal of Pharmaceutics*. v.599, 120443. 2021. <https://doi.org/10.1016/j.ijpharm.2021.120443>.
- Ehsanipour EA, Sheng X, Behan JW, Wang X, Butturini A, Avramis VI, Mittelman SD. Adipocytes cause leukemia cell resistance to L-asparaginase via release of glutamine. *Cancer Res*. 15;73(10):2998-3006. 2013. doi: 10.1158/0008-5472.CAN-12-4402.
- Farber S, Diamond LK. Temporary remissions in acute leukemia in children produced by folic acid antagonist, 4-aminopteroyl-glutamic acid. *N Engl J Med*. 3;238(23):787-93. 1948. doi: 10.1056/NEJM194806032382301.
- FDA. Drugs@FDA: FDA Approved Drug Products - Elspar. [s.l: s.n.]. Disponível em: <https://www.accessdata.fda.gov/scripts/cder/daf/index.cfm?event=overview.process&ApplNo=101063>
- FDA. Drugs@FDA: FDA Approved Drug Products - Oncaspar. [s.l: s.n.]. Disponível em: <https://www.accessdata.fda.gov/scripts/cder/daf/index.cfm?event=BasicSearch.process>
- FDA. Drugs@FDA: FDA Approved Drug Products - Erwinaze. [s.l: s.n.]. Disponível em: <https://www.accessdata.fda.gov/scripts/cder/daf/index.cfm?event=overview.process&ApplNo=125359>
- FDA; CDER; CBER. Guidance for Industry Immunogenicity Assessment for Therapeutic Protein Products. Disponível em <http://www.fda.gov/Drugs/GuidanceComplianceRegulatoryInformation/Guidances/default.htm#/>
- Figueiredo L, Cole PD, Drachtman RA. Asparaginase *Erwinia chrysanthemi* as a component of a multi-agent chemotherapeutic regimen for the treatment of patients with acute lymphoblastic leukemia who have developed hypersensitivity to *E. coli*-derived asparaginase. *Expert Rev Hematol*. 9(3):227-34. 2016. doi: 10.1586/17474086.2016.1142370. Globocan, 2020. LEUKEMIA. <https://gco.iarc.fr/today/data/factsheets/cancers/36-Leukaemia-fact-sheet.pdf>
- Hesse F, Wagner R. Developments and improvements in the manufacturing of human therapeutics with mammalian cell cultures. *Trends Biotechnol*. 18(4):173-80. 2000. doi: 10.1016/s0167-7799(99)01420-1.
- Holleman A, Cheok MH, den Boer ML, Yang W, Veerman AJ, Kazemier KM, Pei D, Cheng C, Pui CH, Relling MV, Janka-Schaub GE, Pieters R, Evans WE. Gene-expression patterns in drug-resistant acute lymphoblastic leukemia cells and response to treatment. *N Engl J Med*. 5;351(6):533-42. 2004. doi: 10.1056/NEJMoa033513.
- Huebbers JW, Buyel JF. On the verge of the market - Plant factories for the automated and standardized production of biopharmaceuticals. *Biotechnol Adv*. 46:107681. 2021. doi: 10.1016/j.biotechadv.2020.107681.
- INCA. Leucemia Agudas na Infância e Adolescência. *Revista Brasileira de Cancerologia*, v. 47, n. 3, p. 245–257, 2001. Disponível em: <http://www1.inca.gov.br/rbc/n_47/v03/pdf/normas.pdf>.
- Irani ZA, Kerkhoven EJ, Shojaosadati SA, Nielsen J. Genome-scale metabolic model of *Pichia pastoris* with native and humanized glycosylation of recombinant proteins. *Biotechnol Bioeng*. 2016 May;113(5):961-9. doi: 10.1002/bit.25863. Epub 2015 Nov 2. PMID: 26480251.
- Iwamoto S, Mihara K, Downing JR, Pui CH, Campana D. Mesenchymal cells regulate the response of acute lymphoblastic leukemia cells to asparaginase. *J Clin Invest*. 117(4):1049-57. 2007. doi: 10.1172/JCI30235.

- Jacobs PP, Geysens S, Vervecken W, Contreras R, Callewaert N. Engineering complex-type N-glycosylation in *Pichia pastoris* using GlycoSwitch technology. *Nat Protoc.*4(1):58-70. 2009. doi: 10.1038/nprot.2008.213.
- Kaser EC, Zhao L, D'mello KP, Zhu Z, Xiao H, Wakefield MR, Bai Q, Fang Y. The role of various interleukins in acute myeloid leukemia. *Med Oncol.* 2021. doi: 10.1007/s12032-021-01498-7.
- Kastilan R, Boes A, Spiegel H, Voepel N, Chudobová I, Hellwig S, Buyel JF, Reimann A, Fischer R. Improvement of a fermentation process for the production of two PfAMA1-DiCo-based malaria vaccine candidates in *Pichia pastoris*. *Sci Rep.* 20;7(1):11991. 2017. doi: 10.1038/s41598-017-11819-4.
- Kidd JG. Regression of transplanted lymphomas induced in vivo by means of normal guinea pig serum. I. Course of transplanted cancers of various kinds in mice and rats given guinea pig serum, horse serum, or rabbit serum. *J Exp Med.* 98(6):565-82. 1953. doi: 10.1084/jem.98.6.565.
- Kilikian BV, Pessoa A. Purificação de produtos biotecnológicos: operações e processos com aplicação industrial. 1. ed. São Paulo: Edgard Blücher Ltda, 2020. v. 1. 760p.
- Knott SRV, Wagenblast E, Khan S, Kim SY, Soto M, Wagner M, Turgeon MO, Fish L, Erard N, Gable AL, Maceli AR, Dickopf S, Papachristou EK, D'Santos CS, Carey LA, Wilkinson JE, Harrell JC, Perou CM, Goodarzi H, Poulogiannis G, Hannon GJ. Asparagine bioavailability governs metastasis in a model of breast cancer. *Nature.* 15;554(7692):378-381. 2018. doi: 10.1038/nature25465.
- Kurtzman CP. Biotechnological strains of *Komagataella* (*Pichia*) *pastoris* are *Komagataella phaffii* as determined from multigene sequence analysis. *J Ind Microbiol Biotechnol.* 36(11):1435-8. 2009. doi: 10.1007/s10295-009-0638-4.
- Lin-Gibson S, Srinivasan V. Recent Industrial Roadmaps to Enable Smart Manufacturing of Biopharmaceuticals. *IEEE Transactions on Automation Science and Engineering.* v18, pp. 176-183. 2021. doi: 10.1109/TASE.2019.2951018.
- Lopes AM, Oliveira-Nascimento L, Ribeiro A, Tairum CA Jr, Breyer CA, Oliveira MA, Monteiro G, Souza-Motta CM, Magalhães PO, Avendaño JG, Cavaco-Paulo AM, Mazzola PG, Rangel-Yagui CO, Sette LD, Converti A, Pessoa A. Therapeutic L-asparaginase: upstream, downstream and beyond. *Crit Rev Biotechnol.* 37(1):82-99. 2017. doi: 10.3109/07388551.2015.1120705.
- Mattanovich D, Branduardi P, Dato L, Gasser B, Sauer M, Porro D. Recombinant protein production in yeasts. *Methods Mol Biol.* 824:329-58. 2012. doi: 10.1007/978-1-61779-433-9_17.
- Michelozzi IM, Granata V, De Ponti G, Alberti G, Tomasoni C, Antolini L, Gambacorti-Passerini C, Gentner B, Dazzi F, Biondi A, Coliva T, Rizzari C, Pievani A, Serafini M. Acute myeloid leukaemia niche regulates response to L-asparaginase. *Br J Haematol.* Aug;186(3):420-430. 2019. doi: 10.1111/bjh.15920.
- Naqvi Z, Khan RH, Saleemuddin M. A procedure for the purification of beta-lactoglobulin from bovine milk using gel filtration chromatography at low pH. *Preparative Biochemistry & Biotechnology.* 40:4, 326-336. 2010. doi: 10.1080/10826068.2010.525405
- Nomme J, Su Y, Konrad M, Lavie A. Structures of apo and product-bound human L-asparaginase: insights into the mechanism of autoproteolysis and substrate hydrolysis. *Biochemistry.* 28;51(34):6816-26. 2012. doi: 10.1021/bi300870g.
- Offman MN, Krol M, Patel N, Krishnan S, Liu J, Saha V, Bates PA. Rational engineering of L-asparaginase reveals importance of dual activity for cancer cell toxicity. *Blood.* 3;117(5):1614-21. 2011. doi: 10.1182/blood-2010-07-298422.
- Ortega JA, Nesbit ME, Donaldson MH, Hittle RE, Weiner J, Karon M, Hammond D. L-Asparaginase, vincristine, and prednisone for induction of first remission in acute lymphocytic leukemia. *Cancer Research,* v. 37. p. 535-540. 1977.
- Pacheco B, Crombet L, Loppnau P, Cossar D. A screening strategy for heterologous protein expression in *Escherichia coli* with the highest return of investment. *Protein Expression and Purification.* v. 81, p. 33-41, 2012. doi: 10.1016/j.pep.2011.08.030.
- Patel N, Krishnan S, Offman MN, Krol M, Moss CX, Leighton C, van Delft FW, Holland M, Liu J, Alexander S, Dempsey C, Ariffin H, Essink M, Eden TO, Watts C, Bates PA, Saha V. A dyad of

- lymphoblastic lysosomal cysteine proteases degrades the antileukemic drug L-asparaginase. *J Clin Invest.* 119(7):1964-73. 2009. doi: 10.1172/JCI37977.
- Pasut G, Veronese FM. State of the art in PEGylation: the great versatility achieved after forty years of research. *J Control Release.* 20;161(2):461-72. 2012. doi: 10.1016/j.jconrel.2011.10.037.
- Pieters R, Hunger SP, Boos J, Rizzari C, Silverman L, Baruchel A, Goekbuget N, Schrappe M, Pui CH. L-asparaginase treatment in acute lymphoblastic leukemia: a focus on Erwinia asparaginase. *Cancer.* 15;117(2):238-49. 2011. doi: 10.1002/cncr.25489.
- Potvin G, Ahmad A, Zhang Z. Bioprocess engineering aspects of heterologous protein production in *Pichia pastoris*: A review. *Biochemical Engineering Journal.* 64, 91-105. 2012. <https://doi.org/10.1016/j.bej.2010.07.017>.
- Pourhossein M, & Korbekandi H. Cloning, expression, purification and characterisation of *Erwinia carotovora* L-asparaginase in *Escherichia coli*. *Advanced biomedical research.* 3, 82. 2014. <https://doi.org/10.4103/2277-9175.127995>.
- Pui CH, Evans WE. A 50-year journey to cure childhood acute lymphoblastic leukemia. *Semin Hematol.* 50(3):185-96. 2013. doi: 10.1053/j.seminhematol.2013.06.007.
- Pui CH, Robinson LL, Look AT. Acute lymphoblastic leukaemia. *Lancet.* v. 371. p. 1030– 1043. 2008. [https://doi.org/10.1016/S0140-6736\(08\)60457-2](https://doi.org/10.1016/S0140-6736(08)60457-2).
- Rizzari C, Conter V, Starý J, Colombini A, Moericke A, Schrappe M. Optimizing asparaginase therapy for acute lymphoblastic leukemia. *Curr Opin Oncol.* 1:S1-9. 2013. doi: 10.1097/CCO.0b013e32835d7d85.
- Saba CF, Hafeman SD, Vail DM, Thamm DH. Combination chemotherapy with continuous L-asparaginase, lomustine, and prednisone for relapsed canine lymphoma. *J Vet Intern Med.* 23(5):1058-63. 2009. doi: 10.1111/j.1939-1676.2009.0357.x.
- Scherf U, Ross DT, Waltham M, Smith LH, Lee JK, Tanabe L, Kohn KW, Reinhold WC, Myers TG, Andrews DT, Scudiero DA, Eisen MB, Sausville EA, Pommier Y, Botstein D, Brown PO, Weinstein JN. A gene expression database for the molecular pharmacology of cancer. *Nat Genet.* 24(3):236-44. 2000. doi: 10.1038/73439.
- Shiromizu S, Kusunose N, Matsunaga N, Koyanagi S, Ohdo S. Optimizing the dosing schedule of L-asparaginase improves its anti-tumor activity in breast tumor-bearing mice. *J Pharmacol Sci.* 136(4):228-233. 2018. doi: 10.1016/j.jphs.2018.01.008.
- Skropeta D. The effect of individual N-glycans on enzyme activity. *Bioorg Med Chem.* 17(7):2645-53. 2009. doi: 10.1016/j.bmc.2009.02.037.
- Soares PAG, Vaz AFM, Correia MTS, Pessoa-Junior A, Cunha MGC. Purification of bromelain from pineapple wastes by ethanol precipitation. *Separation and Purification Technology.* v. 98, p.389-395, 2012.
- Song P, Ye L, Fan J, Li Y, Zeng X, Wang Z, Wang S, Zhang G, Yang P, Cao Z, & Ju D. Asparaginase induces apoptosis and cytoprotective autophagy in chronic myeloid leukemia cells. *Oncotarget.* 6(6). 3861–3873. 2015. <https://doi.org/10.18632/oncotarget.2869>.
- Sousa AS, Guimarães AP, Gonçalves CV, Silva IJ, Cavalcante CL, Azevedo DCS. Purification and Characterization of Microbial Hyaluronic Acid by Solvent Precipitation and Size-Exclusion Chromatography. *Separation Science and Technology.* 44:4, 906-923. 2009. doi: 10.1080/01496390802691281.
- Steiner M, Hochreiter D, Kasper DC, Kornmüller R, Pichler H, Haas OA, Pötschger U, Hutter C, Dworzak MN, Mann G, Attarbaschi A. Asparagine and aspartic acid concentrations in bone marrow versus peripheral blood during Berlin-Frankfurt-Münster-based induction therapy for childhood acute lymphoblastic leukemia. *Leuk Lymphoma.* 53(9):1682-7. 2012. doi: 10.3109/10428194.2012.668681.
- Sugimoto H, Odani S, Yamashita S. Cloning and Expression of cDNA Encoding Rat Liver 60-kDa Lysophospholipase Containing an Asparaginase-like Region and Ankyrin Repeat. *The Journal Of Biological Chemistry,* v. 273, p. 12536–12542, 1998. <https://doi.org/10.1074/jbc.273.20.12536>.
- Tong WH, Pieters R, Kaspers GJ, te Loo DM, Bierings MB, van den Bos C, Kollen WJ, Hop WC, Lanvers-Kaminsky C, Relling MV, Tissing WJ, van der Sluis IM. A prospective study on drug monitoring of

- PEGasparaginase and Erwinia asparaginase and asparaginase antibodies in pediatric acute lymphoblastic leukemia. *Blood*, 123(13), 2026–2033. (2014). <https://doi.org/10.1182/blood-2013-10-534347>.
- van der Meer LT, Terry SY, van Ingen Schenau DS, Andree KC, Franssen GM, Roeleveld DM, Metselaar JM, Reinheckel T, Hoogerbrugge PM, Boerman OC, van Leeuwen FN. In Vivo Imaging of Antileukemic Drug Asparaginase Reveals a Rapid Macrophage-Mediated Clearance from the Bone Marrow. *J Nucl Med*. 58(2):214-220. 2017. doi: 10.2967/jnumed.116.177741.
- Verma N, Kumar K, Kaur G, Anand S. L-asparaginase: a promising chemotherapeutic agent. *Critical reviews in biotechnology*, v. 27, n. 1, p. 45–62, 2007. doi: 10.1080/07388550601173926.
- Vervecken W, Callewaert N, Kaigorodov V, Geysens S, Contreras R. Modification of the N-glycosylation pathway to produce homogeneous, human-like glycans using GlycoSwitch plasmids. *Methods Mol Biol*. 389:119-38. 2007. doi: 10.1007/978-1-59745-456-8_9.
- Vimal, A., & Kumar, A. L-Asparaginase: a feasible therapeutic molecule for multiple diseases. *Biotech*. 8(6), 278. (2018). <https://doi.org/10.1007/s13205-018-1282-3>.
- Zhang YQ, Tao ML, Shen WD, Zhou YZ, Ding Y, Ma Y, Zhou WL. Immobilization of L-asparaginase on the microparticles of the natural silk sericin protein and its characters. *Biomaterials*. 25(17):3751-9. 2004. doi: 10.1016/j.biomaterials.2003.10.019.
- Zhang W, Sinha J, Smith LA, Inan M, Meagher MM. Maximization of production of secreted recombinant proteins in *Pichia pastoris* fed-batch fermentation. *Biotechnol Prog*. 21(2):386-93. 2005. doi: 10.1021/bp049811n.

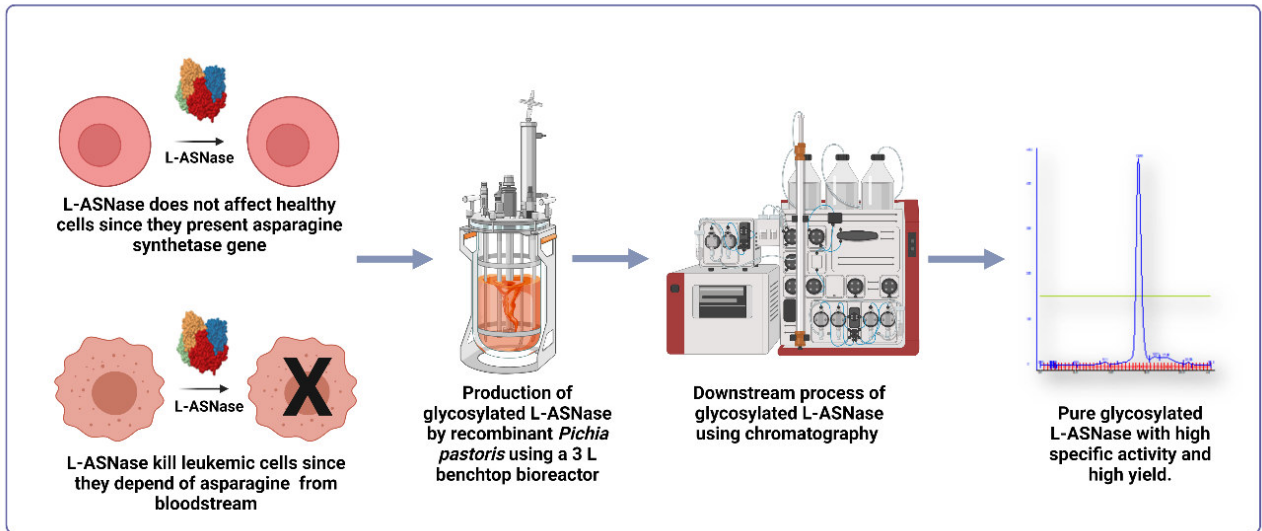
Chapter 2

Upstream and downstream processing of L-asparaginase with human-like glycosylation pattern expressed by recombinant *Pichia pastoris*

Abstract

L-asparaginase (L-ASNase) is a life-saving medication used in the treatment of Acute Lymphoblastic Leukaemia (a blood cancer that affects over 60,000 people yearly, most of whom are children) and has shown potential for preventing breast cancer metastasis. However, L-ASNase still requires improvement since up to 60% of the patients develop hypersensitivity to the treatment due to its immunogenicity, which may cause serious side effects. To address this issue, this work describes the optimization of the production process of an L-ASNase from *Erwinia chrysanthemi* expressed extracellularly by *Pichia pastoris* with human-like glycosylation pattern in a 3L benchtop bioreactor, as well as its downstream purification process. After purification, it was possible to reach a final yield of 54.93% with a purification factor of 70.93 fold. The proteomics analyses confirmed the attainment of an extremely pure enzyme and the cytotoxicity assay demonstrated its anti-leukemic activity after glycosylation through the reduction of 65% and 44% in cell viability for MOLT-4 and Jurkat line, respectively. Hence, this work paves the way for production scale-up and pre-clinical trials of this promising novel medication, which may help improve the remission rates and quality of life for many cancer patients around the world.

Keywords Leukemia; Bioprocess; Biopharmaceutical; Protein purification; L-asparaginase.



Graph Abstract. Schematic representation of the methodology used to produce and purify the glycosylated L-ASNase.

1. Introduction

Leukemias are characterized by intense multiplication and by large numbers of immature lymphoid and myeloid cells in the bloodstream. Among the different types of leukemia, Acute Lymphoblastic Leukemia (ALL) is an aggressive malignancy occurring especially in children and adolescents but can also occur in young adults (Brumano et al., 2019).

Several factors may lead to the translocation and chromosomal mutations that cause ALL, such as bone marrow changes, obesity, growth factors, or random mutations (Avramis, 2012). Subsequently, normal hematopoietic elements are hijacked by immature lymphoid cells, resulting in decreased erythrocyte and platelet counts. As a result, patients develop anemia and can experience symptoms such as fatigue, pallor, higher vulnerability to infections, and bleeding episodes (Brumano et al., 2019). Adult survival rates are over 60 % in developed countries and exceeds 90 % for children treated in modern research centers (Pui and Evans, 2013; Inaba et al., 2013).

L-Asparaginase (ASNase) (EC 3.5.1.1, L-Asparagine amidohydrolase) is one of the main therapeutic agents used in the treatment of leukemias, such as ALL. Currently, the commercially available L-ASNases approved by the FDA for therapeutic purposes have been sourced from bacteria (*E. coli* and *E. chrysanthemi*) (Brumano et al., 2019). This tetrameric protein has around 330 amino acid residues per monomer, a molar mass between 140 – 160 kDa, and catalyzes the L-asparagine (Asn) hydrolysis reaction. The component monomers are arranged in 14 β -sheets and 8 α -helices. The isoelectric point

(pI) for the *E. chrysanthemi* ASNase is 8.6 and it has optimal activity under human physiological conditions (37°C and pH 7.2) (Pourhossein and Korbekandi, 2014; Zhang et al., 2003).

Leukemic lymphoblasts are often deficient in expression levels of the asparagine synthetase gene (ASNS) (EC 6.3.5.4), which causes an insufficient synthesis of Asn. As a result, neoplastic cells become dependent on Asn from the bloodstream. Once L-ASNase is injected, it depletes Asn from the bloodstream into L-aspartate and ammonia (Brumano et al., 2019). Decreasing the levels of this and other amino acids leads to the inhibition of constitutive protein synthesis for the leukemic blasts resulting in their apoptosis (Avramis, 2012). On the other hand, most healthy cells are self-sufficient in the production of this amino acid and are not affected by the action of L-ASNase (Nomme et al., 2012).

However, the administration of these exogenous proteins may induce an immune response, producing anti-asparaginase antibodies. This is the main cause of reduced drug efficacy, resulting in reduced L-ASNase activity and undesirable effects such as pancreatitis, coagulation disorders, and diabetes (Effer et al., 2020; Costa-Silva et al., 2020). To overcome these side effects, a few publications have evaluated chemical modifications such as encapsulation (Apolinario et al., 2018) and PEGylation (where the enzyme is covalently bound to polyethyleneglycol (PEG) (Torres-Obreque et al., 2019; Menegueti et al., 2019). These modifications reduce the immunogenicity of the molecule by masking the epitopes that otherwise activate the immune system and the PEG polymer stabilizes the enzyme and increases its half-life. However, the only chemical modification currently approved by the FDA for L-ASNase for human use is PEGylation (Effer et al., 2020).

While chemical reactions can improve biopharmaceuticals, the PEGylation reaction can also be emulated through a biological route, exploring the tools from the recent trends that molecular biology had brought. More specifically, a great deal of attention has been drawn towards exploiting the potential of substituted by post-translational modifications, such as glycosylation, in new biotherapeutics. Glycosylated proteins are covered with oligosaccharides, which, similarly to PEGylation, provide stability and correct folding, and may influence both its cellular activity and its biological function (Vervecken et al., 2004). Oligosaccharides may be bound to the Asn residues to form N-glycans (which is more common), or to the threonine or serine residues, forming

O-glycans (Skropeta, 2009). This tends to decrease adverse reactions such as those observed with the use of L-ASNases from bacterial sources (Effer et al., 2020).

Yeasts gained attention as a host system for the expression of recombinant proteins as they are eukaryotic organisms able to perform glycosylation. Among them, the most well-known systems to express recombinant proteins are *Saccharomyces cerevisiae* and *Pichia pastoris*. Similarly to *E. coli*, *S. cerevisiae* expresses two L-ASNase proteoforms. However, contrary to mammalian cells, protein glycosylation in yeasts results in high-mannose N-glycans that may cause immunogenic reactions when interacting with human mannose receptors present in immune cells, which results in rapid clearance from the bloodstream (De Pourcq et al., 2010).

To overcome these limitations, the N-glycosylation pathway in yeasts has been reengineered to produce glycoproteins with human-like glycosylation patterns (De Pourcq et al., 2010; Hopkins et al., 2011). Furthermore, the levels of hyper-mannosylation in *P. pastoris* are naturally much lower (approximately 50 residues) than in *S. cerevisiae* (~500 residues) (De Pourcq et al., 2010). When engineered, *P. pastoris* adds only 5 residues of mannose in the final oligosaccharide.

As described in a previous study, our research group has constructed a new *P. pastoris* strain (Glycoswitch_pJAG-s1_ashb) that can express an active extracellular L-ASNase from *E. chrysanthemi* with human-like glycosylation (Effer et al., 2019). The present study presents a critical development for the upstream and downstream processing of an innovative glycosylated L-ASNase proteoform obtained by this biotechnological route using a benchtop bioreactor and purified by crossflow filtration and high-resolution techniques. This study also presents the final yield of the process and the specific activity of the new recombinant L-ASNase.

2. Material and methods

2.1. Upstream

2.1.1. Expression system

The recombinant *Pichia pastoris* Glycoswitch® Superman5 (his⁻) strain is used to express the *ashb* gene (i.e. amino acid residues 22–348 UniprotKB – P06608) from *E. chrysanthemi*. This construction used the pJAG-s1_ashb expression vector as previously described (Effer et al., 2019). The L-ASNase is glycosylated and secreted into the cellular medium (Effer et al., 2020).

2.1.2. Determination of *Pichia pastoris* cell concentration

A calibration curve was constructed, correlating optical density (OD₆₀₀) with dry cell mass. Thus, 5 mL of triplicate samples were taken throughout the culture and centrifuged at 3000xg for 20 min, 4°C. The precipitate (cells, cell debris, and culture medium) was resuspended to the same volume (with 9% physiological solution), homogenized, and centrifuged under the same conditions (3000xg, 20 min). Absorbance was read on a spectrophotometer (Beckman DU 640 and Hitachi U1800) at 600 nm. Another part was filtered in a filtration system (vacuum pump plus 0.45 µm diameter pore cellulose nitrate membrane filter) to determine cell dry mass concentration (gL⁻¹). The previously dried membranes with the determined masses were placed in an oven at 100°C for 24 h (Olsson and Nielsen, 1997). Finally, dried membranes were weighted.

2.1.3. Experimental design for shake flask cultivation

To establish the variables that lead to higher extracellular expression of glycosylated L-ASNase, we chose its enzymatic activity. Hence, we used a fractional factorial design 2⁴⁻¹ to find the statistically significant variables followed by optimization experiments. The levels and coded levels (-1, 0, 1) of the independent variables are shown in Table 1a.

After evaluating the statistically significant variables, a second experimental design was created, which is shown in Table 1b. The surface response regressions and Analyses of Variance (ANOVAs) were performed using the package rsm in R (Lenth RV (2009) “Response-Surface Methods in R, Using rsm”, Journal of Statistical Software, 32(7), 1–17. <https://www.jstatsoft.org/v32/i07/>).

Table 1. (a) 2^{4-1} Fractional factorial design with triplicate at the central point for L-ASNase production. Variables studied: temperature (X_1 , °C); initial inoculum (X_2 , X_0); inductor concentration (MeOH, X_3); periodicity of induction (Δt induction, X_4).

Experiment		Temperature (°C)				X ₀ (g/L)	[MeOH] (%)	Δt induction (h)	
		x1	x2	x3	x4				
Fractionate Factorial Design 2 ⁴⁻¹	1	-1	-1	-1	-1	15.0	1.0	0.5	12
	2	+1	-1	-1	+1	35.0	1.0	0.5	36
	3	-1	+1	-1	+1	15.0	3.0	0.5	36
	4	+1	+1	-1	-1	35.0	3.0	0.5	12
	5	-1	-1	+1	+1	15.0	1.0	1.5	36
	6	+1	-1	+1	-1	35.0	1.0	1.5	12
	7	-1	+1	+1	-1	15.0	3.0	1.5	12
	8	+1	+1	+1	+1	35.0	3.0	1.5	36
Central Point	*PC1	0	0	0	0	25.0	2.0	1.0	24
	*PC2	0	0	0	0	25.0	2.0	1.0	24
	*PC3	0	0	0	0	25.0	2.0	1.0	24

Table 1. (b) Experimental design for optimizing L-ASNase production. Variables studied: temperature (X_1 , °C) and inductor concentration (MeOH, X_2).

Experiment		Temperature (°C)		[MeOH] (%)
		X_1	X_2	
Factorial Design 2^2	1	-1	-1	10.0
	2	+1	-1	50.0
	3	-1	+1	10.0
	4	+1	+1	50.0
Central point	*PC1	0	0	30.0
	*PC2	0	0	30.0
	*PC3	0	0	30.0

An Eppendorf tube containing approximately 1 mL of cell stock was pre-inoculated in a 500 mL Erlenmeyer with baffles and a useful volume of 100 mL BMGY (1M pH 6.0) (buffered glycerol complex medium: yeast extract, 10.0 g L⁻¹; peptone, 20.0 g L⁻¹; yeast nitrogen base, 3.4 g L⁻¹; ammonium sulfate, 10.0 g L⁻¹; glycerol, 10 g L⁻¹) medium incubated in a shaker at 30°C and 250 rpm for 20 h.

For inoculum preparation, after 20 h of pre-inoculum culture, the optical density of cells was measured. The cell concentration of the pre-inoculum was determined using a calibration curve (absorbance as a function of dry cell mass). The required volumes were then centrifugated in Falcon tubes at 5 °C for 10 min at 3000xg. Cells were resuspended in a freshly prepared medium and inoculated into a 250 mL Erlenmeyer shaker flask containing 50 mL of BMGY culture medium with potassium phosphate buffer and then incubated in a shaker at 30°C and 250 rpm for 24 h.

At the end of the growth phase, the induction was started, in which the conditions mentioned in Table 1 (a) and (b) were studied. The enzymatic activity was measured every 24 hours after the induction.

2.1.4. Measurement of L-asparaginase activity

At this stage, ASNase activity was determined by the formation of L-aspartyl- β -hydroxamic acid (AHA) using the modified microplate protocol (Drainas et al., 1977).

2.1.5. Production of L-ASNase with human-like glycosylation pattern in a bench bioreactor

Using the optimized shaker conditions, batch cultivation was carried out using the BIOFLO™/CelliGen® 115 bioreactor (New Brunswick) containing 1 L of complex medium (BMGY) with potassium phosphate buffer (1M pH 6). Glycerol 1% (v/v) was used as a carbon source until exhaustion. Once all glycerol had been consumed, the induction phase began, in which the system was fed with methanol. The temperature was maintained at 35°C throughout the cultivation and aeration was maintained at 1 vvm and initial agitation at 700 rpm and a target value of 20% dissolved oxygen was kept with cascade control of agitation between 700 and 1000 rpm.

2.2. Downstream

2.2.1. Crossflow filtration

A study was performed to evaluate the purity of glycosylated L-ASNase obtained by biotechnological route from the complex medium. Thus, two strategies were implemented.

Strategy 1: After 24 h of culture induction, a 5 mL sample was collected from the reactor and, after centrifugation (3000 \times g for 10 min at 4 °C), its activity was measured in the supernatant. Then, the extracellular medium containing L-ASNase was transferred to four 250 mL centrifuge vials each. The medium was then centrifuged at 3000 \times g for 10 minutes at 4°C. After that, the supernatant was redistributed to 50 mL centrifuge vials and centrifuged again at 10,000 \times g for 10 min. Finally, the whole collected medium was vacuum filtered on a 0.45 μ m membrane.

Strategy 2: After 24 h of culture induction, a 5 mL sample was taken from the reactor and, after centrifugation (3000 \times g for 10 min at 4 °C), its activity was measured. Then the extracellular medium containing L-ASNase was transferred to four 250 mL centrifuge vials each. The medium was then centrifuged at 3000 \times g for 10 min at 4 °C to separate the medium from the cells. After this time, a 300 kDa cut-off membrane was

used to remove the remaining cell debris by crossflow ultrafiltration. Thus, the permeate was collected for the next steps.

Extracellular media from strategies 1 and 2 were separately concentrated and diafiltered using the Sartoflow Slice 200 Benchtop System (120V) ultrafilter (Sartorius® Stedim Biotec) under the following conditions: flow rate of 400 mL min⁻¹; 30 psi of transmembrane pressure; polyethersulfone membrane; and three different pore sizes were studied separately (10, 30 and 100 kDa). The medium was then concentrated tenfold and buffer exchange was performed by the addition of acetate buffer (50 mM pH 5.2) upon reaching the desired (pH 5.2) to perform the next step of the purification process: the cation exchange chromatography.

2.2.2. Cationic exchange chromatography

A 20 mL SP HP column (GE Healthcare, USA) was used for cation exchange. To equilibrate the column, three column volumes (CV) of sodium acetate buffer (50 mM, pH 5.3 with 100 mM Glycine) were used. The sample was loaded into the column using the Akta Start (GE Healthcare, USA) peristaltic pump with a flow rate of 0.5 mL min⁻¹ to ensure that the protein binds with the column resin. Finally, the column was washed with 1.5 column volume of the same buffer to remove the excess of contaminant proteins. The target protein was eluted with 50 mM sodium acetate buffer, pH 5.3 with 100 mM Glycine, and by step gradient using NaCl 1 M on the following steps 40 mM, 60 mM, 100 mM. Samples of 500 µL were collected to measure enzyme activity, total protein concentration, and purity using SDS-PAGE. The remaining enzyme was purified by gel filtration.

2.2.3. Size-exclusion chromatography

After Cationic Exchange Chromatography, size-exclusion was performed using the Superdex™ 200 Increase 10/300 GL column (GE Healthcare, USA). The column was washed with water and equilibrated with two column volumes at pH 5.5 sodium acetate buffer with 100 mM glycine. The protein was eluted with 1.5 column volumes of the same buffer at a flow rate of 0.75 mL min⁻¹.

2.2.4. Determination of L-ASNase activity

Pure enzyme activity was estimated using the Nessler method, where 1 unit represents the release of 1 μmol ammonia per minute. In a 96-well plate, 168 μL Asn (44 mM), 148 μL 50 mM Tris HCl buffer (pH 8.6), 37 μL ultra-pure water, and 17 μL sample were added. After 10 min incubating at 37°C, the reaction was stopped by adding 17 μL of 1.5 M trichloroacetic acid. In another 96-well plate, 279 μL of ultra-pure water, 37 μL of Nessler's reagent, and 37 μL of the previous reaction were added and the absorbances read at 440 nm in a plate reader SpectraMax (Molecular Devices). The absorbance measurement was then compared to the standard curve previously made with the Nessler reagent and ammonium sulfate at concentrations of 0.05, 0.1, 0.25, 0.5, 1.0, and 2.5 mM.

2.2.5. Polyacrylamide gel electrophoresis (SDS-PAGE)

For SDS-PAGE, 20 μL of samples from each purification step were transferred to a microtube, and 5 μL of Laemmli sample buffer + dithiothreitol (DTT) were added and then heated at 95 °C for 5 min.

Using a 12 % acrylamide separating gel, samples were loaded into the lanes and the protein marker (BioRad) was loaded into the first and the last lane. The voltage was set to 120 V and the running buffer (tris-glycine pH 8.5 + SDS 1% (w/v) was added until the top of the electrophoresis system. When the run was completed, the polyacrylamide gel was stained with Coomassie Blue R-250 for 1 h, and then it was destained overnight with solution (40 v/v % methanol, 20 v/v % acetic acid).

2.2.6. Total protein assay

Total protein was determined by the BCA (bicinchoninic acid assay) method. Initially, a calibration curve was constructed using BSA (bovine serum albumin) in the range 0.1-1.2 mg mL⁻¹. Then, before measuring the protein concentration, interferences were removed using the Non-Interfering Protein AssayTM (Calbiochem®) kit. A solution of bicinchoninic acid (50 parts) plus copper sulfate (1 part) was prepared for each sample. From this mixture, 200 μL were aliquoted into an Eppendorf tube and 25 μL of the sample were added. After homogenization, it was incubated for 30 min at 37 °C. Finally, the absorbance was measured at 562 nm.

2.2.7. Proteomics analysis by LC-MS/MS

This analysis was performed to assess the final purity of the glycosylated L-ASNase. In-gel reduction, alkylation, and digestion with trypsin (Sigma-Aldrich; Trypsin sequencing grade) was performed on the gel sample prior to the analysis by mass spectrometry. Cysteine residues were reduced with dithiothreitol (10 mM) and derivatized by treatment with iodoacetamide (55 mM) to form stable carbamidomethyl derivatives. Trypsin digestion was carried out overnight at room temperature after initial incubation at 37 °C for 2 hours.

The peptide sample was suspended in 30 µL of resuspension buffer (2% acetonitrile (ACN) in 0.05% formic acid (FA)), 10 µL of which were injected to be analyzed by LC-MS/MS. Chromatographic separation was performed using a U3000 UHPLC NanoLC system (ThermoFisherScientific, UK). Peptides were resolved by reversed-phase chromatography in a 75 µm C18 column (50 cm length) using a three-step linear gradient of 80% ACN in 0.1% FA. The gradient was set to elute the peptides at a flow rate of 250 nL.min⁻¹ over 60 min. The eluate was ionized by electrospray ionization using an Orbitrap Fusion Lumos (ThermoFisherScientific, UK) operating using Xcalibur v4.1.5. The instrument was first programmed using a “Universal_CID” method by defining a 3 secs cycle time between a full MS scan and MS/MS fragmentation. This method takes advantage of the multiple analyzers on Orbitrap-Fusion-Lumos and drives the system to use all available parallelizable time, resulting in decreasing the dependence on method parameters (such as DDA). The instrument was programmed to acquire in the automated data-dependent switching mode, selecting precursor ions based on their intensity for sequencing by collision-induced fragmentation using a TopN CID method. The MS/MS analyses were conducted using collision energy profiles that were chosen based on the mass-to-charge ratio (m/z) and the charge state of the peptide.

2.2.8. Cell culture and cytotoxicity assay

T-ALL strains (Jurkat and MOLT-4) were purchased from ATCC. In order to monitor the effect of the Glycosylated L-ASNase, we used the (3-(4,5-dimethylthiazol-2-yl)-2,5-diphenyltetrazolium bromide) test (MTT) as described by Mosmann. In a 96 well plate, 2x10⁴ cells from each lineage were incubated with asparaginase (0.01-1.00 IU.mL⁻¹) and 150 µL of RPMI-1640 medium supplemented with 10% of fetal bovine serum at

37 °C at 5% of CO₂. After 72 hours, 0.33 µg.mL⁻¹ of MTT was added and incubated for 4 hours at 37 °C. After this time, 100 µL of SDS 10% and HCl 0.01 N was added to each well and incubated overnight. The absorbance was determined at 570 nm to measure the survival rate and we considered the cells incubated just with the vehicle as 100% to calculate the IC₅₀ value.

3. Results and Discussion

Table 2a shows the Analysis of Variance (ANOVA) of a first-order model for the dependency of the L-ASNase activity on the cultivation temperature (°C), inoculum concentration (X_0 [g/L]), MeOH concentration (%), and periodicity of the induction phase (Δt). Among these first-order terms, only the temperature seemed to have a statistically significant p-value (0.007), while the other terms contributed very little to the variance of L-ASNase activity. Table 2b shows the ANOVA of a linear model for the dependency of the L-ASNase activity on the cultivation temperature (°C) alone, which achieved a p-value of 0.001. Given the positive sign of the temperature term in these models, higher cultivation temperatures (30°C to 35°C) seem to favor higher L-ASNase activities, although this dependency does not seem to be linear, which results in the R-squared values of these models not being very high.

Table 2. Analysis of variance (ANOVA) of the fractional factorial design 2^{4-1} used for screening the statistically significant variables for the production of L-ASNase in shaker flasks considering (a) first-order effects of the 4 variables tested and (b) only the first-order effect of temperature.

- a) L-ASNase activity as a function of the first-order effects of cultivation temperature (°C), inoculum concentration (X_0 [g/L]), MeOH concentration (%), and periodicity of the induction phase (Δt).

	Estimate	Std. Error	t-value	p-value
(Intercept)	-105.9	277.3	-0.38	0.716
Temperature (°C)	25.5	6.37	4.01	0.007
X_0 (g/L)	22.9	63.7	0.36	0.731
[MeOH] (%)	78.8	127.3	0.62	0.559
Δt induction (h)	-0.96	5.3	-0.18	0.862

Multiple R-squared: 0.73, adjusted R-squared: 0.56, F-statistic: 4.15, p-value: 0.06.

- b) L-ASNase activity as a function of the first-order effect of cultivation temperature (°C) alone.

	Estimate	Std. Error	t-value	p-value
(Intercept)	-4.45	143.4	-0.03	0.976
Temperature (°C)	25.5	5.43	4.7	0.001

Multiple R-squared: 0.71, adjusted R-squared: 0.68, F-statistic: 22.06, p-value: 0.001.

A second experimental design was then created for the optimization of the cultivation temperature and MeOH concentration, the second of which was included in this analysis because previous studies have indicated its importance for the expression of glycosylated proteins in *P. pastoris*, even though the screening experiments have not supported its statistical significance in our process. The model coefficients shown in Table 3 confirm that the MeOH concentration indeed has a very small and statistically insignificant effect on the L-ASNase activity. As shown in Figure 1 the optimal cultivation temperature is between 25°C and 35°C and the MeOH concentration has little to no effect on the process output.

Table 3. Analysis of variance (ANOVA) of the experimental design used for optimizing the cultivation temperature (°C) and MeOH concentration (%) for the production of L-ASNase in shaker flasks.

	Estimate	Std. Error	t-value	p-value
(Intercept)	-233.5	120	-1.94	0.148
Temperature (°C)	51.9	8.45	6.14	0.009
[MeOH] (%)	-1.71	24.0	-0.07	0.948
Temperature ² (°C ²)	-0.86	0.138	-6.23	0.008

Multiple R-squared: 0.93, adjusted R-squared: 0.86, F-statistic: 12.95, p-value: 0.03.

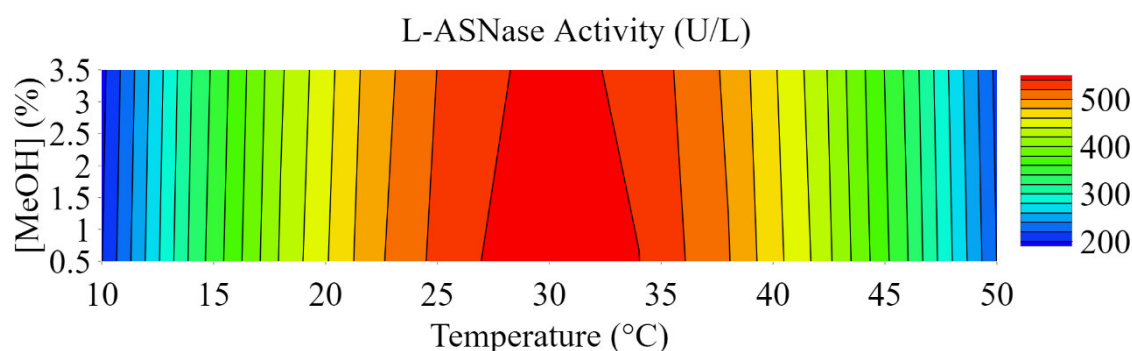


Figure 1. Response surface analysis of the L-ASNase activity as a function of cultivation temperature (°C) and MeOH concentration (%) plotted using plotly in R (<https://cran.r-project.org/web/packages/plotly/citation.html>).

In our previous study, we have found that L-ASNase was expressed as two different variants (Effer et al., 2020). When it was expressed in its higher molecular mass (Erw240), the enzymatic activity was not adequate for clinical application. Therefore, we have sought to express only the tetramer with one glycosylation site, which requires a careful selection of the cultivation temperature as reported by previous works (Woo et al., 2008; Donaldson et al., 1999).

As shown in Figure 2a, under the cultivation optimized conditions, ASNase activity reached 800 UL⁻¹ in the bioreactor after 24 h of cultivation. The parameters that were controlled during the production of L-ASNase in a bioreactor were agitation, temperature, available oxygen, and pH. Figure 2b shows the available oxygen profile and pH variation along the bioprocess.

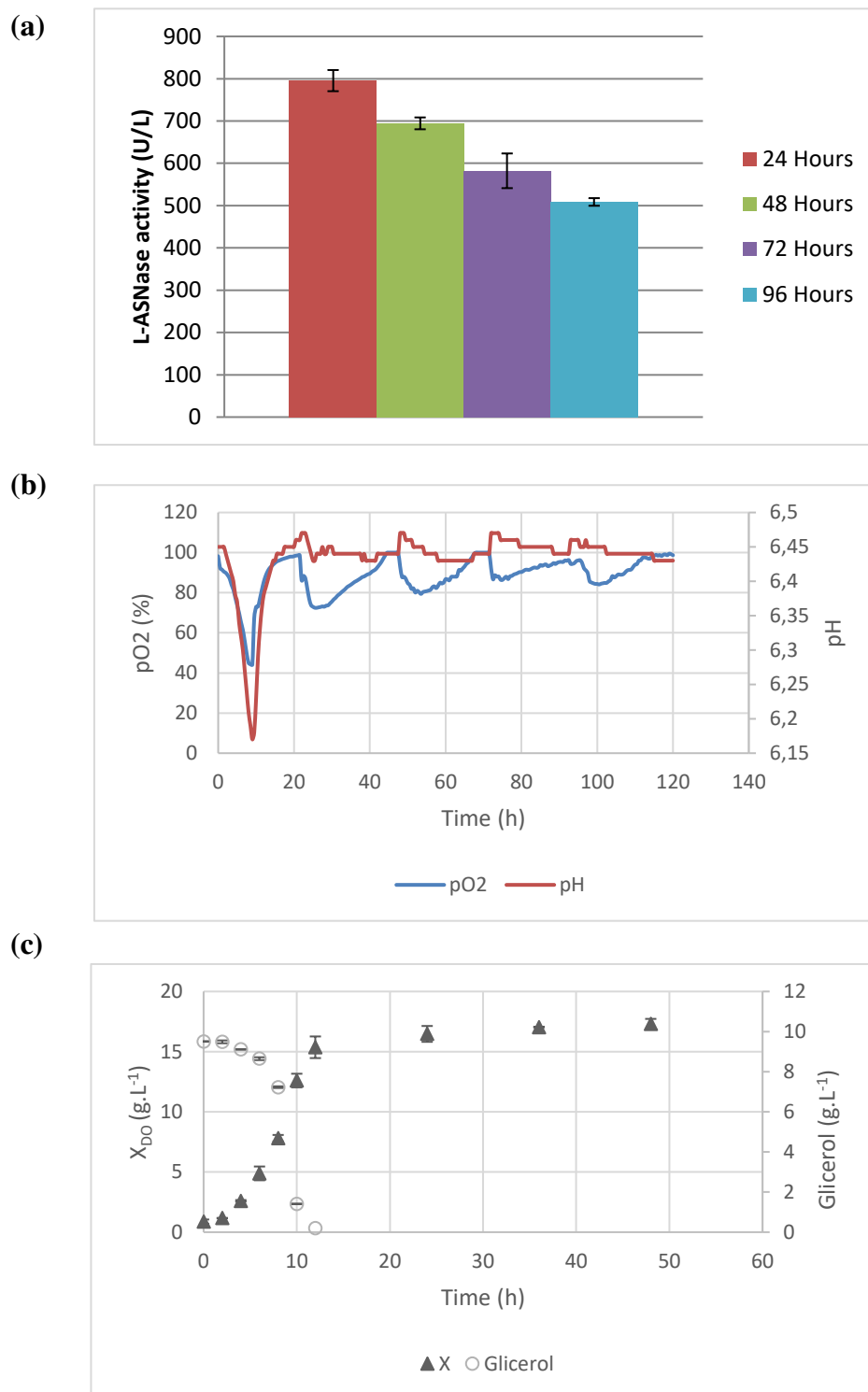
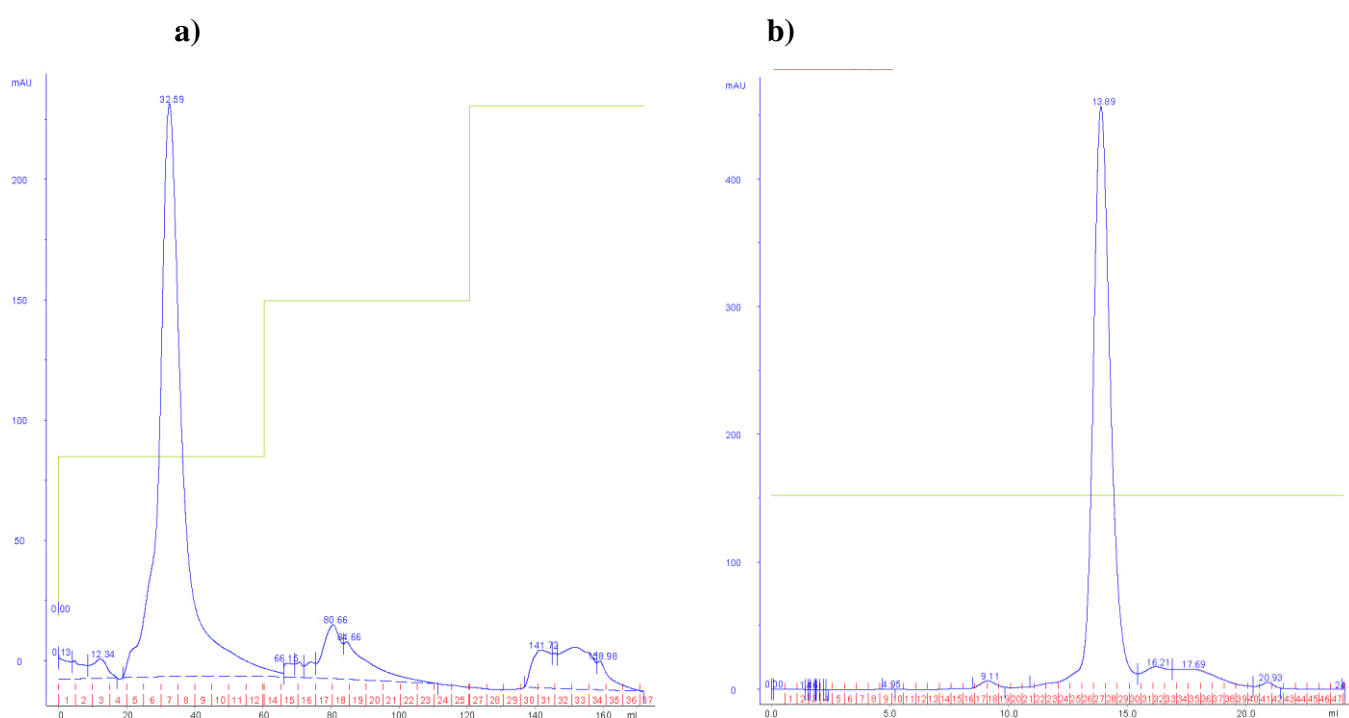


Figure 2. a) L-ASNase activity along 96 hours of batch cultivation. b) Profile of variation in pH and oxygen consumption by *Pichia pastoris* during glycosylated L-ASNase production under optimized cultivation conditions by batch mode. c) Cell growth and substrate consumption.

Figure 2b shows high demand for oxygen during the first 12 h of cultivation due to the exponential growth phase of the strain, which is corroborated by Figure 2c. A spike of oxygen concentration was noted at approximately 24 h after inoculation where the amount of oxygen available returns to nearly 100% when the exponential growth phase ended and the stationary phase began (Figure 2c). It was also observed that the pH decreased, albeit slightly, during the exponential growth phase. After 24 h, the pulse methanol feed began to induce L-ASNase expression, which coincides with a decrease in the oxygen concentration. This corroborates the conclusions derived from the first round of cultivation experiments using shaker flasks that showed that the period of induction Δt was not a relevant variable for L-ASNase production since protein production occurred for 24 h with a single methanol pulse.

Glycoproteins are promising in the biopharmaceutical field. The newly developed glycosylated L-ASNase can be seen in the chromatograms shown in Figure 3.



contaminate the product. After size exclusion chromatography (Figure 3b) we had a very well-resolved active peak and another fraction that showed low activity attributable to other L-ASNase proteoforms expressed in smaller amounts. It further shows an active L-ASNase peak eluted in a time corresponding to a 160 kDa protein, which suggests that the enzyme expressed in *P. pastoris Glycoswitch*[®] preserved the original tetrameric configuration of L-ASNase observed in *E. coli* and *E. chrysanthemi*.

Figure 4 shows the SDS-PAGE throughout the downstream process of our L-ASNase in which the increasingly concentrated and pure 40 kDa band can be observed, which corresponds to the glycosylated L-ASNase monomer. In our previous work, we have analyzed the L-ASNase presented in this research through mass spectrophotometry. We have found that this L-ASNase is glycosylated in the epitope ASN₁₇₀ with the glycan GlcNAc₂Man₇ (Effer et al., 2020).

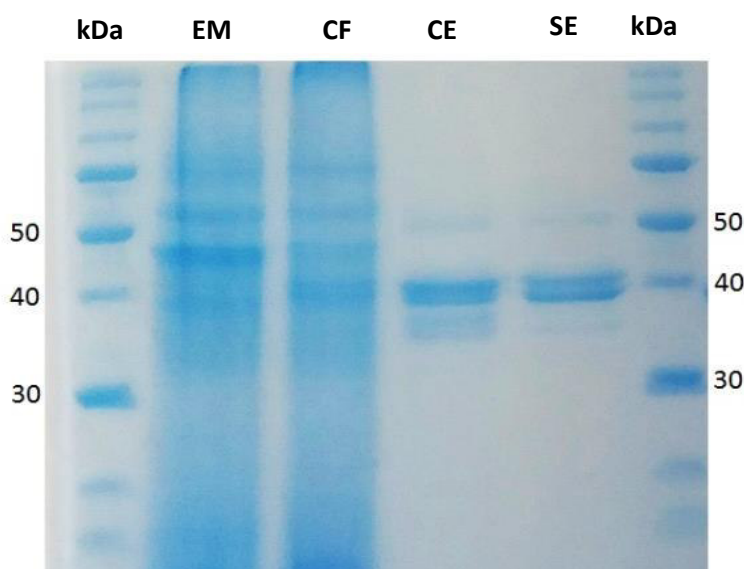


Figure 4. SDS-PAGE of glycosylated L-ASNase from each purification step: Extracellular Medium (EM); Crossflow filtration (CF); Cationic Exchange chromatography (CE); Size exclusion chromatography (SE).

It is well known that injectable biopharmaceuticals must have a very high purity to avoid undesirable side effects. Thus, to verify the purity of our L-ASNase after our downstream process, we performed proteomic analysis by LC-MS/MS to identify potential remaining contaminants. Table 4 shows the results of proteomics of the glycosylated L-ASNase after the purification process.

Table 4. Proteins identified by LC-MS/MS analyses from L-ASNase with human-like glycosylation pattern expressed extracellularly by recombinant *Pichia pastoris* after protein purification.

Accession	Identified protein	Spectral peptides count	kDa
ASPG_DICCH	L-Asparaginase	212	38
TRY1_BOVIN	Cationic trypsin	18	26
ACTB_XENLA	Cluster of actin	8	42

Given the absence of contaminating proteins in the final purified fraction, we can conclude that our process yielded an extremely pure protein after downstream processing. The contaminants detected by the proteomic analysis come from the sample preparation. Therefore, our purification process is significantly better than the ones currently used for commercial production, having the potential for scaling up and eventually reaching the market after clinical trials. Recently, Zenatti and collaborators (2018) performed a similar analysis by LC-MS/MS of the impurities from the two L-ASNases available in the Brazilian market used to treat ALL. Their findings had shown a very high amount of impurities in Leuginase® in contrast to the impurities from Aginasa® (Zenatti et al., 2018).

While biopharmaceutical product purity is critical in process development, the process yield is just as relevant in an industrial production setting. Hence, we evaluated the L-ASNase yield and enrichment after each step of the downstream process (shown in Tables 5a and 5b) for the two purification strategies tested.

Table 5a. Purification process of L-ASNase with human-like glycosylation pattern expressed extracellularly by recombinant *Pichia pastoris* using a 10 kDa cassette during crossflow filtration (strategy 1).

Purification steps	Volume (mL)	Activity (U/mL)	[Total Proteins] mg/mL	Total Activity (IU)	Total Proteins (mg)	Specific Activity (U/mg)	Purification fold	Yield (%)
Extracellular Medium	700	1.45	0.25	1014.62	178.29	5.69	1	100
Crossflow filtration and diafiltration	140	5.22	0.33	731.29	45.91	15.93	2.80	72.08
Cationic exchange chromatography	1.25	332.91	2.60	416.14	3.25	128.04	22.50	41.01
Size exclusion chromatography	1.5	265.92	1.05	398.88	1.58	253.26	44.50	39.31

Table 5b. Purification process of L-ASNase with human-like glycosylation pattern expressed extracellularly by recombinant *Pichia pastoris* using a 300 kDa cassette before the 10 kDa cassette during crossflow filtration (strategy 2).

Purification steps	Volume (mL)	Activity (U/mL)	Total Proteins mg/mL	Total Activity (IU)	Total Proteins (mg)	Specific activity (U/mg)	Purification fold	Yield (%)
Extracellular medium	500	3.49	0.52	1743.46	260.33	6.70	1	100
Cross flow filtration and diafiltration	85	20.14	1.03	1712.07	87.29	19.61	2.93	98.20
Cationic Exchange Chromatography	1.83	539.54	1.76	987.32	3.22	307.09	45.85	56.63
Size Exclusion Chromatography	4	239.43	0.50	957.74	2.02	475.03	70.93	54.93

Tables 5a and 5b show a loss of approximately 28% of the enzyme activity and a yield of 72.08% after strategy 1, while strategy 2 resulted in 98.20 % recovery of the enzyme. In both cases, the enzyme is unlikely to have been lost to the permeate since this fraction did not present detectable L-ASNase activity and the molecular weight of the enzyme is over one order of magnitude larger than the 10kDa membrane pore-size. However, this loss can be attributed to protein adsorption on the membrane.

Given a possible loss resulting from the use of the filter in conventional filtration (strategy 1), we decided to change the clarification steps prior to crossflow filtration. Thus, centrifugation and conventional filtration were excluded and crossflow filtration with a 300 kDa cut-off membrane was adopted. Since the protein was approximately 140 to 160 kDa, using strategy 2, we first collected the permeate from this step, and then this permeate went through crossflow filtration using a 10 kDa cassette.

The clarification steps prior to crossflow filtration are necessary because we need to ensure complete removal of cells from the extracellular medium (where L-ASNase is contained) to avoid column clogging in the later stage of cation exchange chromatography. From Table 5a and 5b, we can notice that the overall yields of the purification processes were 39.31% and 54.93% for strategies 1 and 2, respectively.

In table 5a, we can also observe that there was a loss of 31.07% and 41.57% after cation exchange chromatography. However, no enzymatic activity was detected in the column outlet during the loading, thus ruling out the possibility that the column was saturated.

After adopting strategy 2 as a protocol, we evaluated the recovery and yield factor with the 30 and 100 kDa cassettes. The results are provided in Table 6.

Table 6. Evaluation of purification fold and final yield of the downstream process from the glycosylated L-ASNase through crossflow filtration using cassettes with variable cut-off sizes.

Cut off (kDa)	Purification fold	Final yield (%)
10 (strategy 1)	44.50	39.31
10 (strategy 2)	70.93	54.93
30 (strategy 2)	102.65	45.17
100 (strategy 2)	45.85	15.88

From Table 6 we can conclude that the strategy with the highest yield was strategy 2 using the 10 kDa diameter cut-off cassette. Using the 100 kDa cassette we had the highest loss. Interestingly, using the 30 kDa cassette we obtained a lower yield, but also the highest purification factor among all the studied conditions. This difference can be explained because the membrane pore size is an average of the value indicated by the manufacturer, however, there may be few pores with a larger diameter than that indicated by the manufacturer, thus explaining this significant loss when the 100 kDa cassette was employed.

In a study conducted by De Castro Girão and collaborators (2016), a glycosylated L-ASNase obtained from *S. cerevisiae* was expressed in *P. pastoris*. The authors firstly employed size exclusion chromatography, and then ion-exchange chromatography (MONO-Q). A single active peak in molecular exclusion and four active peaks in cation exchange were obtained, which, according to the authors, were attributed to different proteoforms related to different post-translational modifications. The final yield of the process and the specific activity obtained were, respectively, 51.3 % and 204.4 U_{mg}⁻¹ (De Castro Girão et al., 2016).

Lopes and coauthors (2019) found an estimated weight for their L-ASNase of 178 kDa after gel filtration. The final yield reached by the authors after affinity chromatography was 11.4% with a specific activity of 5.4 U_{mg}⁻¹ from a L-ASNase from *S. cerevisiae* expressed in *E. coli* (Lopes et al., 2019).

Studies undertaken by Kante and collaborators (2018) evaluated the production and purification of recombinant human asparaginase expressed in *E. coli* by crossflow filtration at different temperatures (22, 25, and 28 °C) and transmembrane pressures (12, 16, 20 and 25 psi). They reported that using 12 and 16 psi transmembrane pressure provided a process yield of 70% and 74%, respectively (Kante et al., 2018). The

recombinant human asparaginase was purified using cation exchange chromatography (SP-Sepharose FF) in gradient mode elution and resulted in a 51% yield and specific activity of 200 U mg^{-1} (Kante et al., 2018). Their findings corroborate with our yield of 72.08% using 15 psi transmembrane pressure and the same membrane pore size 10 kDa as in the present study.

Other studies reported the recovery of L-ASNase from *Bacillus lincheniformis* by ultrafiltration, reaching a 94.81% yield (Mahajan et al., 2014). Since ultrafiltration is a process involving pressure action, the optimal transmembrane pressure (TMP) filtration operation is also very important to protect the protein's native structure. The lower recovery yield may be due to the formation of protein aggregates caused by the high pressure drop of the solution feed in the membrane (Kante et al., 2018).

Trang and coauthors (2016) studied the purification of L-ASNase from *E. chrysanthemi* expressed by *E. coli*, and after two chromatographic steps (Sephacryl and DEAE) the authors obtained a final yield of 17.8% with a specific activity of 312.8 U mg^{-1} (Trang et al., 2016). Another study obtained an 86% of yield and a specific activity of 190 U mg^{-1} using affinity chromatography from an extracellularly L-ASNase expressed in *E. coli* (Kushoo et al., 2004).

Other studies employed anionic exchange chromatography (DEAE column) and size exclusion chromatography to purify a L-ASNase from *E. coli* and obtained 50.8% and 190 U mg^{-1} of final yield and specific activity (Upadhyay, et al 2014).

Our findings, shown after cation exchange and size exclusion chromatography, provided a specific activity of 128.04 U mg^{-1} , 253.26 U mg^{-1} , respectively, and a yield of 56.63% and 54.93%, respectively. Table 7 summarizes the yield and specific activities reported in the literature from the purification process of other recombinant L-ASNase and in the present work.

Table 7. Final yield and specific activity of different recombinant L-ASNase reported in the literature.

L-ASNase source	Purification Methodology	Specific activity (U/mg)	Final yield (%)	Reference
<i>Escherichia coli</i>	Cross flow filtration and cationic exchange	200.0	51.0	Kante et al, 2018
<i>Bacillus lincheniformis</i>	Cross flow filtration, precipitation, ionic exchange, size exclusion	697.1	33.0	Mahajan et al, 2014
<i>Escherichia coli</i>	Anionic exchange and size exclusion	190.0	50.8	Upadhyay et al, 2014
<i>Erwinia chrysanthemi</i> expressed by <i>Escherichia coli</i>	Anionic exchange	312.8	17.8	Trang et al, 2016
<i>Escherichia coli</i>	Affinity chromatography	190.0	86.0	Khushoo et al 2004
<i>Saccharomyces cerevisiae</i> expressed by <i>Escherichia coli</i>	Affinity chromatography	5.4	11.4	Lopes et al 2019
<i>Saccharomyces cerevisiae</i> expressed by <i>Pichia pastoris</i>	Cross flow filtration, size exclusion, anionic exchange	204.4	51.3	Girão et al, 2016
<i>Erwinia chrysanthemi</i> expressed by <i>Pichia pastoris</i>	Cross flow filtration, cationic exchange, size exclusion	475.0	54.9	This work

Finally, we analyzed the cytotoxic effect of these mutant L-ASNase against two commonly used ALL cell lines, MOLT-4 and Jurkat, which have different genotypes, phenotypes, and different described sensitivities to ASNase (Figure 5). Our results show that the MOLT-4 lineage was more sensitive to L-ASNase than Jurkat (MOLT-4 IC₅₀ = 0.3 unit/mL; Jurkat IC₅₀ = 0.6 unit/mL). After 72 h, we detected reductions of 65% and 44% in the cell viability of the MOLT-4 and Jurkat lines, respectively. Therefore, glycosylation preserved L-ASNase cytotoxic activity against these leukemic lines. These outcomes corroborate as described by Rodrigues and collaborators (2020) that found the IC₅₀ for the MOLT-4 cell line was 0.29 U/mL for their recombinant L-ASNases and the IC₅₀ for the Jurkat lineage for one of their proteoforms was also 0.60 U/mL.

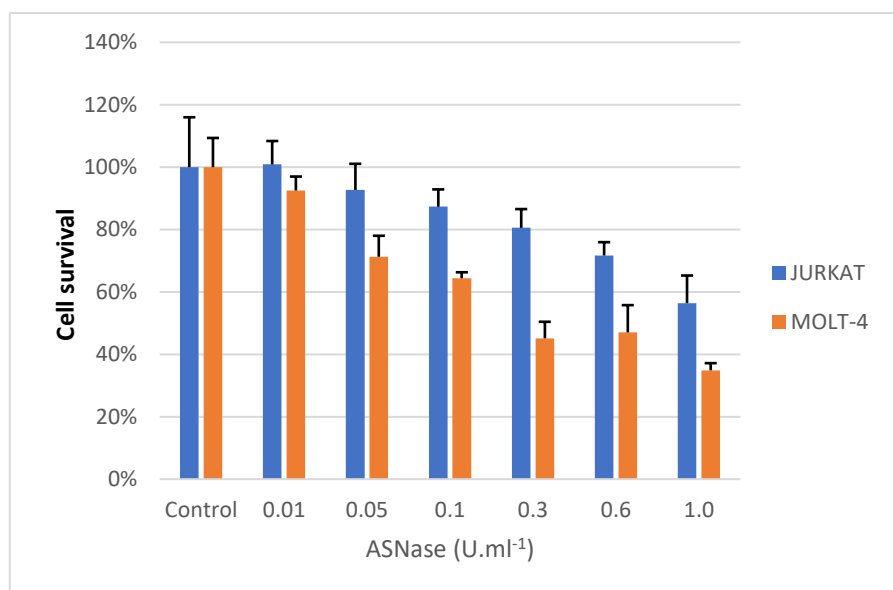


Figure 5. Cell viability of ALL cell lines treated with glycosylated L-ASNase. Cytotoxicity was evaluated by the MTT reduction test. The cells were incubated with 6 concentrations (0.01, 0.05, 0.1, 0.3, 0.6 and 1 U/mL) of ASNase at 37 °C for 72 h (MOLT-4 and JURKAT cell lines) and analysed spectrophotometrically after MTT reduction.

4. Conclusion

In summary, the newly identified recombinant glycosylated L-ASNase had shown a higher expression level when the bioprocess was conducted under 35 °C and 1.5% (v/v) of methanol during the induction phase in a 3 L benchtop bioreactor. In addition, we successfully identified the bottlenecks of the downstream process and optimized the crossflow filtration achieving 98.20 % of yield in this step and a final yield of 54.90 with a specific activity of 475 Umg⁻¹. The proteomics data suggested that under the optimized purification conditions it is possible to obtain a protein with fewer contaminants than the presented in Aginasa®.

References

- Apolinário, A.C., Magoñ, M.S., Pessoa, A., Rangel-Yagui, C. de O., 2018. Challenges for the self-assembly of poly(Ethylene glycol)-poly(lactic acid) (PEG-PLA) into polymersomes: Beyond the theoretical paradigms. *Nanomaterials* 8. <https://doi.org/10.3390/nano8060373>
- Avramis, V.I., 2012. Asparaginases: Biochemical pharmacology and modes of drug resistance. *Anticancer Res.*
- Brumano, L.P., da Silva, F.V.S., Costa-Silva, T.A., Apolinário, A.C., Santos, J.H.P.M., Kleingesinds, E.K., Monteiro, G., Rangel-Yagui, C. de O., Benyahia, B., Junior, A.P., 2019. Development of L-asparaginase biobetters: Current research status and review of the desirable quality profiles. *Front. Bioeng. Biotechnol.* <https://doi.org/10.3389/fbioe.2018.00212>
- De Castro Girão, L.F., Da Rocha, S.L.G., Sobral, R.S., Dinis Ano Bom, A.P., Franco Sampaio, A.L., Da Silva, J.G., Ferrara, M.A., Da Silva Bon, E.P., Perales, J., 2016. *Saccharomyces cerevisiae* asparaginase II, a potential antileukemic drug: Purification and characterization of the enzyme expressed in *Pichia pastoris*. *Protein Expr. Purif.* 120, 118–125. <https://doi.org/10.1016/j.pep.2015.12.012>
- De Pourcq, K., De Schutter, K., Callewaert, N., 2010. Engineering of glycosylation in yeast and other fungi: Current state and perspectives. *Appl. Microbiol. Biotechnol.* 87, 1617–1631. <https://doi.org/10.1007/s00253-010-2721-1>
- Drainas, C., Kinghorn, J.R., Pateman, J.A., 1977. Aspartic hydroxamate resistance and asparaginase regulation in the fungus *Aspergillus nidulans*. *J. Gen. Microbiol.* 98, 493–501. <https://doi.org/10.1099/00221287-98-2-493>
- Effer, B., Kleingesinds, E.K., Lima, G.M., Costa, I.M., Sánchez-Moguel, I., Pessoa, A., Santiago, V.F., Palmisano, G., Farías, J.G., Monteiro, G., 2020. Glycosylation of Erwinase results in active protein less recognized by antibodies. *Biochem. Eng. J.* 163. <https://doi.org/10.1016/j.bej.2020.107750>
- Effer, B., Meira, G., Cabarca, S., Pessoa, A., Farias, J., Monteiro, G., 2019. L-asparaginase from *E. chrysanthemi* expressed in Glycoswitch: Effect of His-tag fusion on the extracellular expression. *Prep. Biochem. Biotechnol.* 0, 1–7. <https://doi.org/10.1080/10826068.2019.1599396>
- Hopkins, D., Gomathinayagam, S., Rittenhour, A.M., Du, M., Hoyt, E., Karaveg, K., Mitchell, T., Nett, J.H., Sharkey, N.J., Stadheim, T.A., Li, H., Hamilton, S.R., 2011. Elimination of β -mannose glycan structures in *Pichia pastoris*. *Glycobiology* 21, 1616–1626. <https://doi.org/10.1093/glycob/cwr108>
- Inaba, H., Greaves, M., Mullighan, C.G., 2013. Acute lymphoblastic leukaemia. *Lancet.* [https://doi.org/10.1016/S0140-6736\(12\)62187-4](https://doi.org/10.1016/S0140-6736(12)62187-4)
- Kante, R.K., Vemula, S., Somavarapu, S., Mallu, M.R., Boje Gowd, B.H., Ronda, S.R., 2018. Optimized upstream and downstream process conditions for the improved production of recombinant human asparaginase (rhASP) from *Escherichia coli* and its characterization. *Biologicals* 56, 45–53. <https://doi.org/10.1016/j.biologicals.2018.10.002>
- Khushoo, A., Pal, Y., Singh, B.N., Mukherjee, K.J., 2004. Extracellular expression and single step purification of recombinant *Escherichia coli* l-asparaginase II. *Protein Expr. Purif.* 38, 29–36. <https://doi.org/10.1016/j.pep.2004.07.009>
- Lopes, W., Santos, B.A.F. dos, Sampaio, A.L.F., Gregório Alves Fontão, A.P., Nascimento, H.J., Jurgilas, P.B., Torres, F.A.G., Bon, E.P. da S., Almeida, R.V., Ferrara, M.A., 2019. Expression, purification, and characterization of asparaginase II from *Saccharomyces cerevisiae* in *Escherichia coli*. *Protein Expr. Purif.* 159, 21–26. <https://doi.org/10.1016/j.pep.2019.02.012>
- Mahajan, R. V., Kumar, V., Rajendran, V., Saran, S., Ghosh, P.C., Saxena, R.K., 2014. Purification and characterization of a novel and robust L-asparaginase having low-glutaminase activity from *Bacillus licheniformis*: In vitro evaluation of anti-cancerous properties. *PLoS One* 9. <https://doi.org/10.1371/journal.pone.0099037>
- Nomme, J., Su, Y., Konrad, M., Lavie, A., 2012. Structures of apo and product-bound human l-asparaginase: Insights into the mechanism of autoproteolysis and substrate hydrolysis. *Biochemistry.* <https://doi.org/10.1021/bi300870g>
- Olsson, L., Nielsen, J., 1997. On-line and in situ monitoring of biomass in submerged cultivations. *Trends*

Biotechnol. [https://doi.org/10.1016/S0167-7799\(97\)01136-0](https://doi.org/10.1016/S0167-7799(97)01136-0)

- Pourhossein, M., Korbekandi, H., 2014. Cloning, expression, purification and characterisation of *Erwinia carotovora* L-asparaginase in *Escherichia coli*. *Adv. Biomed. Res.* <https://doi.org/10.4103/2277-9175.127995>
- Pui, C.H., Evans, W.E., 2013. A 50-year journey to cure childhood acute lymphoblastic leukemia. *Semin. Hematol.* <https://doi.org/10.1053/j.seminhematol.2013.06.007>
- Rodrigues, M.A.D., Pimenta, M. V., Costa, I.M., Zenatti, P.P., Migita, N.A., Yunes, J.A., Rangel-Yagui, C.O., de Sá, M.M., Pessoa, A., Costa-Silva, T.A., Toyama, M.H., Breyer, C.A., de Oliveira, M.A., Santiago, V.F., Palmisano, G., Barbosa, C.M.V., Hebeda, C.B., Farsky, S.H.P., Monteiro, G., 2020. Influence of lysosomal protease sensitivity in the immunogenicity of the antitumor biopharmaceutical asparaginase. *Biochem. Pharmacol.* 182. <https://doi.org/10.1016/j.bcp.2020.114230>
- Skropeta, D., 2009. The effect of individual N-glycans on enzyme activity. *Bioorganic Med. Chem.* <https://doi.org/10.1016/j.bmc.2009.02.037>
- Torres-Obreque, K., Meneguetti, G.P., Custódio, D., Monteiro, G., Pessoa-Junior, A., de Oliveira Rangel-Yagui, C., 2019. Production of a novel N-terminal PEGylated crisantaspase. *Biotechnol. Appl. Biochem.* 66, 281–289. <https://doi.org/10.1002/bab.1723>
- Trang, T.H.N., Cuong, T.N., Thanh, S.L.N., Tuyen, T. Do, 2016. Optimization, purification and characterization of recombinant L-asparaginase II in *Escherichia coli*. *African J. Biotechnol.* 15, 1681–1691. <https://doi.org/10.5897/ajb2016.15425>
- Upadhyay, A.K., Singh, A., Mukherjee, K.J., Panda, A.K., 2014. Refolding and purification of recombinant L-asparaginase from inclusion bodies of *E. coli* into active tetrameric protein. *Front. Microbiol.* 5, 1–10. <https://doi.org/10.3389/fmicb.2014.00486>
- Vervecken, W., Kaigorodov, V., Callewaert, N., Geysens, S., De Vusser, K., Contreras, R., 2004. In vivo synthesis of mammalian-like, hybrid-type N-glycans in *Pichia pastoris*. *Appl. Environ. Microbiol.* <https://doi.org/10.1128/AEM.70.5.2639-2646.2004>
- Woo, S.A., Jeon, J.J., Jeong, Y.R., Seung, J.L., Sung, K.Y., 2008. Effect of culture temperature on erythropoietin production and glycosylation in a perfusion culture of recombinant CHO cells. *Biotechnol. Bioeng.* 101, 1234–1244. <https://doi.org/10.1002/bit.22006>
- Zenatti, P.P., Migita, N.A., Cury, N.M., Mendes-Silva, R.A., Gozzo, F.C., de Campos-Lima, P.O., Yunes, J.A., Brandalise, S.R., 2018. Low Bioavailability and High Immunogenicity of a New Brand of *E. coli* L-Asparaginase with Active Host Contaminating Proteins. *EBioMedicine.* <https://doi.org/10.1016/j.ebiom.2018.03.005>

Chapter 3

Biochemical, kinetical and thermodynamics characterization of the glycosylated L-ASNase

Abstract

The importance of L-ASNase as a biopharmaceutical product to treat Acute Lymphoblastic Leukemia (ALL) is recognized worldwide. Kinetical and biochemical properties are extremely important when a protein is used for therapeutical purposes because it is mandatory that a potential biopharmaceutical presents compatible parameters with the final patient (human or animal). Thermostability is also another main property required for biocatalysts by therapeutic proteins. It represents an important advantage in the manufacturing process and is critical to the success or failure in the development of a viable drug. In this sense, this chapter discloses about biochemical, kinetical, thermostability and thermodynamic parameters of this new glycosylated proteoform that can enable its use as a potential alternative for the treatment of ALL. At pH 8.0 and 50 °C the enzyme showed its optimum activity. Kinetic parameters, k_M and V_{max} of purified enzyme, with a specific activity of 302.02 Umg^{-1} , were found to be 7.64×10^{-5} M and $0.065 \mu mol \text{ min}^{-1}$, respectively. Thermostability was investigated by unfolding and refolding processes. The thermodynamic study showed that the enzyme irreversible deactivation is well described by first-order kinetics. Activation energy of the enzyme-catalysed reaction (E^*) was estimated to be 26.8 $kJ \text{ mol}^{-1}$. Half-life decreased progressively at high temperatures, and higher half-life was observed (4.85 h) at 50 °C. The activation energy of denaturation (E^*_d) was 120 $kJ \text{ mol}^{-1}$, which represents the required energy to overcome the energy barrier of the unfolding process. Finally, higher and positive values of ΔH and ΔG demonstrated higher structural stability of this novel L-ASNase. The outcomes of this work demonstrated that the glycosylated L-ASNase presents the appropriate biochemical parameters for therapeutical purposes and it is thermostable, particularly below 60 °C, which could be an important advantage for biopharmaceutical shelf-life storage, especially in countries with limited biotechnological investment and deficient cold chain.

Keywords: Michaelis-Menten constant. Enthalpy. Entrophy. Enzyme denaturation.

1. Introduction

The use of therapeutic proteins for human and animal health is a feat in itself. One key strategy in the field of enzymology is the study of kinetic and biochemical parameters. Establishing aspects underlying enzyme-catalyzed reactions, from substrate binding over the mechanism of rate acceleration, will facilitate obtaining the correct evaluation for therapeutic purposes (Rufer, 2021).

The Michaelis-Menten constant (k_M) is a measurable parameter for comparing enzyme affinity to a substrate. The lower the k_M value, the higher the enzyme affinity for that substrate and, in a therapeutic context, a more efficient enzyme (Beckett and Gervais, 2019). When there is a sufficiently low concentration of substrate, the catalytic sites of the enzyme are free to bind with it. The rate of the reaction catalyzed by the enzyme rapidly increases as the concentration of substrate increases. Once the catalytic sites of the enzyme are completely bound with a substrate, there is a plateau in the reaction velocity, which corresponds to the maximum reaction velocity (V_{max}). Thus, the substrate concentration is then sufficiently high that as soon as there is a free active site it quickly becomes bound again. The lower the enzyme affinity, the higher the concentration of substrate required to achieve a reasonable reaction velocity. Another important kinetic parameter is the turnover number (k_{cat}) which estimates the amount of substrate in which one enzyme can turn over into a product per second. Therapeutic proteins like L-ASNase must present a low k_M value and a high k_{cat} value (Rufer, 2021; Beckett and Gervais, 2019).

Protein stability has gained tremendous attention in the biopharmaceutical industry. Efficient stabilization strategies can potentially reduce efforts in protein manufacturing and formulation, increase the probability of success in the development of a viable drug as well as improve safety (Asial et al., 2013). Moreover, highly stable proteins are more cost-effective products. Thermodynamically unstable proteins occupy the unfolded states to a greater degree, and unfolded proteins are generally biologically inactive and more likely to generate immune responses (Rostad et al., 2017).

Previous studies described the complete characterization of protein thermostability based on two contributions: (i) the thermodynamic stability, defined as the difference in free energy between the folded and unfolded states (ΔG), and (ii) the thermal resistance, described by the melting temperature (T_m) (Miotto et al., 2019; Pucci et al., 2014; Souza et al., 2015). In this sense, thermostability is usually kinetically

modeled like a first-order deactivation reaction, which describes the enzyme irreversible inactivation (denaturation) and half-life ($t_{1/2}$) (Foo, 2003). Additionally, this kinetic model allows estimation of thermodynamic parameters such as Gibbs free energy, enthalpy, and entropy of irreversible inactivation, which are of paramount importance to understand the thermodynamic behavior of enzyme denaturation phenomenon (Santos et al., 2019).

Crisantaspase is the ASNase from *Erwinia chrysanthemi*, which was approved by the FDA in 2011 as the second therapeutic option to treat ALL (Chien et al., 2014). Although it has approximately twice the asparaginase activity of *E. coli* ASNase, its half-life is significantly shorter (10 h, compared to 30 h for the *E. coli* enzyme) (Avramis, 2012; Nguyen et al, 2016). In this sense, this chapter aimed to investigate the biochemical, kinetic and thermostability of the glycosylated L-ASNase. This study can contribute to the development of biobetters of this protein, as well as bring insights for other glycoprotein drugs.

2. Material and Methods

2.1. Optimum pH and temperature

To determine the optimum pH for protein activity, enzymatic assays were carried out by Nesslerization, as described above, at 37 °C in 50 mM of different buffers: acetate (pH: 4.0, 4.5, 5, 5.5); sodium phosphate (pH: 6.0, 6.5, 7.0, 7.5, 8.0); tris-HCl (pH: 8.5, 9.0); glycine-sodium hydroxide (pH: 9.5, 10.0). To determine the optimum temperature, enzymatic activity was measured by the same method at temperature range between 15-65 °C.

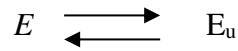
2.2. Kinetic parameters

The kinetic parameters of the purified proteins were determined by spectrophotometry using an adapted NADH-consumption-coupled assay (Balcão et al., 2001). The ammonia released during the reaction is used to produce glutamate in the presence of glutamate dehydrogenase (GDH) and reduced beta-nicotinamide adenine dinucleotide (β -NADH) (Sigma-Aldrich, Germany). NADH oxidation was measured spectrophotometrically at 340 nm at 37 °C. An extinction coefficient of $0.7516 \mu\text{mol}^{-1} \text{cm}^{-1}$ was used. Reactions were performed in 96-well microplate and contained 50 mM

sodium phosphate pH 7.5; 0.005 mM, 0.01 mM, 0.02 mM, 0.04 mM, 0.08 mM, 0.16 mM, 0.335 mM, 0.67 mM, 1.3 mM, 2.68 mM of either Asn or Gln, 0.13 mM β -NADH, 1 mM alfa-ketoglutarate, 1 U GDH (diluted in 50 mM sodium phosphate pH 7.4; 50 % glycerol) and 50 ng of L-ASNase. The substrate affinity and turnover number were determined using non-linear regression analysis of experimental steady-state data in GraphPad Prism version 5.0 software (GraphPad Software, Inc.).

2.3. Thermodynamic study

Thermal inactivation of enzymes can be described by an enzyme unfolding equilibrium (Converti et al., 2002):



where E and E_u are the folded and unfolded forms of the enzyme, respectively, related to a time-dependent irreversible denaturation and characterized by a first-order rate constant (k_d). At temperatures below the optimum temperature (T < T_{opt}), the equilibrium tends to the left side predominating the native or folded form, and the rate constant of the enzyme-catalysed reaction (k₀) is described by the Arrhenius model.

On the other hand, when T > T_{opt}, the equilibrium tends to the right side, predominating the unfolded form (Roels, 1983). This equilibrium model can be described by Eq. (1):

$$k_0 = \frac{A \exp \frac{-E^*}{RT}}{1 + B \exp \frac{-\Delta H_U^0}{RT}} \quad (1)$$

where E* is the activation energy of enzyme reaction; R the ideal gas constant (8.314 J K⁻¹ mol⁻¹); A and B the Arrhenius and an additional pre-exponential factor, respectively; and ΔH_U^0 the standard enthalpy variation of the inactivation equilibrium previously described. If the unfolded form of the enzyme is predominant, with temperature above the optimum one, Eq. (1) simplifies to Eq. (2):

$$k_0 = \frac{A}{B} \exp \frac{\Delta H_U^0 - E^*}{RT} \quad (2)$$

The E^* and ΔH_U^0 were estimated from the slopes of the straight lines of $\ln v_0$ vs. $1/T$, according to the Arrhenius equation and Eq. (2), respectively. For the enzyme irreversible thermo-inactivation (denaturation), the transition state theory was used (Glasstone et al., 1941). This process can be described by first-order reaction kinetics Eq. (3):

$$v_d = k_d E \quad (3)$$

where v_d is the rate of enzyme denaturation and E represents the active enzyme concentration measured as enzyme activity. k_d was estimated at each temperature from the slope of the straight line of $\ln \psi$ vs. time, where ψ is the activity coefficient, defined as the ratio between E and E_0 , i.e. the activity before exposition to temperature.

The activation energy of irreversible enzyme denaturation (E_d^*) was then estimated from the slope of the straight line of $\ln k_d$ vs. $1/T$. The enthalpy of activation (ΔH), Gibbs free energy of activation (ΔG) and entropy of activation (ΔS) of the thermal denaturation were finally estimated according to the Eqs. (4) to (6) (Melikoglu et al., 2013):

$$\Delta H = E_d^* - RT \quad (4)$$

$$\Delta G = -RT \ln \frac{k_d h}{k_B T} \quad (5)$$

$$\Delta S = \frac{\Delta H - \Delta G}{T} \quad (6)$$

where k_B and h are the Boltzmann and Planck constants, respectively.

Finally, the enzyme half-life ($t_{1/2}$), defined as the time of exposure required at a specific temperature to reduce E to one half of E_0 , was calculated by Eq. (7) (Zhou et al., 2016):

$$t_{1/2} = \frac{\ln 2}{k_d} \quad (7)$$

3. Results and Discussion

3.1. Optimum pH and temperature

The effect of pH on L-ASNase enzymatic activity was investigated at the range of pH between 4.0 – 12.0 and the temperature effect on L-ASNase enzymatic activity was measured at the range of 15.0 – 60.0 °C (Figure 1).

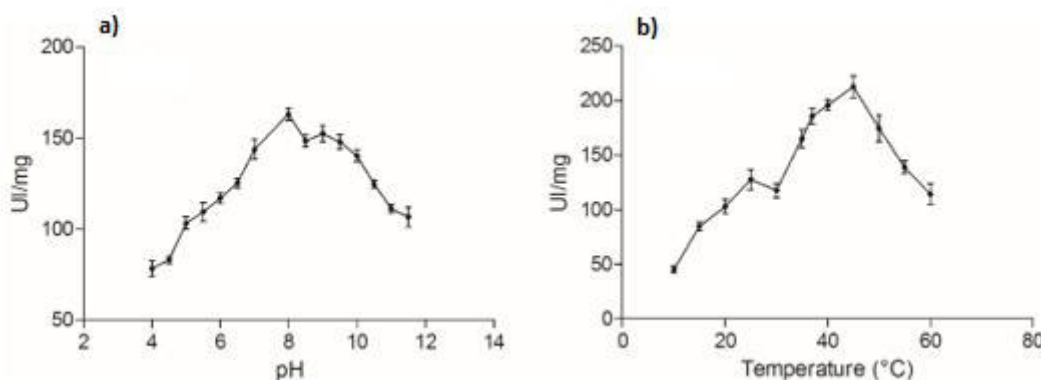


Figure 1. Evaluation of optimum a) pH and b) temperature of the glycosylated L-ASNase. Adapted from Effer et al, 2020.

From Figure 1 it is possible to observe that at the pH range between 7.0 - 10.0, the enzyme presented higher activity, being 8.0 the optimum pH for enzymatic activity and the optimum temperature was 50 °C. These data suggest that the glycosylated L-ASNase is suitable for therapeutic application under physiological conditions.

3.2. Kinetic parameters

The specific activity of the L-ASNase was calculated by the initial velocity of Asn or Gln hydrolysis as a function of enzyme concentration (Figure 2). When Asn was used as the substrate, the activity found was 302.02 U_{mg}⁻¹. The glutaminase specific activity was 7.5 % of L-ASNase activity.

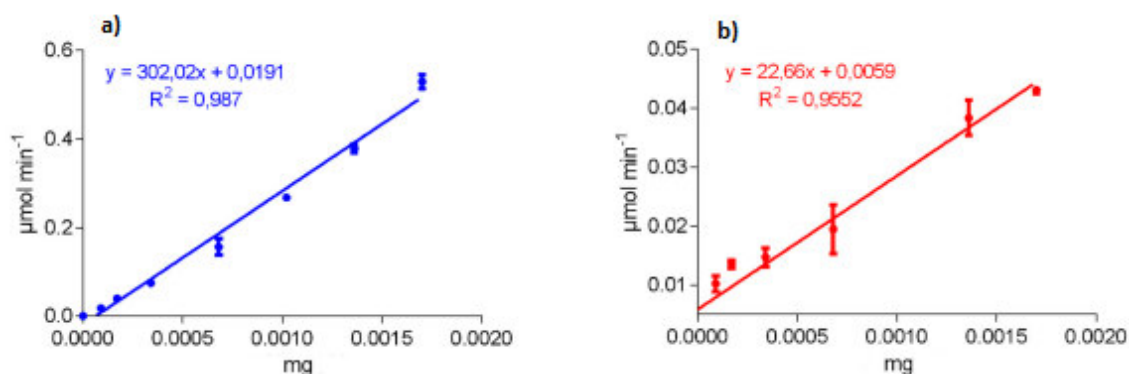


Figure 2. Determination of specific activity of the glycosylated L-ASNase for a) L-asparagine b) L-glutamine. Adapted from Effer et al., 2020.

The kinetic profile of glycosylated L-ASNase was investigated and the enzyme presented a Michaelian behavior. The Michaelis–Menten curves for the two substrates are presented in Figure 3 and the kinetic parameters are summarized in Table 1.

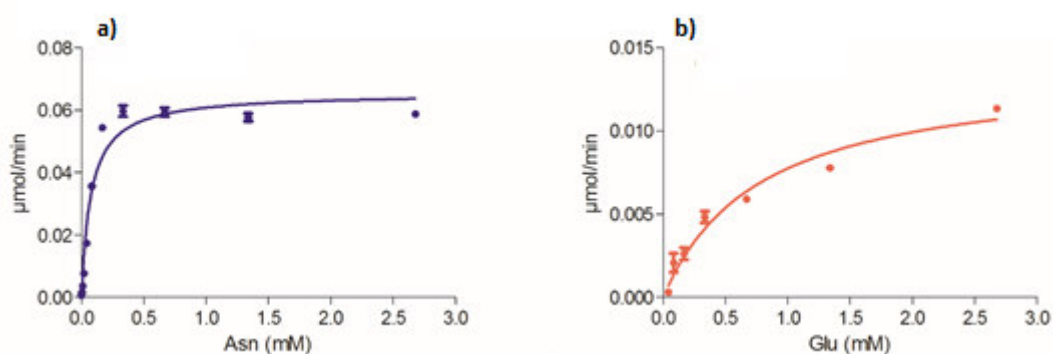


Figure 3. The kinetic parameters of the glycosylated L-ASNase were determined by coupled assay with NADH oxidation using different concentrations of either a) Asn or b) Gln as a substrate. Adapted from Effer et al., 2020.

Table 1. Kinetic parameters of the glycosylated L-ASNase.

L-Asparagine			L-Glutamine		
k_M (μM)	k_{cat} (s^{-1})	V_{max} ($\mu\text{mol min}^{-1}$)	k_M (M)	k_{cat} (s^{-1})	V_{max} ($\mu\text{mol min}^{-1}$)
76.4	58.96	0.065	7.8×10^{-4}	12.43	0.014

(Adapted from Effer et al., 2020).

Studies undertaken by Torres-Obreque and collaborators (2019) founded the k_M value for their PEGylated crisantaspase of 150 μM . This outcome is very interesting because the k_M of the glycosylated L-ASNase is 76.4 μM (Table 1) which means the affinity for Asn is two times higher than the PEGylated version. Albeit PEG tends to provide a more stable protein, the site where PEG is bound to the protein can interfere with its mobility, thus decreasing its affinity for a substrate.

3.3. Thermodynamic properties

The commercial L-ASNase are exposed to several stress factors during manufacturing and storage, among which temperature variation stands out as the main factor leading to protein denaturation. Evaluation of enzyme thermodynamic parameters is an elegant form to study denaturation with temperature. The thermodynamic parameters of the glycosylated L-ASNase was investigated at temperature range between 20.0 – 70.0 $^{\circ}\text{C}$, which was found that 50.0 $^{\circ}\text{C}$ was the temperature with the highest activity (T_{opt}). The semi-log plots of relative activity [$\ln(v_0/v_{\text{opt}})$] vs $1/T$ (Figure 4) show two different trends, below and above T_{opt} , following a typical Arrhenius behaviour.

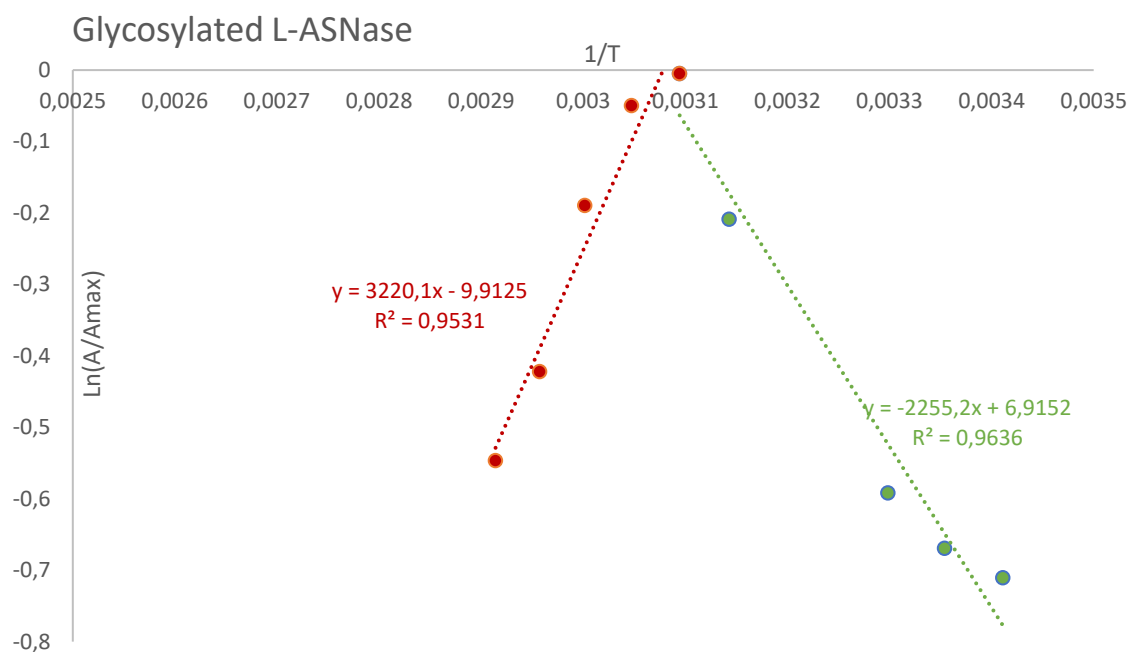


Figure 4. Arrhenius-type plots of relative activity of glycosylated L-ASNase.

A linear decrease can be observed at temperatures below 50 $^{\circ}\text{C}$, while higher temperatures led to an opposite trend corresponding to enzyme unfolding. Based on these results, the activation energy (E^*) of the enzyme-catalysed reaction was estimated in 26.8

kJ mol^{-1} . Low E^* value indicates that not much energy is required to convert L-Asn into L-aspartate and ammonium.

3.4. Thermostability and half-life

Residual activity tests were carried out as a function of time, in the temperature range 50–70 °C (Figure 5). The residual activities followed the typical first-order decay due to denaturation. The thermodynamic parameters of the irreversible denaturation process are summarized in Table 2.

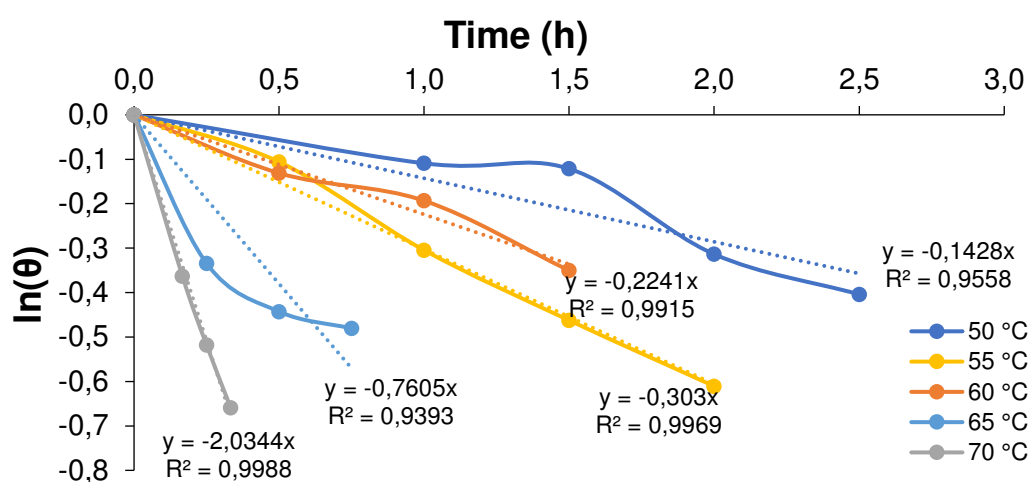


Figure 5. Semi-log plots of the residual enzymatic activity of glycosylated L-ASNase along the time.

Table 2. Thermodynamic and kinetic parameters of the irreversible thermal deactivation (denaturation) of glycosylated L-ASNase.

T(°C)	k_d (h^{-1})	$t_{1/2}$ (h)	ΔH^*_d (kJ/mol)	ΔG^*_d (kJ/mol)	ΔS^*_d (kJ/mol K)
50	0.14	4.85	119.46	14.14	1.46
55	0.22	3.09	119.48	13.43	1.59
60	0.30	2.29	119.51	12.46	1.74
65	0.76	0.91	119.52	11.77	1.84
70	2.03	0.34	119.54	10.98	1.87

As is well known, the half-life ($t_{1/2}$), which is the time required for the enzyme activity to drop down to 50% of the starting value at a given temperature, represents one of the main economic factors to be considered in many industrial applications. A high $t_{1/2}$

reflects long-term stability, especially during storage, and generally higher commercial potential of an enzyme drug. This parameter decreased progressively with increasing temperature, likely due to breaking of strong electrostatic and hydrogen bonds responsible for the enzyme secondary and/or tertiary structure (Almeida et al., 2020). In contrast, the first-order rate constant of enzyme thermoinactivation (k_d) increased with the temperature. At 50 °C the k_d value was 0.14 h^{-1} , while the estimated $t_{1/2}$ value was 4.85 h, thus demonstrating that glycosylation does not confer a wide thermoprotection effect for the enzyme.

The activation energy of denaturation (E^*_d) was $120.0 \text{ kJ mol}^{-1}$ ($R^2 > 0.941$) and it was estimated from the semi-log plot of $\ln(k_d)$ vs. $1/T$ (Figure 6). This parameter, which in the case of a protein represents the required energy to overcome the energy barrier that holds together the secondary and/or tertiary structure, thereby resulting in the irreversible point of denaturation.

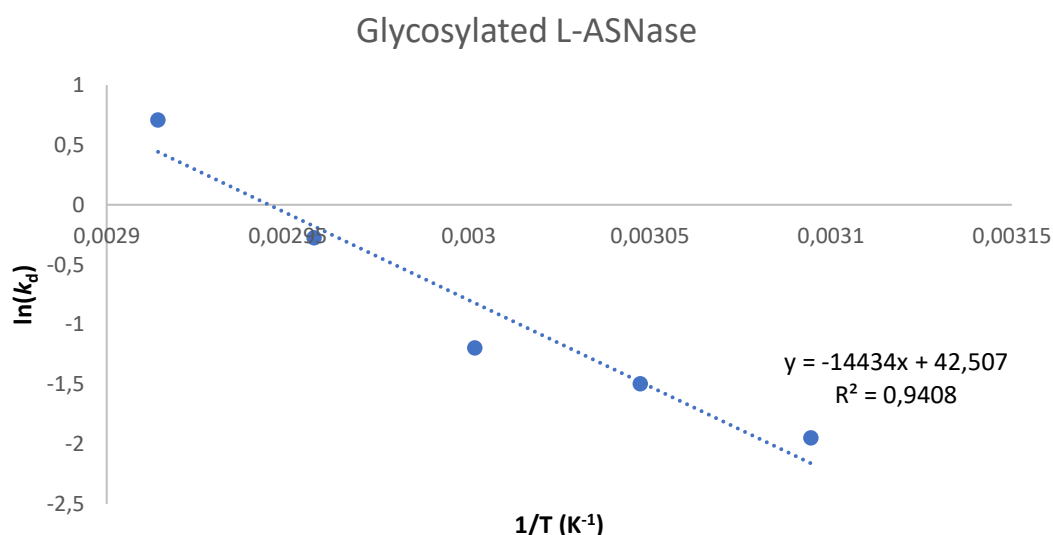


Figure 6. Semi-log plots of the first-order denaturation constant (k_d) vs. the reciprocal temperature ($1/T$). The slopes of the resulting straight lines were used to estimate the activation energie (E^*_d) of irreversible inactivation (denaturation).

Applying equations (4) – (6), the activation enthalpy (ΔH), Gibbs free energy (ΔG) and entropy (ΔS) of the glycosylated L-ASNase denaturation were also calculated (Table 1). These parameters are relevant to shed further light on the denaturation phenomenon (Chan et al., 2011). ΔH is an especially important thermodynamic parameter that expresses the total amount of energy required for enzyme denaturation (Marangoni, 2003) and has been proposed to be related to the breakdown of noncovalent bonds, including

hydrogen bonds and van der Waals forces (Melikoglu et al, 2013). Specifically, $\Delta H > 0$ indicates that the denaturation of the enzyme was exothermic.

On the other hand, ΔG relies to the spontaneity of the process based on the sum of enthalpic and entropic contributions; therefore, it allows more accurately predicting the stability of enzyme (Sousa et al., 2015). The positive value indicates that enzyme denaturation is a non-spontaneous event, as reported for other thermosensitive enzymes (Santos et al., 2019).

Finally, as for the entropy of the system, positive values of ΔS point to an increase in the randomness degree of the transition states compared to the starting enzymes. Protein thermal denaturation often implies positive ΔS values, especially for large proteins with a quaternary structure with more than one subunit such as the tetrameric protein investigated in the present study.

4. Conclusion

The outcomes of this chapter provide a basis for the design of enzyme-based biopharmaceuticals for future industrial and therapeutic use with the appropriate biochemical and kinetical parameters. Our results demonstrated that the glycosylated L-ASNase presents a high affinity for asparagine and its optimum activity at pH 8.0 and 50 °C. As for thermostability parameters, the half-life observed was 4.85 h, and the activation energy was estimated at 26.8 kJ mol⁻¹, which means the amount of required energy for denaturation. Likewise, higher positive values of ΔH and ΔG suggest higher resistance to denaturation and higher structural stability.

References

- Almeida GM, Mendonça CMN, Converti A, Oliveira RPS. Kinetic and thermodynamic parameters of nisin thermoinactivation. *J. Food Eng.* 280:109986. 2020. <https://doi.org/10.1016/j.jfoodeng.2020.109986>.
- Asial I, Cheng YX, Engman H, Dollhopf M, Wu B, Nordlund P, Cornvik T. Engineering protein thermostability using a generic activity-independent biophysical screen inside the cell, *Nat. Commun.* 4:2901.2013. <https://doi.org/10.1038/ncomms3901>.
- Avramis VI. Asparaginases: Biochemical pharmacology and modes of drug resistance, *Anticancer Res.* 32:2423–2437. 2012.
- Balção VM, Mateo C, Ferna R, Malcata FX. Structural and functional stabilization of L-sparaginase via multisubunit immobilization onto highly activated supports. *Biotechnol. Prog.* 17:537–542. 2001. <https://doi.org/10.1021/bp000163r>.
- Beckett A, Gervais D. What makes a good new therapeutic L-asparaginase? *World J Microbiol Biotechnol.* 24;35(10):152. 2019. doi: 10.1007/s11274-019-2731-9.

- Chan CH, Yu TH, Wong KB. Stabilizing salt-bridge enhances protein thermostability by reducing the heat capacity change of unfolding. *PLoS One*. 6(6):e21624. 2011. doi: 10.1371/journal.pone.0021624.
- Chien WW, Allas S, Rachinel N, Sahakian P, Julien M, Le Beux C, Lacroix CE, Abribat T, Salles G. Pharmacology, immunogenicity, and efficacy of a novel pegylated recombinant *Erwinia chrysanthemi*-derived L-asparaginase. *Invest. New Drugs*. 32:795–805. 2014. <https://doi.org/10.1007/s10637-014-0102-9>.
- Converti A, Del Borghi A, Gandolfi R, Lodi A, Molinari F, Palazzi E. Reactivity and stability of mycelium-bound carboxylesterase from *Aspergillus oryzae*. *Biotechnol Bioeng*. 2002 Jan 20;77(2):232-7. doi: 10.1002/bit.10124.
- Effer B, Kleingesinds EK, Lima GM, Costa IM, Sánchez-Moguel I, Pessoa A, Santiago VF, Palmisano G, Farias JG, Monteiro G. Glycosylation of Erwinase results in active protein less recognized by antibodies. *Biochemical Engineering Journal*. 163, 107750. 2020. <https://doi.org/10.1016/j.bej.2020.107750>.
- Foo Y. *Enzyme Kinetics: A Modern Approach*. A.G. Marangoni. New York: John Wiley & Sons, Inc., 244 pp., 89.95, hardcover. ISBN 0-471-15985-9., *Clin. Chem*. 49:838–838. 2003. <https://doi.org/10.1373/49.5.838>.
- Glasstone S, Laidler KJ, Eyring H. *The Theory of Rate Processes*, New York, 1941. <https://doi.org/10.1021/ed019p249.1>.
- Marangoni AG. *Enzyme Kinetics: A Modern Approach*, John Wiley & Sons, New Jersey, 2003. <https://doi.org/10.1002/0471267295>.
- Melikoglu M, Lin CSK, Webb C. Kinetic studies on the multi-enzyme solution produced via solid state fermentation of waste bread by *Aspergillus awamori*. *Biochem. Eng. J.* 80:76–82. 2013. <https://doi.org/10.1016/j.bej.2013.09.016>.
- Miotto M, Olimpieri PP, Di Rienzo L, Ambrosetti F, Corsi P, Lepore R, Tartaglia GG, Milanetti E. Insights on protein thermal stability: A graph representation of molecular interactions. *Bioinformatics*. 35:2569–2577. 2019. <https://doi.org/10.1093/bioinformatics/bty1011>.
- Nguyen HA, Su Y, Lavie A. Structural Insight into Substrate Selectivity of *Erwinia chrysanthemi* L-Asparaginase. *Biochemistry*. 55:1246–1253. 2016. <https://doi.org/10.1021/acs.biochem.5b01351>.
- Pucci F, Dhanani M, Dehouck Y, Rooman M. Protein thermostability prediction within homologous families using temperature-dependent statistical potentials. *PLoS One*. 9:e91659. 2014. <https://doi.org/10.1371/journal.pone.0091659>.
- Roles J. *Energetics and kinetics in biotechnology*, New York, 1983.
- Rostad CA, Stobart CC, Todd SO, Molina SA, Lee S, Blanco JCG, Moore ML. Enhancing the Thermostability and Immunogenicity of a Respiratory Syncytial Virus (RSV) Live-Attenuated Vaccine by Incorporating Unique RSV Line19F Protein Residues. *J. Virol*. 92:e01568-17. 2017. <https://doi.org/10.1128/jvi.01568-17>.
- Rufer AC. Drug discovery for enzymes. *Drug Discov Today*. 26(4):875-886. 2021. doi: 10.1016/j.drudis.2021.01.006.
- Santos JHP, Carretero G, Ventura SPM, Converti A, Rangel-Yagui CO. PEGylation as an efficient tool to enhance cytochrome c thermostability: a kinetic and thermodynamic study, *J. Mater. Chem. B*. 7:4432–4439. 2019. <https://doi.org/10.1039/C9TB00590K>.
- Souza PM, Aliakbarian B, Filho EX, Magalhães PO, Junior AP, Converti A, Perego P. Kinetic and thermodynamic studies of a novel acid protease from *Aspergillus foetidus*. *Int J Biol Macromol*. 81:17-21. 2015. doi: 10.1016/j.ijbiomac.2015.07.043.

- Torres-Obreque K, Meneguetti GP, Custódio D, Monteiro G, Pessoa-Junior A, de Oliveira Rangel-Yagui C. Production of a novel N-terminal PEGylated crisantaspase. *Biotechnol Appl Biochem*. 66(3):281-289. 2019. doi: 10.1002/bab.1723.
- Zhou JQ, He T, Wang JW. PEGylation of cytochrome c at the level of lysine residues mediated by a microbial transglutaminase. *Biotechnol Lett*. 38(7):1121-9. 2016. doi: 10.1007/s10529-016-2083-6.

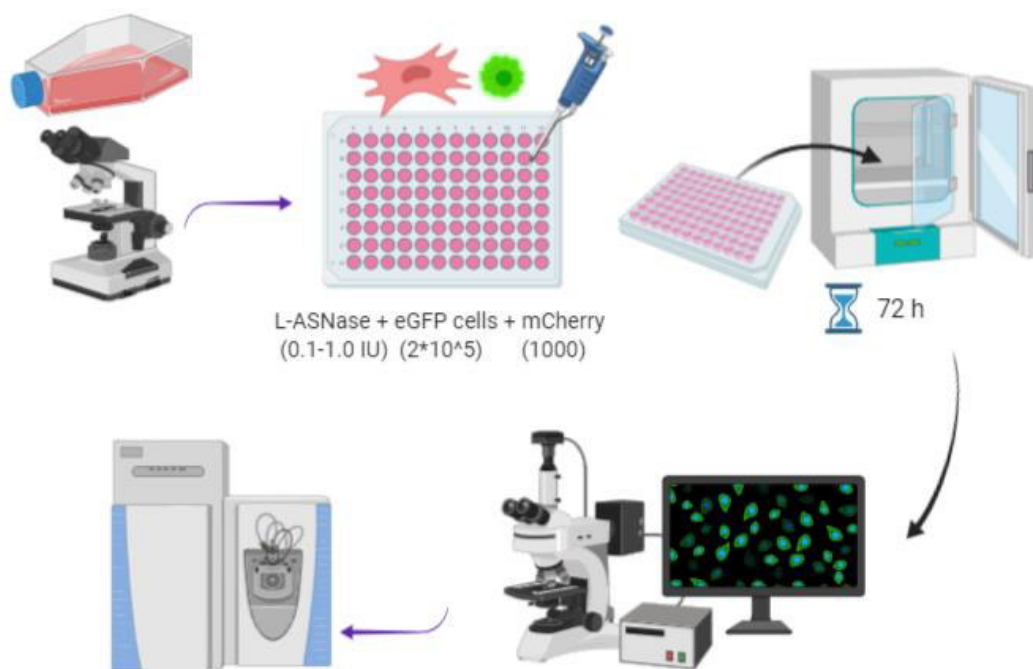
Chapter 4

Evaluation of the concomitant impact of a recombinant glycosylated L-asparaginase on ALL and AML cancer cells and the bone marrow tumour microenvironment using a high throughput fluorescent-based *in vitro* experimental platform

Abstract

ALL is a disorder of the immune system that is characterized by overproduction of immature lymphoblasts that, among some mutations, have become unable to synthesize the amino acid L-asparagine (Asn) and become dependent on this amino acid from the bloodstream. The response of the tumor microenvironment to anticancer drugs can influence treatment efficacy. This chapter investigated the concomitant impact of the glycosylated L-ASNase on ALL and AML and on the tumor microenvironment of leukemic cells. For this purpose, a fluorescence-based experiment model that employs the mCherry-labelled bone marrow fibroblastic stroma cells HS5, co-cultured with enhanced green fluorescent protein (eGFP)-labelled tumor cell lines was used. It was evaluated the eGFP-ALL cell proliferation, apoptosis, and adhesion on mCherryHS5. Cells were seeded in a 96 well plate to determine the effect of the recombinant protein on cell proliferation. In parallel, we seeded 96 well plates to analyze the effect of ASNases on cell viability by FACS analysis to determine the percentage of apoptotic cells. The outcomes showed that the eGFP-Hb11-19 and eGFP-SEMK2 cell lines were more susceptible for the action of L-ASNase. The treatment of the eGFP-REH cell line showed the lowest effectiveness, likely due to the production of cathepsin B, a lysosomal cysteine protease, by this cell line. The AML cell line eGFP-MV4-11 showed similar results to REH cells, suggesting that L-ASNase may also be used for AML treatment in addition to ALL. Finally, it was observed a lower effectiveness of the drug when tumour cells were co-culture with stromal cells than when tumour cells were cultured on their own. These data suggest that the microenvironment of stromal cells offer some cytoprotection to tumour cells against L-ASNase drug treatment.

Keywords: Bone marrow. Microenvironment. Co-culture models. Bioluminescence.



Graphical abstract. Schematic representation of the methodology used for image acquisition of ALL/AML cell cultures.

1. Introduction

Acute Lymphoid Leukaemia (ALL) represents the most frequently diagnosed leukemia in children and young adults (90%). In first world countries the rate of cure reach 80% for children and 50-60% for adults (Lopez-Millan et al., 2019; Brumano et al., 2019). Acute Myeloid leukaemia (AML) is a heterogeneous blood cancer and represents the most frequently diagnosed leukaemia in adults (25%) and accounts for 15–20% cases in children (Siveen et al., 2017). Despite continuous advance in the comprehension of AML prognosis, patients are still subject to a high rate of relapse (Siveen et al., 2017).

Leukemic stem cells (LSC) are a heterogeneous group of cells responsible for initiating and maintaining the disease (Michelozzi et al., 2019). Furthermore, the refractoriness of the LSC to conventional chemotherapies determines the relapse of leukemia (Siveen et al., 2017). This is due to the protection provided by mesenchymal stromal cells in the bone marrow (BM) microenvironment which works as a sanctuary where leukemic blasts and LSC can acquire a drug-resistant phenotype and evade the treatment (Michelozzi et al., 2019; Korn, 2017). In addition, we can find in BM mature immune cell types, such as T and B cells, dendritic cells, and macrophages, that play a protective role for leukemic cells environment (Michelozzi et al., 2019).

Among the main therapies used to treat ALL is L-Asparaginase (L-ASNase). Its mechanism consists of a starving mechanism where L-asparagine (Asn) and L-glutamine (Glu) are depleted from blood and BM (Steiner et al., 2012). Under deprived conditions of these two amino acids, the leukemic cells suffer apoptosis (Brumano et al., 2019).

Currently, the ASNase formulations available have challenges to overcome due to either side effects caused by impurities or by the immune system. According to Patel and collaborators (2009) therapy failure is caused by the inactivation of ASNase by cellular lysosomal cysteine proteases. It is important to pinpoint that microenvironmental cells, such as macrophages, can produce cathepsin B (CTSB) and contribute to ASNase turnover *in vivo* in mice (Michelozzi et al., 2019; Van Der Meer et al., 2014).

The anti-leukemic effect of L-ASNase has been extensively investigated in ALL, but only partially in AML (Michelozzi et al., 2019). Some specific subtypes of AML were reported to be more susceptible to ASNase as compared to others (Zwaan et al., 2000; Okada et al., 2003; Bertuccio et al., 2017). This is due to AML cells present a proclivity addiction in glutamine for their energetic and biosynthetic metabolism (Willems et al., 2013; Jacque et al., 2015; Matre et al., 2016). Hence, the efficacy of L-ASNase should be considered in future studies targeting AML cells.

According to the literature, co-culture models provide a highly relevant drug screening setting for testing L-ASNase as a possible therapeutic intervention in ALL since tumor stroma has been shown to be the major source for Asn to leukemic blasts (Lopez-Millan et al., 2019; Michelozzi et al., 2019).

Bioluminescence technology has been widely used to assess the therapeutic response of tumor cells under the protective influence of BM stroma in a high throughput setting (Ramasamy et al., 2012). By co-culturing m-Cherry HS5 BM fibroblast stroma cells and eGFP-expressing tumor cell lines that frequently originate in the BM, it is possible to evaluate these reciprocal effects by a robust platform. This platform can be scaled up to high throughput using 96 well plates and allows the concomitant assessment of both tumor and BM stroma response to anticancer drugs (Ramasamy et al., 2012). The well-known methodology that evaluates cell viability, the MTT (3-(4,5-Dimethylthiazol-2-yl)-2,5-diphenyltetrazolium bromide) assay, cannot discriminate between the stromal and tumor cell response in co-culture. Hence, this fluorescent-based co-culture methodology allows the evaluation of the reciprocal effect of the stromal cell and anticancer therapy on tumor cells (Ramasamy et al., 2012).

Based on the potential of the glycosylated L-ASNase expressed by *Pichia pastoris*, this chapter aimed to investigate the effect of the glycosylated L-ASNase on leukemic blasts, focusing on the role of different players of the BM microenvironment. The following Human eGFP-ALL cell lines were used in our experiments: Hb11-19, SEMK2 and REH. We also evaluated the action of L-ASNase on the eGFP-AML cell line MV4-11. The fibroblastic HS5 cell line transduced with the red fluorescent protein mCherry was used as a source of bone marrow stromal cells (Ramasamy et al., 2012). We analyzed eGFP-ALL and eGFP-AML cell proliferation, apoptosis and adhesion on mCherryHS5.

2. Materials and Methods

2.1. Enzyme production and purification

The glycosylated L-ASNase was produced using the BIOFLO™/CelliGen® 115 bioreactor (New Brunswick) containing 1 L of complex medium (BMGY) with potassium phosphate buffer (1M pH 6) at 35°C during 48 hours. To purify the protein, crossflow filtration was performed followed by cation exchange chromatography and size exclusion chromatography.

2.2. Enzymatic activity assay

Pure enzyme activity was estimated using the Nessler method, where 1 unit represents the release of 1 μ mol ammonia per minute. In a 96-well plate, 168 μ L Asn (44 mM), 148 μ L 50 mM Tris HCl buffer (pH 8.6), 37 μ L ultra-pure water, and 17 μ L sample were added. After 10 min incubating at 37°C, the reaction was stopped by adding 17 μ L of 1.5 M trichloroacetic acid. In another 96-well plate, 279 μ L of ultra-pure water, 37 μ L of Nessler's reagent, and 37 μ L of the previous reaction were added and the absorbances read at 440 nm in a plate reader SpectraMax (Molecular Devices). The absorbance measurement was then compared to the standard curve previously made with the Nessler reagent and ammonium sulfate at concentrations of 0.05, 0.1, 0.25, 0.5, 1.0, and 2.5 mM.

2.3. Cell culture

All e-GFP cell lines and the human fibroblast HS5 lineage were a kind gift from Dr Yolanda Calle (Roehampton University of London). m-Cherry-HS5 human stromal cell line were cultured in Dulbecco's modified Eagle medium with L-glutamax supplemented with 10 % of fetal bovine serum (FBS). The eGFP-ALL cell lines studies were SEMK2, Hb11-19 and REH. The eGFP-AML cell line studied was MV4-11. All tumor cell lines were cultured in RPMI-1640 medium supplemented with 10% of FBS. All cell lines were cultured at 37 °C in a humidified atmosphere in the presence of 5% of CO₂, 95% air.

2.4. Determination of cell proliferation and viability of tumor cells in co-culture with m-Cherry HS5 cells

m-Cherry fibroblastic stroma cells were seeded at 5×10^3 cells/per well in a 96-well plate and incubated overnight. GFP-positive cells were seeded alone or layered on m-Cherry HS5 cells in triplicate per condition (Figure 1). We evaluated the effect of 2 drug treatment plus untreated control of eGFP cells seeded alone or in co-culture with BM microenvironment cell after leaving blank wells for calculation of background values. The fluorescence intensity per well was read at 488 nm/528 nm and at 584 nm/607 nm to detect the numbers of e-GFP tumor cells and m-Cherry HS5 cells, respectively, using a FLx800 multidetector microplate reader (Biotek Instruments, Potton, Bedfordshire, UK) at day 0 and day 3. The proliferation index was calculated by dividing the fluorescence intensity in the same well at day 3/day0 after subtracting the average of the background values of the corresponding condition (eGFP cultured alone or in co-culture). The various tumor cell lines cultured alone or in co-culture were treated with concentrations of L-ASNase in the range of 0.1 - 1.0 UI.

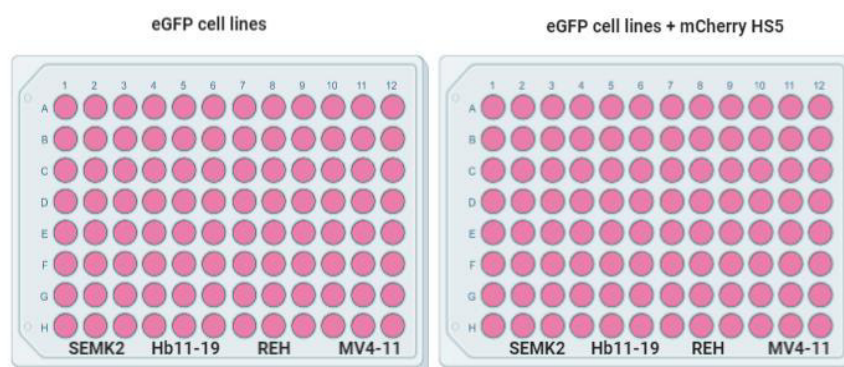


Figure 1. Evaluation of cytotoxicity of glycosylated L-ASNase using co-culture models with eGFP-ALL and eGFP-AML cell lines cultured by their own and co-cultured with BM mCherry HS5 cells.

2.5. Fluorescent Microscopy

Cells seeded in 96 well plates were imaged using an Elipse Nikon fluorescence microscope equipped with a motorised stage and an environmental chamber with controlled temperature and CO₂ levels. Images were captured and exported as JPEG files using NIS-Elements Nikon software.

2.6. Flow cytometry analysis

Cell suspensions of cultured cells were prepared at day 3 for fluorescence activated cell sorting (FACS) analysis using a BD Accuri flow cytometer. Analysis of FSS and SC as well as the levels of emission of fluorescence of eGFP ($\lambda_{excitation}$ 395 nm; $\lambda_{emission}$). Data were analysed using the BD Accuri C6 Analysis software.

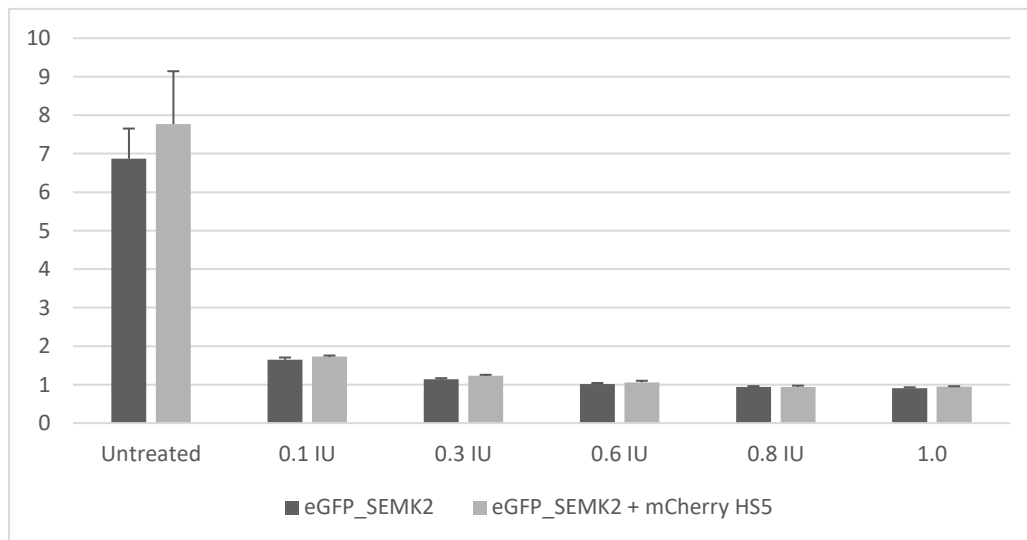
2.7. Intracellular amino acid quantification

Intracellular amino acids from Hb119, REH, and MV411 lineages were measured by UPLC-MS/MS using precolumn derivatization with 6-aminoquinolyl-N-hydroxysuccinimidyl carbamate (AccQTag kit) (Gray et al., 2017)

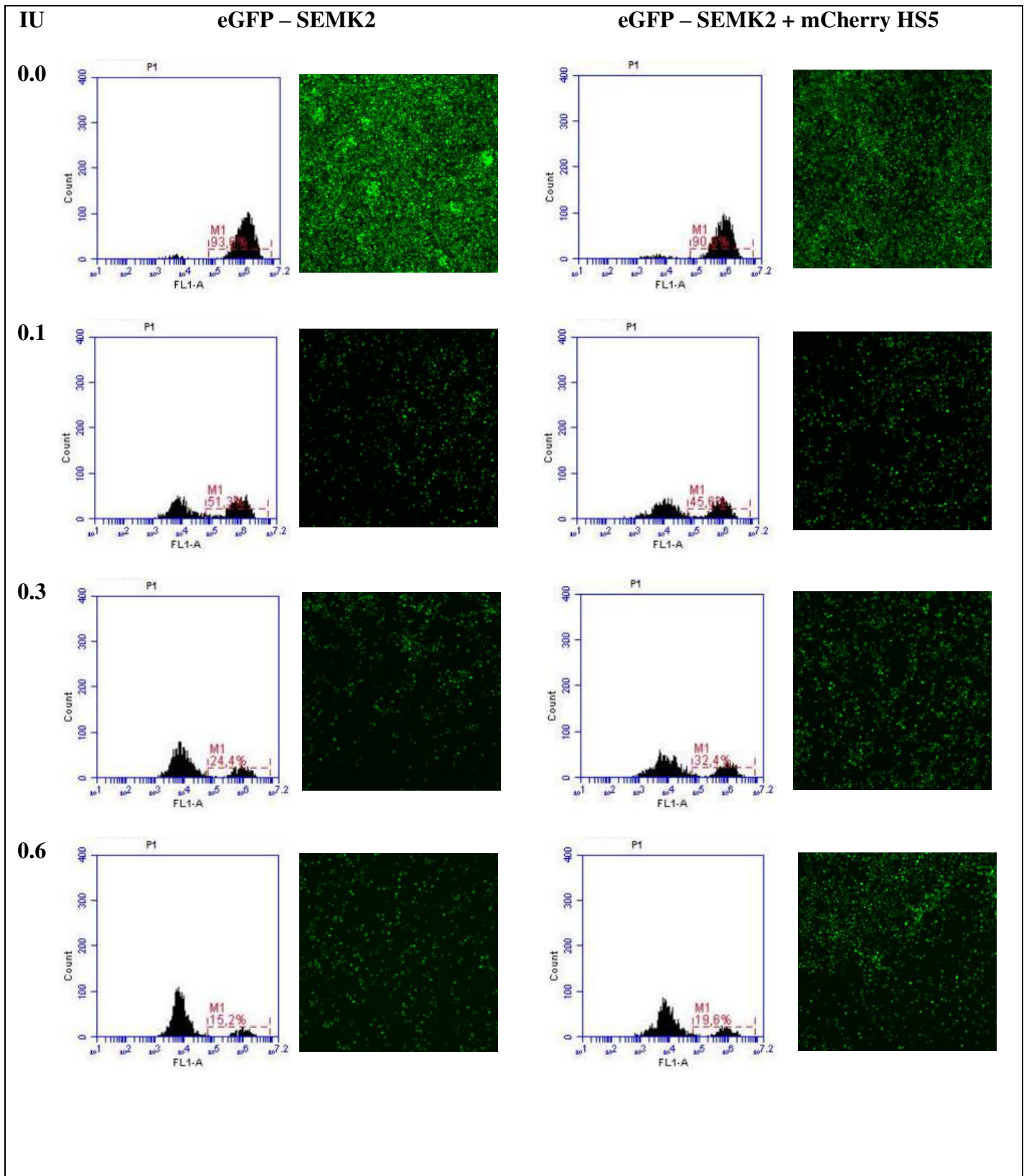
3. Results and Discussion

The anti-leukemic and anticancer effect of L-ASNases has been extensively investigated however, the effect of the recombinant glycosylated L-ASNase on human leukemic cells has not been fully elucidated. Therefore, in order to study the effect of purified recombinant L-ASNase on human leukemic cell lines, eGFP-SEMK2 cells were cultured on their own and co-culture with the BM stroma fibroblast cell line HS5 (Figure 2) treated with different concentrations of the purified enzyme. Our data showed that after 72 h of treatment, significant morphological changes were observed (Figure 2).

(A)



(B)



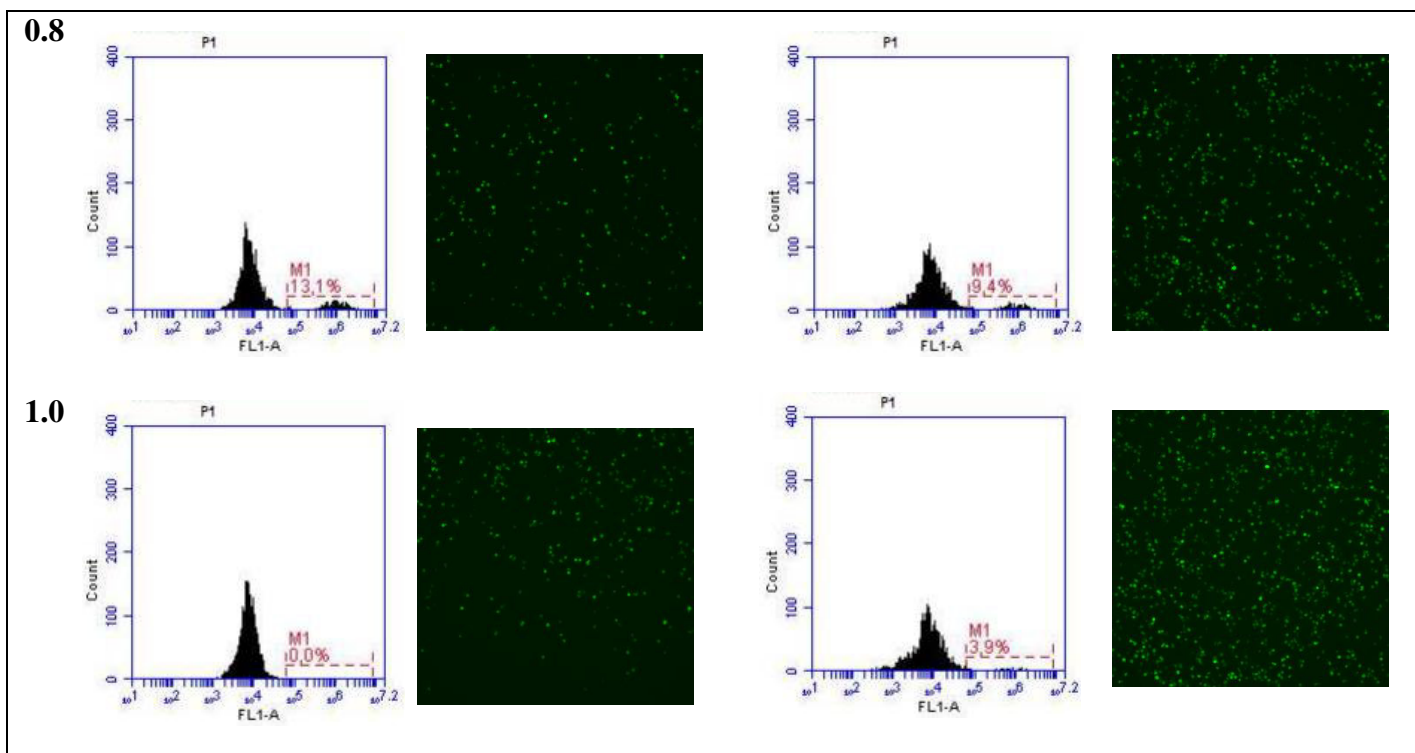


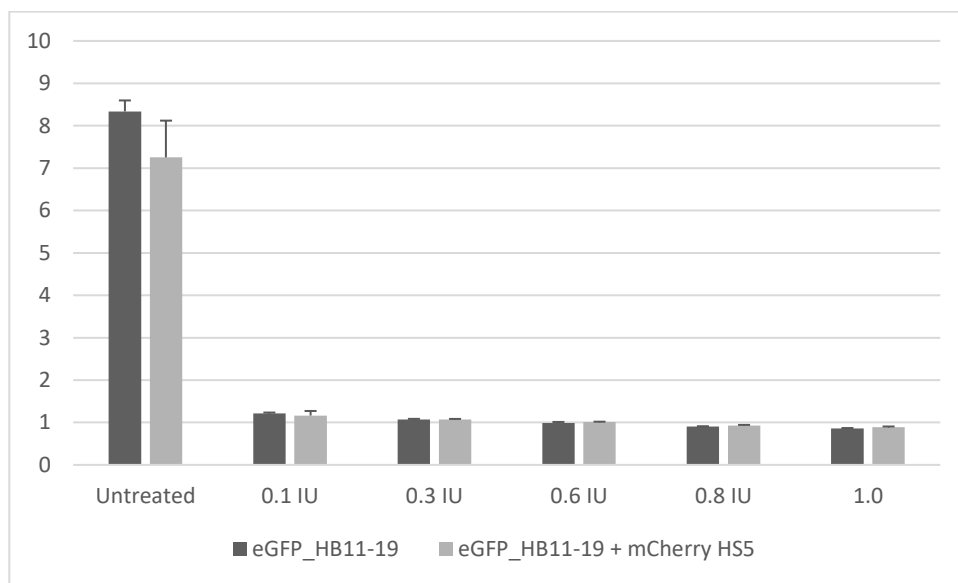
Figure 2. Glycosylated L-ASNase blocks proliferation of the ALL cell line SEMK2 in the presence of BM stromal cells. Evaluation of A) tumor cell proliferation and B) cell apoptosis of eGFP-SEMK2 lineage after 72 hours of treatment with glycosylated L-ASNase in the range of 0.1-1.0 IU cultured alone or co-cultured with mCherry HS5 BM stroma cells. Micrographs showing the presence of GFP-ALL cells acquired using a 10X magnification lens. Glycosylated L-ASNase inhibited proliferation of SEMK2 cells cultured alone or in the presence of the BM stromal cell line HS5.

From Figure 2A we observed that L-ASNase was efficient in all concentrations studied here for this strain. Thus, we conclude that we can still study ranges with lower concentrations of L-ASNase since the lower the concentrations of L-ASNase, the lower the number of side effects in the patient, in addition to reducing the effective cost of treatment. From Figure 2B we can see that with the lowest concentration of L-ASNase we reduced the cell population from 93.6% to 51.3% when the cells are culture alone. We observed that with the gradual increase in the concentration of L-ASNase, the population of viable cells was practically eradicated. This is a valuable result as it proves that L-ASNase did not only have a cytostatic activity but also presented a cytotoxic activity because it reduced the viability of cell population already there. When compared with the co-cultured models, we can see that at concentrations 0.3 IU, 0.6 IU and 1.0 IU we can observe a significantly higher prevalence of small (lower than 10% at the highest concentration of glycosylated L-ASNase) population viable cells even after treatment in these cell co-culture models. This data indicate that the bone marrow microenvironment provides a protective environment for the leukemic blast. Finally, from Figure 2B we can

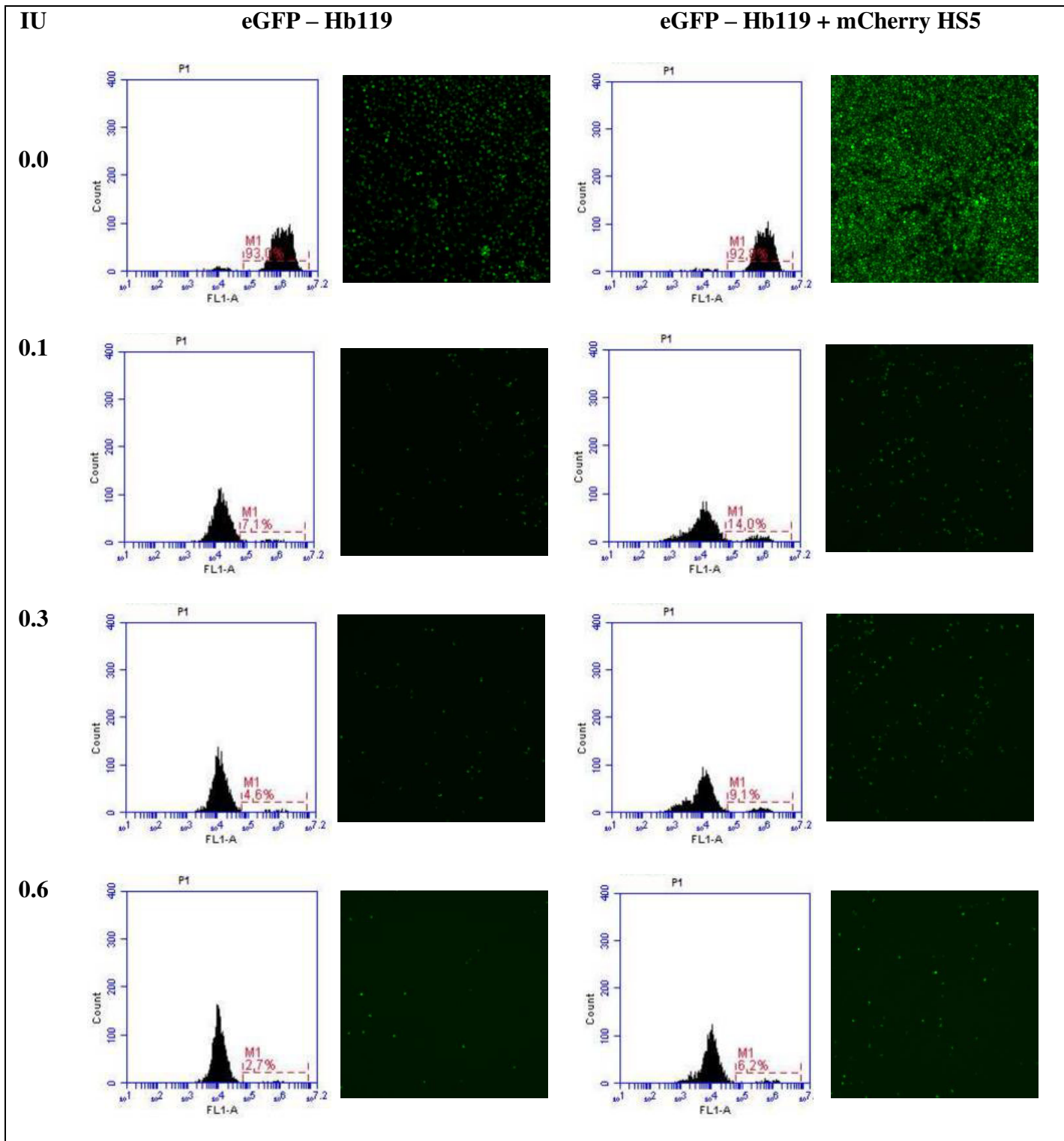
observe in the fluorescence micrographs that as we increase the concentrations of L-ASNase, the smaller the number of viable cells, which corroborates with the initially observed. Herein, we can observe a higher prevalence of cell populations in co-culture models, reaffirming the hypothesis of a protective environment for leukemic cells provided by the BM.

Our data showed a cytotoxic and cytostatic effect of glycosylated L-ASNase on eGFP- Hb11-9 lineage cultured by its own and co-culture with the BM stroma fibroblast cell line HS5 (Figure 3).

(A)



(B)



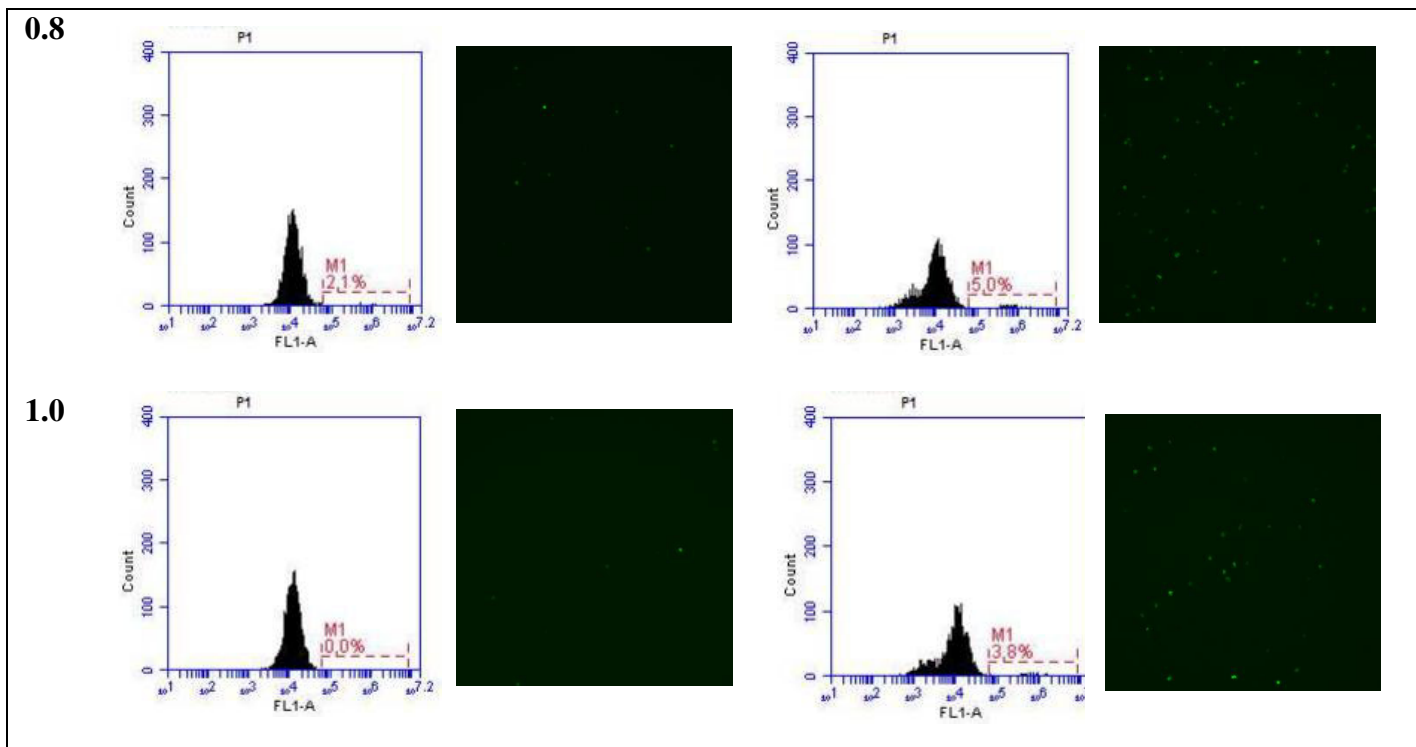


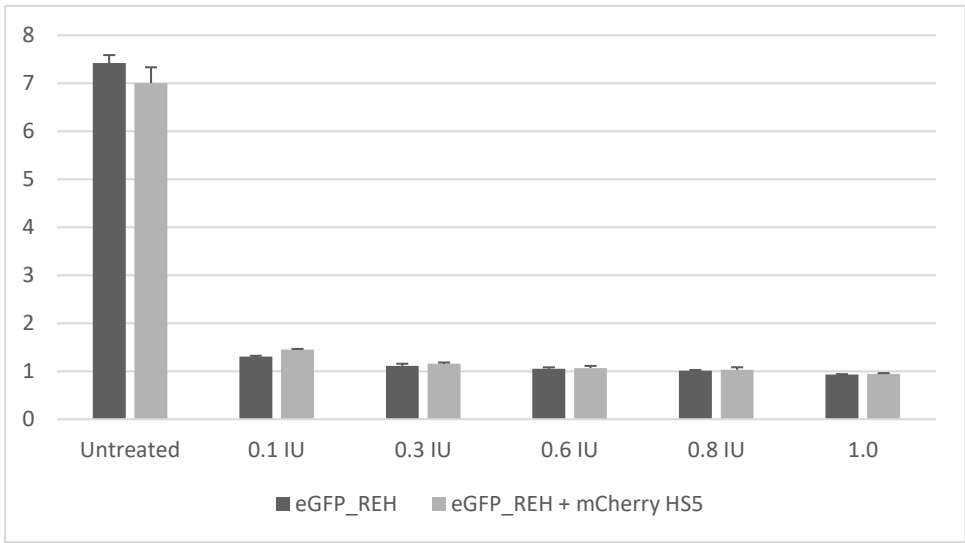
Figure 3. Glycosylated L-ASNase blocks proliferation of the ALL cell line Hb11-9 in the presence of BM stromal cells. Evaluation of: A) tumor cell proliferation and B) cell apoptosis of eGFP-Hb11-9 lineage after 72 hours of treatment with glycosylated L-ASNase in the range of 0.1-1.0 IU cultured alone or co-cultured with mCherry HS5 BM stroma cells. Micrographs showing the presence of GFP-ALL cells acquired using a 10X magnification lens. Glycosylated L-ASNase inhibited proliferation of Hb11-9 cells cultured alone or in the presence of the BM stromal cell line HS5.

From Figure 3A we observed that the Hb11-9 strain was the most sensitive lineage to the treatment of L-ASNase in all concentrations studied here. Thus, we conclude that we can still study lower concentrations of L-ASNase for this strain in order to determine the IC₅₀ values. From Figure 3B we can see that with the lowest concentration of L-ASNase we reduced the cell population from 93.0% to 7.1% when the cells are grown alone. We observed that with the gradual increase in the concentration of L-ASNase, the population of viable cells was completely eradicated. This is a valuable result as it proves that L-ASNase did not only have a cytostatic activity, that is, it not only prevented cell proliferation, but also presented a cytotoxic activity because it reduced the cell population already there. When compared to co-cultured models, we can see that at all concentrations of L-ASNase, the resulting cell population was at least twice the resulting cell population when only eGFP cells were cultured. This result reaffirms that the bone marrow microenvironment provides a protective environment for the leukemic blast, explaining possible resistance to treatments and relapses. Finally, from Figure 3B we can see in the fluorescence micrographs that as we increase the concentrations of L-ASNase, the smaller

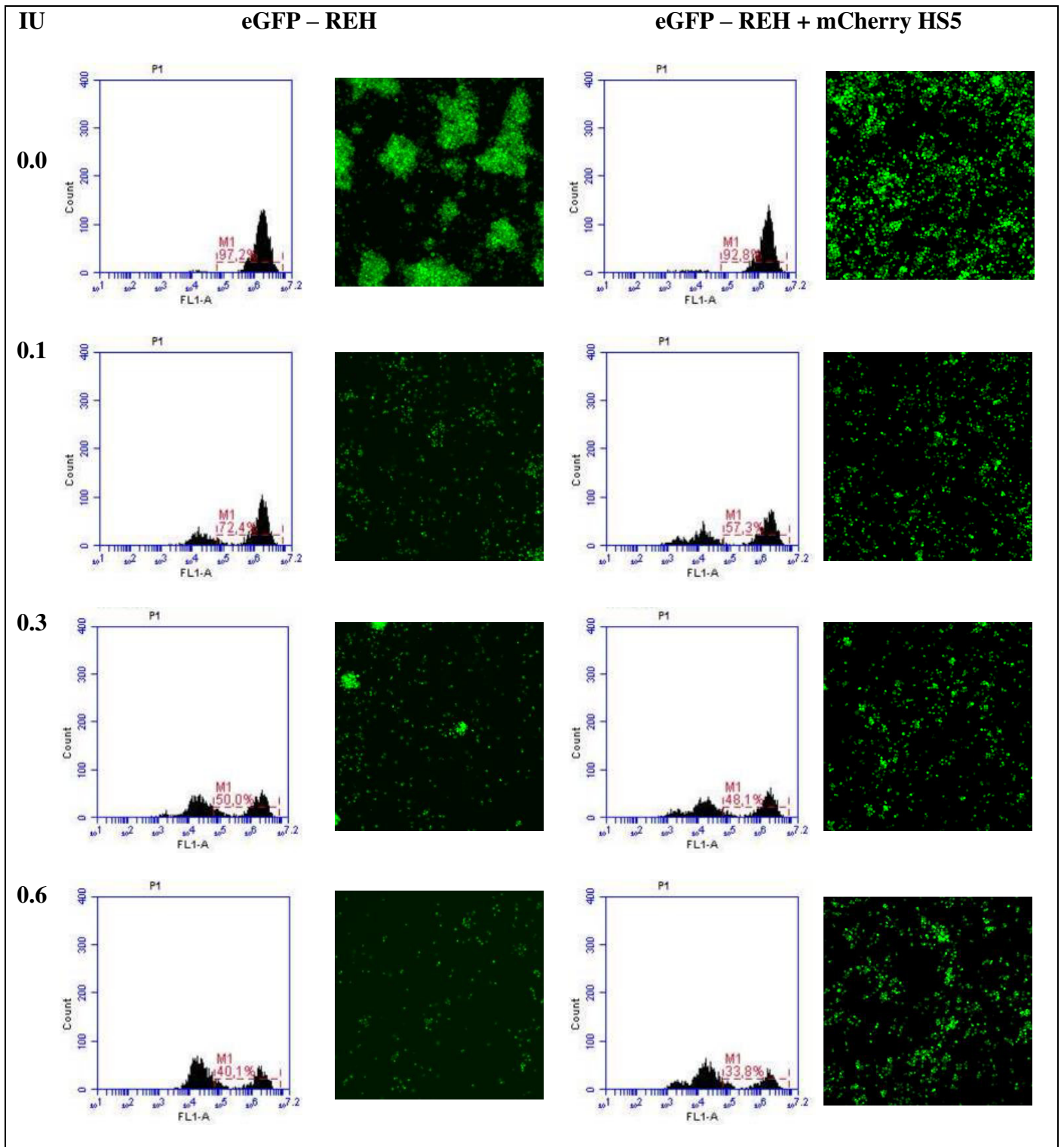
the number of viable cells, which corroborates with what was initially observed. Herein, we can observe that we have a higher prevalence of cell populations in co-culture models, reaffirming the hypothesis that bone marrow provides a protective environment for leukemic cells.

Our data showed a cytotoxic and cytostatic effect of glycosylated L-ASNase on eGFP- REH lineage cultured by its own and co-culture with the BM stroma fibroblast cell line HS5 (Figure 4).

(A)



(B)



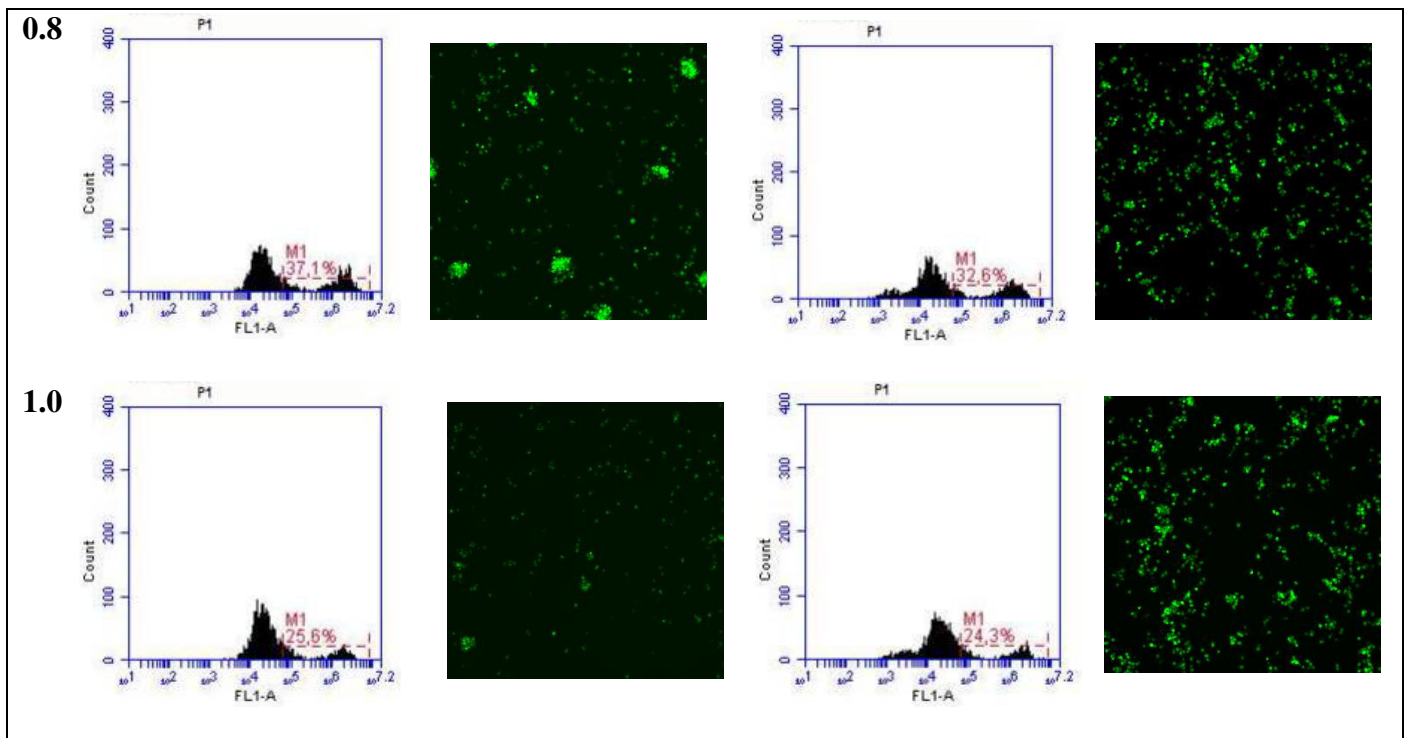
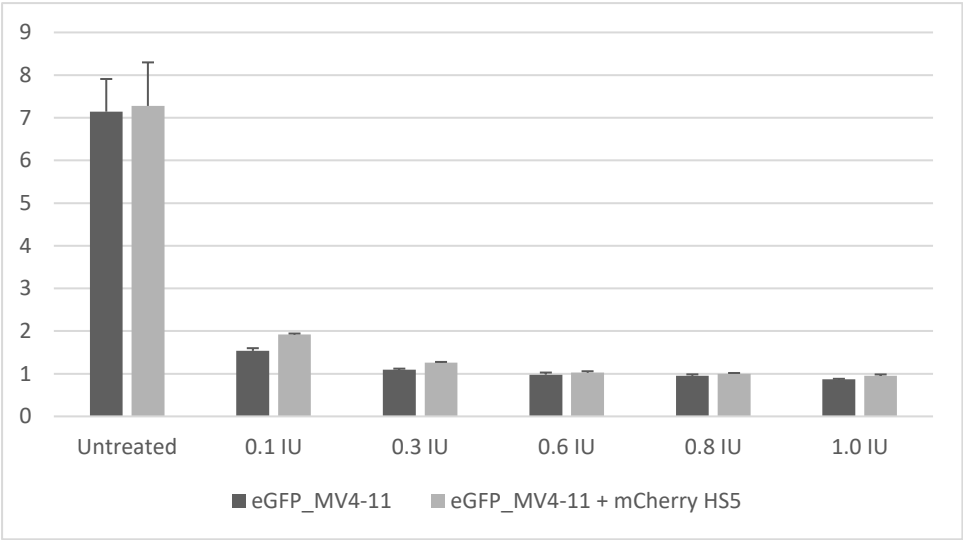


Figure 4. Glycosylated L-ASNase blocks proliferation of the ALL cell line REH in the presence of BM stromal cells. Evaluation of: A) tumor cell proliferation and B) cell apoptosis of eGFP-REH lineage after 72 hours of treatment with glycosylated L-ASNase in the range of 0.1-1.0 IU cultured alone or co-cultured with mCherry HS5 BM stroma cells. Micrographs showing the presence of eGFP-ALL cells acquired using a 10X magnification lens. Glycosylated L-ASNase inhibited proliferation of REH cells cultured alone or in the presence of the BM stromal cell line HS5.

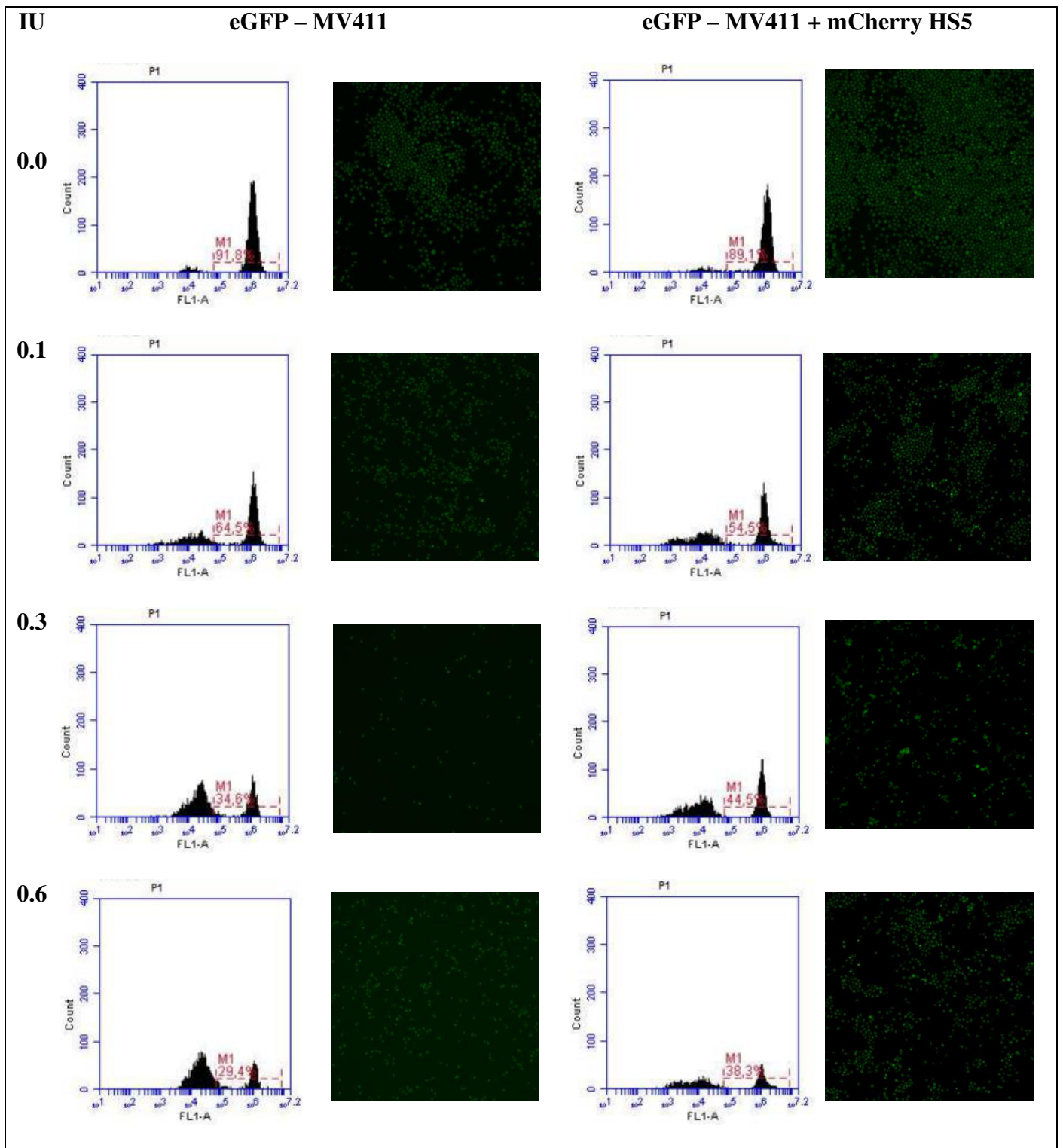
From Figure 4A we observed that the REH strain was the most resistant of all to the treatment of L-ASNase in all the concentrations studied here. From Figure 4B we can see that with the lowest concentration of L-ASNase we reduced the cell population from 97.2% to 72.4% when the cells are grown alone. This result shows that different ALL cell lines can exhibit diametrically opposite behaviours. We observed that with the gradual increase in the concentration of L-ASNase, the population of viable cells was not completely eradicated, thus suggesting that higher doses are required for this cell line. When compared to co-cultured models, we can observe similar values when cells were culture alone. Finally, from Figure 4B we can see in the fluorescence micrographs a higher prevalence of cell populations even when treated with higher concentrations of L-ASNase.

Our data showed a cytotoxic and cytostatic effect of glycosylated L-ASNase on eGFP- MV4-11 lineage cultured by its own and co-culture with the BM stroma fibroblast cell line HS5 (Figure 5).

(A)



(B)



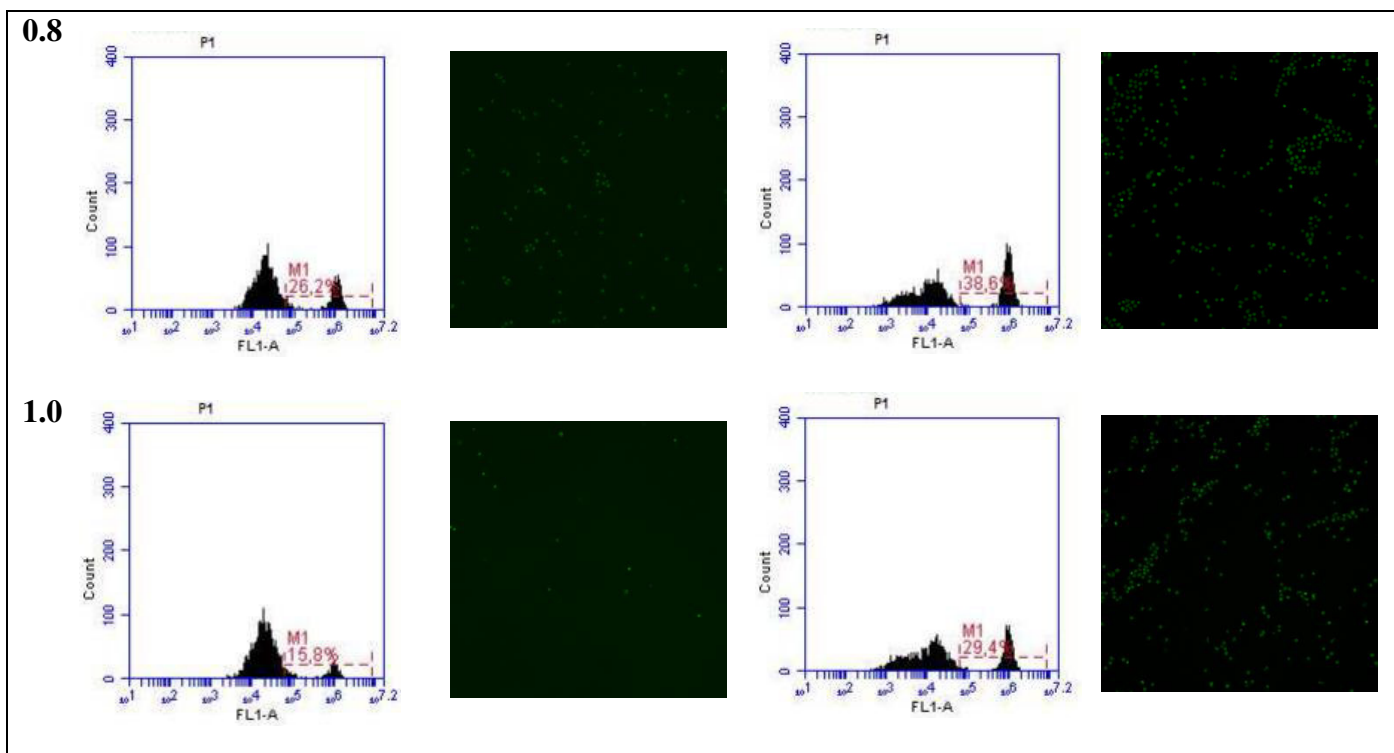


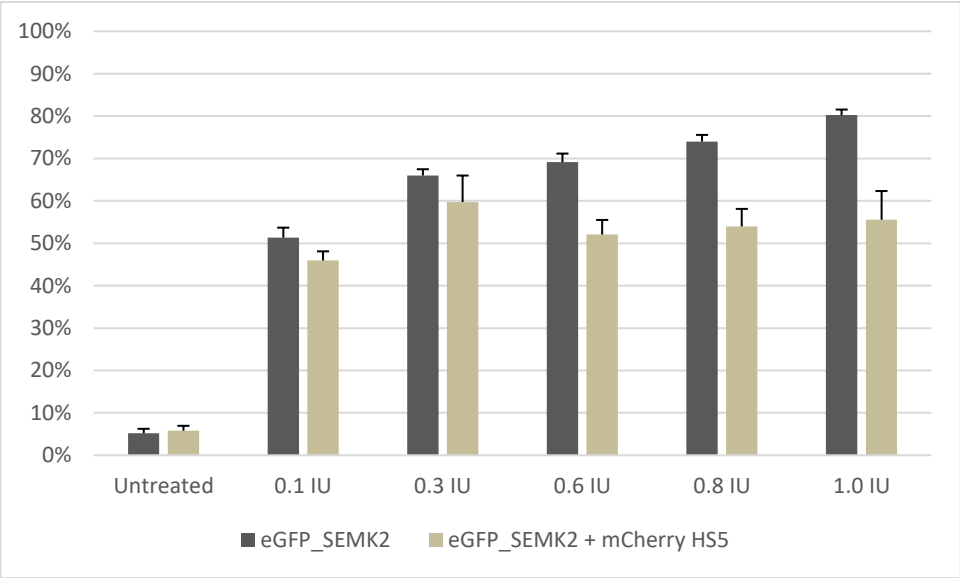
Figure 5. Glycosylated L-ASNase blocks proliferation of the AML cell line MV4-11 in the presence of BM stromal cells. Evaluation of: A) tumor cell proliferation and B) cell apoptosis of eGFP-MV4-11 lineage after 72 hours of treatment with glycosylated L-ASNase in the range of 0.1-1.0 IU cultured alone or co-cultured with mCherry HS5 BM stroma cells. Micrographs showing the presence of GFP-AML cells acquired using a 10X magnification lens. Glycosylated L-ASNase inhibited proliferation of MV4-11 cells cultured alone or in the presence of the BM stromal cell line HS5.

From Figure 5A we observed that the MV4-11 strain showed a similar behaviour to the REH strain. It is worth mentioning that this is a strain of acute myeloid leukaemia and that some studies have been suggesting the action of L-ASNase also as a protocol for the treatment of this leukaemia. From Figure 5B we can see that with the lowest concentration of L-ASNase we reduced the cell population from 91.8% to 67.5% when the cells are grown alone. This result shows that this strain is also susceptible to the action of L-ASNase even though this cell line is self-sufficient in the synthesis of asparagine. We observed that with the gradual increase in the concentration of L-ASNase, the population of viable cells was not eradicated, but reduced to 15.8% with the highest dose of L-ASNase. Thus, this result is extremely promising as it opens a field that has not yet been studied. When compared to co-cultured models, we can see that there is a higher percentage of viable cells in the presence of the bone marrow microenvironment when grown alone. This result reaffirms that the bone marrow microenvironment provides a protective environment for the leukemic blast, explaining possible resistance to treatments and relapses. Finally, we can observe in the fluorescence micrographs a higher

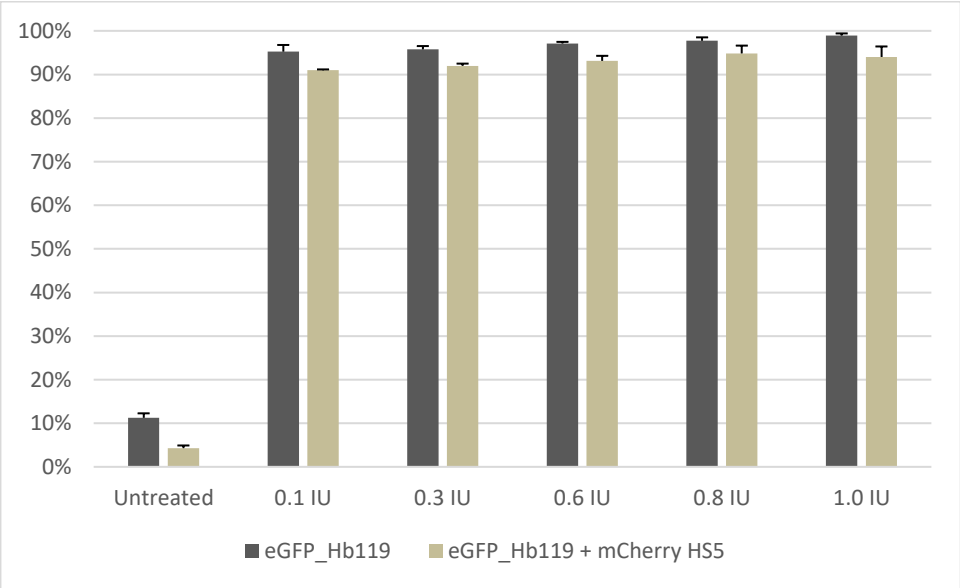
prevalence of cell populations in the models of cell co-culture even when treated with higher concentrations of L-ASNase.

From Figure 6 we can compare the percentage of apoptotic cells when tumor cells were cultured on their own and when co-culture with BM cells. We can conclude that in all conditions there are fewer apoptotic cells in co-culture models reaffirming that fibroblast provides some cytoprotection to tumor cells. It is also possible to observe higher levels of apoptotic cells when the treatment was with higher doses of L-ASNase.

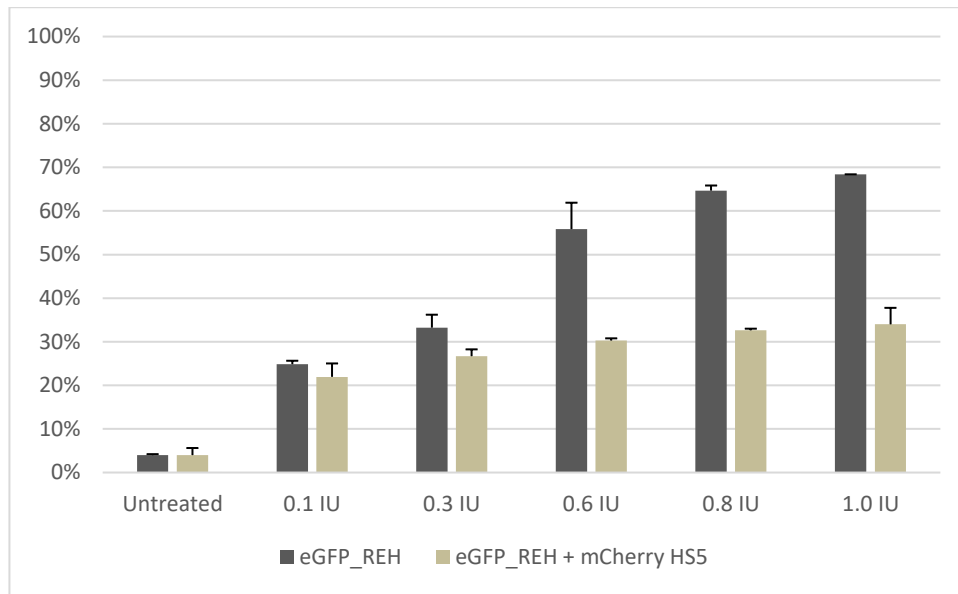
(A)



(B)



(C)



(D)

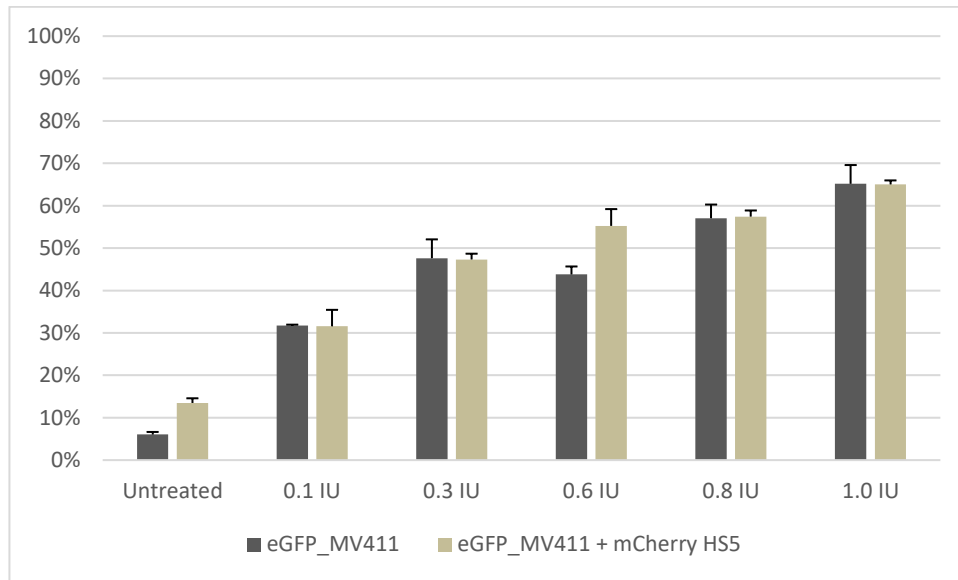


Figure 6. Percentage of cell apoptosis of tumor lineages after 72 hours of treatment with glycosylated L-ASNase in the range of 0.1-1.0 IU cultured alone or co-cultured with mCherry HS5 BM stromal cells. A) eGFP-SEMK2 B) eGFP-Hb119 C) eGFP-REH D) eGFP-MV411.

Our results had shown that the eGFP-Hb11-9 strain was the most sensitive of the four strains, in contrast with the eGFP-REH that was the most resistant lineage. This is because the REH strain express a lysosomal protease, such as CTSB, that inactivate asparaginase. Another and important observation to add is that the stroma cell can also produce CTSB, being one of the explanations for a less effective treatment in co-culture models (Michelozzi et al., 2019).

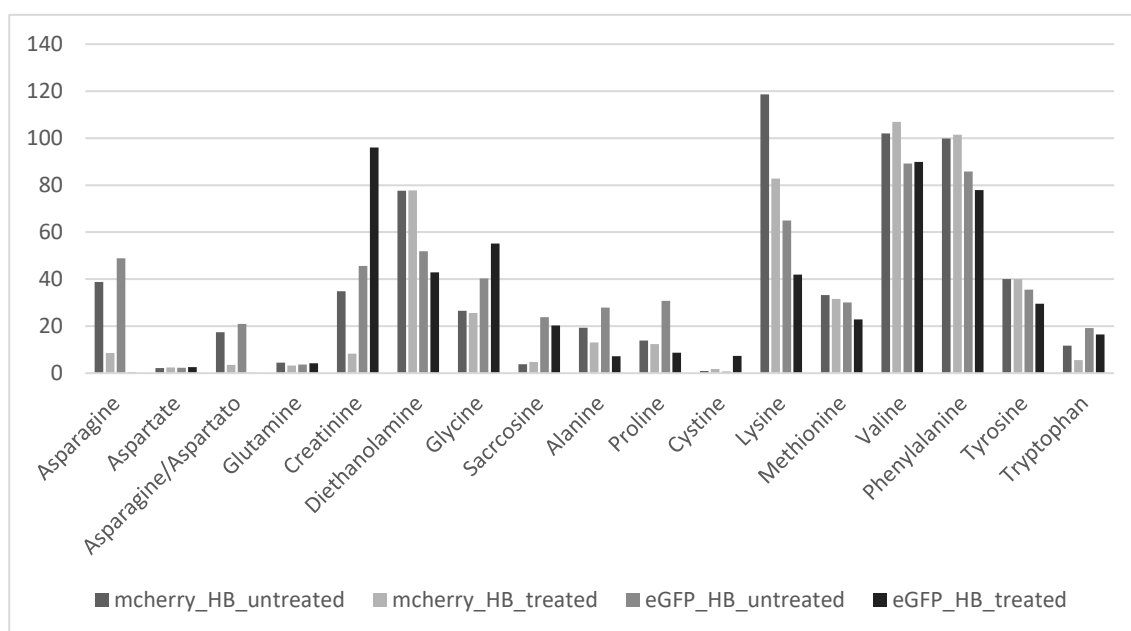
Another extremely interesting outcome to point out is that the AML eGFP-MV411 strain responded to treatment with asparaginase. This suggests that this biopharmaceutical can also be used to treat this disorder in combination with other chemotherapeutic agents.

In a recent study, different cell lines were tested against four different L-asparaginase proteoforms. Although the study was conducted using the MTT methodology, it was also observed that the REH strain was the most resistant strain to the treatment with L-Asparaginase, while on the other hand, the MOLT-4 lineage was the most sensitive to treatment (Rodrigues et al., 2020).

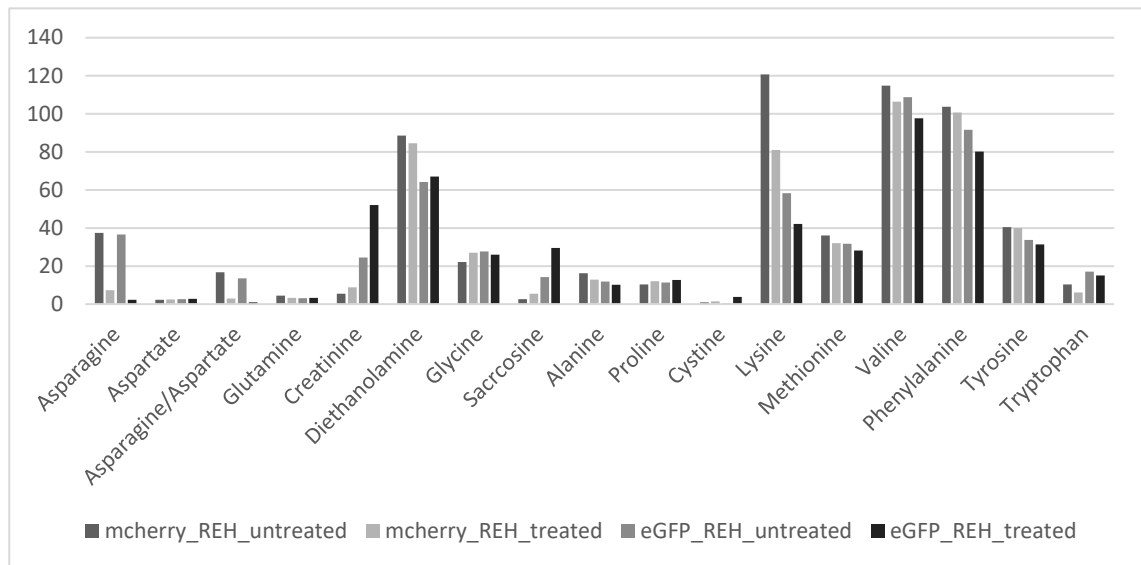
Studies undertaken by Saeed and collaborators (2020) had shown that their recombinant L-ASNase also presented cytotoxicity activity against the AML lineage THP-1. Michelozzi and coauthors (2019) evaluated the cytotoxicity activity of the commercial L-ASNases against THP-1, KG-1 and HL-60. Their findings showed a superior efficacy of Erwinase® in all AML cell lines tested in terms of induction of apoptosis rather than the *E. coli* ASNase (Kidrolase®).

Finally, to estimate the intracellular amino acids after the treatment with the glycosylated L-ASNase, we selected the concentration of 0.3 IU during the first 24 hours and we identified the intracellular metabolites by UPLC-MS/MS in the Hb119, REH and MV411 lineages (Figure 7).

(A)



(B)



(C)

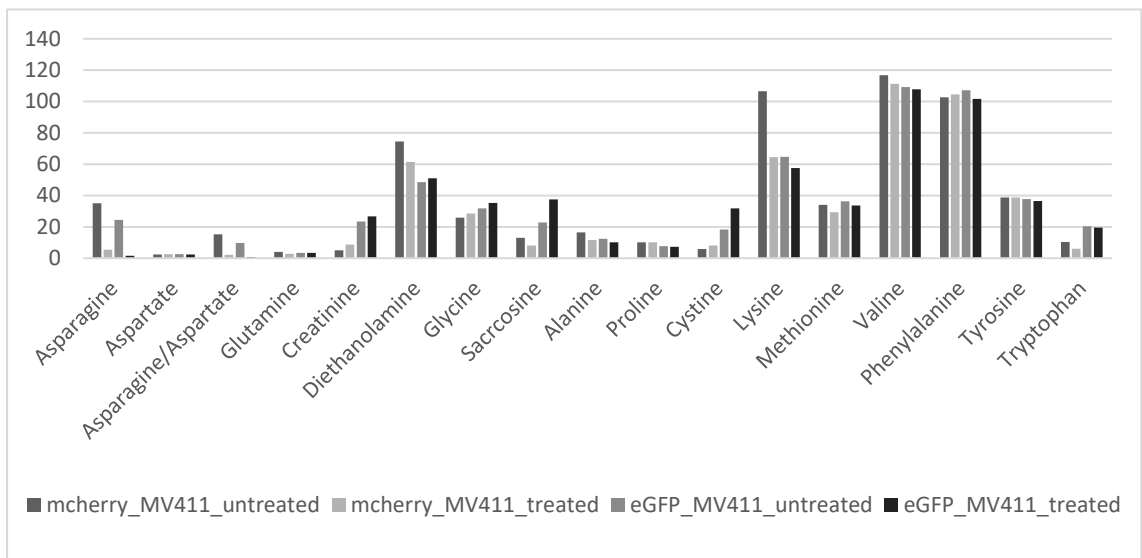


Figure 7. Comparison of intracellular metabolites identified by UPLC-MS/MS after 24 hours of the treatment with the glycosylated L-ASNase. Graphs show absolute levels of each metabolite. The recombinant protein depletes asparagine when tumor cells are culture on their own, however, in the presence of BM stromal cells it is possible to detect asparagine suggesting that the tumor microenvironment influences the response to chemotherapy. L-ASNase concentration: 0.3 IU. Leukemic linages evaluated: A) Hb119 B) REH and C) MV411.

We detected a major decrease in asparagine depletion when tumor cells were cultured on their own. In contrast, when tumor cells were co-cultured with stromal cells, it is possible to notice a higher final asparagine concentration (Figure 7). These data reaffirm that BM provides cytoprotection to tumor cells. In addition, we can observe the highest concentration of lysine for all three lineages studied when the tumor cells were co-cultured with BM. These outcomes are very promising, and it opens a door for future drug discovery targeting also lysine. It is also important to pinpoint that from the lysin perspective, we can see a difference in the response between ALL and AML cells. This comparison shows us that the MV411 lineage presented a higher concentration of lysine even after being treated with the glycosylated L-ASNase. When we analyze both ALL cells, we can observe that the amount of lysine decreased in treated cells.

4. Conclusions

In summary, this study evaluated the cytotoxicity activity of the glycosylated L-ASNase using a methodology that allows the simultaneous analysis of the activity of both tumor and BM stromal cells when co-cultured. To develop new therapeutical biopharmaceuticals a comprehension of how the microenvironment can influence the cancer cells, and further in drug response, is a critical approach. The recombinant enzyme in this study induced a cytotoxic effect in all human leukemic cell lines tested. Thus, all our achievements reaffirm the potential of the glycosylated L-ASNase as a promising alternative enzyme in ALL treatment and open new doors for its further application against AML treatment as well.

References

- Bertuccio SN, Serravalle S, Astolfi A, Lonetti A, Indio V, Leszl A, Pession A, Melchionda F. Identification of a cytogenetic and molecular subgroup of acute myeloid leukemias showing sensitivity to L-Asparaginase. *Oncotarget*. 19;8(66):109915-109923. 2017. doi: 10.18632/oncotarget.18565.
- Brumano LP, da Silva F, Costa-Silva TA, Apolinário AC, Santos J, Kleingesinds EK, Monteiro G, Rangel-Yagui CO, Benyahia B, Junior AP. Development of L-Asparaginase Biobetters: Current Research Status and Review of the Desirable Quality Profiles. *Frontiers in bioengineering and biotechnology*. 6, 212. 2019. <https://doi.org/10.3389/fbioe.2018.00212>.
- Gray N, Zia R, King A, Patel VC, Wendon J, McPhail MJ, Coen M, Plumb RS, Wilson ID, Nicholson JK. High-Speed Quantitative UPLC-MS Analysis of Multiple Amines in Human Plasma and Serum via Precolumn Derivatization with 6-Aminoquinolyl-N-hydroxysuccinimidyl Carbamate: Application to Acetaminophen-Induced Liver Failure. *Anal Chem*. 21;89(4):2478-2487. 2017. doi: 10.1021/acs.analchem.6b04623.

- Korn C, Méndez-Ferrer S. Myeloid malignancies and the microenvironment. *Blood*. 16;129(7):811-822. 2017. doi: 10.1182/blood-2016-09-670224.
- Jacque N, Ronchetti AM, Larrue C, Meunier G, Birsén R, Willems L, Saland E, Decroocq J, Maciel TT, Lambert M, Poulain L, Hospital MA, Sujobert P, Joseph L, Chapuis N, Lacombe C, Moura IC, Demo S, Sarry JE, Recher C, Mayeux P, Tamburini J, Bouscary D. Targeting glutaminolysis has antileukemic activity in acute myeloid leukemia and synergizes with BCL-2 inhibition. *Blood*. 10;126(11):1346-56. 2015. doi: 10.1182/blood-2015-01-621870.
- Lopez-Millan B, Sánchez-Martínez D, Roca-Ho H, Gutiérrez-Agüera F, Molina O, Diaz de la Guardia R, Torres-Ruiz R, Fuster JL, Ballerini P, Suessbier U, Nombela-Arrieta C, Bueno C, Menéndez P. NG2 antigen is a therapeutic target for MLL-rearranged B-cell acute lymphoblastic leukemia. *Leukemia*. 33(7):1557-1569. 2019. doi: 10.1038/s41375-018-0353-0.
- Matre P, Velez J, Jacamo R, Qi Y, Su X, Cai T, Chan SM, Lodi A, Sweeney SR, Ma H, Davis RE, Baran N, Haferlach T, Su X, Flores ER, Gonzalez D, Konoplev S, Samudio I, DiNardo C, Majeti R, Schimmer AD, Li W, Wang T, Tiziani S, Konopleva M. Inhibiting glutaminase in acute myeloid leukemia: metabolic dependency of selected AML subtypes. *Oncotarget*. 29;7(48):79722-79735. 2016. doi: 10.18632/oncotarget.12944.
- Michelozzi IM, Granata V, De Ponti G, Alberti G, Tomasoni C, Antolini L, Gambacorti-Passerini C, Gentner B, Dazzi F, Biondi A, Coliva T, Rizzari C, Pievani A, Serafini M. Acute myeloid leukaemia niche regulates response to L-asparaginase. *Br J Haematol*. 186(3):420-430. 2019. doi: 10.1111/bjh.15920.
- Okada S, Hongo T, Yamada S, Watanabe C, Fujii Y, Ohzeki T, Horikoshi Y, Ito T, Yazaki M, Komada Y, Tawa A. In vitro efficacy of l-asparaginase in childhood acute myeloid leukaemia. *Br J Haematol*. 123(5):802-9. 2003. doi: 10.1046/j.1365-2141.2003.04703.x.
- Patel N, Krishnan S, Offman MN, Krol M, Moss CX, Leighton C, van Delft FW, Holland M, Liu J, Alexander S, Dempsey C, Ariffin H, Essink M, Eden TO, Watts C, Bates PA, Saha V. A dyad of lymphoblastic lysosomal cysteine proteases degrades the antileukemic drug L-asparaginase. *J Clin Invest*. 119(7):1964-73. 2009. doi: 10.1172/JCI37977.
- Ramasamy K, Khatun H, Macpherson L, Caley MP, Sturge J, Mufti GJ, Schey SA, Calle Y. Fluorescence-based experimental model to evaluate the concomitant effect of drugs on the tumour microenvironment and cancer cells. *Br J Haematol*. 157(5):564-79. 2012. doi: 10.1111/j.1365-2141.2012.09103.x.
- Saeed H, Hemida A, El-Nikhely N, Abdel-Fattah M, Shalaby M, Hussein A, Eldoksh A, Ataya F, Aly N, Labrou N, Nematalla H. Highly efficient *Pyrococcus furiosus* recombinant L-asparaginase with no glutaminase activity: Expression, purification, functional characterization, and cytotoxicity on THP-1, A549 and Caco-2 cell lines. *Int J Biol Macromol*. 1;156:812-828. 2020. doi: 10.1016/j.ijbiomac.2020.04.080.
- Siveen KS, Uddin S, Mohammad RM. Targeting acute myeloid leukemia stem cell signaling by natural products. *Mol Cancer*. 2017. 30;16(1):13. doi: 10.1186/s12943-016-0571-x.
- Steiner M, Hochreiter D, Kasper DC, Kornmüller R, Pichler H, Haas OA, Pötschger U, Hutter C, Dworzak MN, Mann G, Attarbaschi A. Asparagine and aspartic acid concentrations in bone marrow versus peripheral blood during Berlin-Frankfurt-Münster-based induction therapy for childhood acute lymphoblastic leukemia. *Leuk Lymphoma*. 53(9):1682-7. 2012. doi: 10.3109/10428194.2012.668681.
- van der Meer LT, Waanders E, Levers M, Venselaar H, Roeleveld D, Boos J, Lanvers C, Brüggemann RJ, Kuiper RP, Hoogerbrugge PM, van Leeuwen FN, te Loo DM. A germ line mutation in cathepsin B points toward a role in asparaginase pharmacokinetics. *Blood*. 6;124(19):3027-9. 2014. doi: 10.1182/blood-2014-06-582627.
- Willems L, Jacque N, Jacquél A, Neveux N, Maciel TT, Lambert M, Schmitt A, Poulain L, Green AS, Uzunov M, Kosmider O, Radford-Weiss I, Moura IC, Auberger P, Ifrah N, Bardet V, Chapuis N, Lacombe C, Mayeux P, Tamburini J, Bouscary D. Inhibiting glutamine uptake represents an attractive

new strategy for treating acute myeloid leukemia. *Blood*. 14;122(20):3521-32. 2013. doi: 10.1182/blood-2013-03-493163.

Zwaan CM, Kaspers GJ, Pieters R, Ramakers-Van Woerden NL, den Boer ML, Wünsche R, Rottier MM, Hähnen K, van Wering ER, Janka-Schaub GE, Creutzig U, Veerman AJ. Cellular drug resistance profiles in childhood acute myeloid leukemia: differences between FAB types and comparison with acute lymphoblastic leukemia. *Blood*. 15;96(8):2879-86. 2000.

Final Remarks

The outcomes from the present thesis are extremely promising and contributed to the development of the upstream and downstream processes of a novel glycosylated L-ASNase with human-like glycosylation pattern extremely pure with high final yield. Our results demonstrated that the glycosylated L-ASNase presents a high affinity for asparagine and its optimum activity at pH 8.0 and 50 °C. The effectiveness of this new L-ASNase proteoform was proven by the high throughput fluorescent-based *in vitro* experimental platform and added a knowledge regarding the study of the tumour microenvironment of which is little explored in Brazil. It is important to highlight that the methodology applied here to assess asparaginase cytotoxicity is a new approach that avoids the use of laboratory animals. Pre-clinical studies must be done in order to evaluate the immune response when this new biopharmaceutical is injected into the bloodstream. Another future work that will expand the knowledge regarding the manufacturing of this drug lies on the economic feasibility of the bioprocess.

List of Publications

1. De Jesus Fontes, Bruno; **Kleingesinds, Eduardo Krebs**; Giovanella, Patricia; Junior, Adalberto Pessoa; Sette, Lara Durães. Laccases produced by *Peniophora* from marine and terrestrial origin: a comparative study. *Biocatalysis and Agricultural Biotechnology*, v. 35, p. 102066, 2021. <https://doi.org/10.1016/j.bcab.2021.102066>
2. De Almeida Parizotto, Letícia; **Krebs Kleingesinds, Eduardo**; Manfrinato Pedrotti Da Rosa, Luiza; Effer, Brian; Meira Lima, Guilherme; Herkenhoff, Marcos Edgar; Li, Zhaopeng; Rinas, Ursula; Monteiro, Gisele; Pessoa, Adalberto; Tonso, Aldo. Increased glycosylated l-asparaginase production through selection of *Pichia pastoris* platform and oxygen-methanol control in fed-batches. *Biochemical Engineering Journal*, v. 173, p. 108083, 2021. <https://doi.org/10.1016/j.bej.2021.108083>
3. Effer, Brian; **Kleingesinds, Eduardo Krebs**; Lima, Guilherme Meira; Costa, Iris Munhoz; Sánchez-Moguel, Ignacio; Pessoa, Adalberto; Santiago, Verônica Feijoli; Palmisano, Giuseppe; Farías, Jorge G.; Monteiro, Gisele. Glycosylation of Erwinase results in active protein less recognized by antibodies. *Biochemical Engineering Journal*, v. 163, p. 107750, 2020. <https://doi.org/10.1016/j.bej.2020.107750>
4. Simas, Rodrigo G; **Krebs Kleingesinds, Eduardo**; Pessoa, Adalberto; Long, Paul F. An improved method for simple and accurate colorimetric determination of L-asparaginase enzyme activity using Nessler's reagent. *Journal of Chemical Technology and Biotechnology*, v. 12, p. jctb.6651, 2020. <https://doi.org/10.1002/jctb.6651>
5. Brumano, Larissa Pereira; Da Silva, Francisco Vitor Santos; Costa-Silva, Tales Alexandre; Apolinário, Alexsandra Conceição; Santos, João Henrique Picado Madalena; **Kleingesinds, Eduardo Krebs**; Monteiro, Gisele; Rangel-Yagui, Carlota De Oliveira; Benyahia, Brahim; Junior, Adalberto Pessoa. Development of L-Asparaginase Biobetters: Current Research Status and Review of the Desirable Quality Profiles. *Frontiers in Bioengineering and Biotechnology*, v. 6, p. 212, 2019. <https://doi.org/10.3389/fbioe.2018.00212>

Additional Files

Academic transcripts

Janus - Sistema Administrativo da Pós-Graduação



Universidade de São Paulo
Faculdade de Ciências Farmacêuticas
FICHA DO ALUNO

9134 - 7570420/1 - Eduardo Krebs Kleingesinds

Email:	ekk@usp.br
Data de Nascimento:	05/04/1993
Cédula de Identidade:	RG - 36.051.283-5 - SP
Local de Nascimento:	Estado de São Paulo
Nacionalidade:	Brasileira
Graduação:	Bacharel em Química - Faculdade de Filosofia, Ciências e Letras de Ribeirão Preto - Universidade de São Paulo - São Paulo - Brasil - 2015
Mestrado:	Mestre em Ciências - Área: Microbiologia Aplicada - Escola de Engenharia de Lorena - Universidade de São Paulo - São Paulo - Brasil - 2017

Curso:	Doutorado
Programa:	Tecnologia Bioquímico-Farmacêutica
Área:	Tecnologia de Fermentações
Data de Matrícula:	24/05/2017
Início da Contagem de Prazo:	24/05/2017
Data Limite para o Depósito:	21/03/2022
Orientador:	Prof(a). Dr(a). Adalberto Pessoa Junior - 24/05/2017 até o presente. Email: pessoajr@usp.br
Proficiência em Línguas:	Inglês, 24/05/2017
Prorrogação(ões):	120 dias Período de 20/11/2021 até 20/03/2022
Data de Aprovação no Exame de Qualificação:	Aprovado em 18/06/2019
Estágio no Exterior:	King's College London, Inglaterra - Período de 01/09/2019 até 31/10/2020
Data do Depósito do Trabalho:	
Título do Trabalho:	
Data Máxima para Aprovação da Banca:	
Data de Aprovação da Banca:	
Data Máxima para Defesa:	
Data da Defesa:	
Resultado da Defesa:	
Histórico de Ocorrências:	Primeira Matrícula em 24/05/2017 Prorrogação em 26/01/2021

Aluno matriculado no Regimento da Pós-Graduação USP (Resolução nº 7493 em vigor a partir de 29/03/2018).

Última ocorrência: Matrícula de Acompanhamento em 19/07/2021

Impresso em: 15/09/2021 07:51:28



Universidade de São Paulo
Faculdade de Ciências Farmacêuticas
FICHA DO ALUNO

9134 - 7570420/1 - Eduardo Krebs Kleingesinds

Sigla	Nome da Disciplina	Início	Término	Carga Horária	Cred.	Freq.	Conc.	Exc.	Situação
TNA5801-1/7	Purificação de Proteínas e Peptídeos (Instituto de Pesquisas Energéticas e Nucleares - Universidade de São Paulo)	29/05/2017	09/07/2017	120	8	100	A	N	Concluída
FBT5776-5/5	Tópicos Especiais de Tecnologia Bioquímico-Farmacêutica II	07/07/2017	20/07/2017	30	2	100	A	N	Concluída
FBF5805-2/4	Delineamento de Experimentos e Ferramentas Estatísticas Aplicadas às Ciências Farmacêuticas	03/08/2017	11/10/2017	90	6	100	A	N	Concluída
QFL5727-3/3	Introdução à Espectrometria de Massas (Instituto de Química - Universidade de São Paulo)	17/08/2017	18/10/2017	90	0	-	-	N	Matrícula cancelada
BTC5700-9/2	Economia de Projetos Biotecnológicos (Curso Interunidades: Biotecnologia - Universidade de São Paulo)	02/10/2017	10/12/2017	90	6	80	A	N	Concluída
QFL5944-2/3	Métodos Avançados em Quimiometria (Instituto de Química - Universidade de São Paulo)	03/10/2017	25/12/2017	120	0	-	-	N	Turma cancelada
FBC5712-2/3	Métodos Modernos de Proteômica na Pesquisa em Análises Clínicas e Toxicológicas	16/10/2017	26/11/2017	60	0	-	-	N	Turma cancelada
ICB5754-1/2	Da Clonagem à Análise de Proteínas – Métodos e Estratégias (Instituto de Ciências Biomédicas - Universidade de São Paulo)	27/08/2018	02/09/2018	30	2	100	A	N	Concluída
FBT5738-2/1	Tópicos Especiais em Tecnologia Bioquímico-Farmacêutica III	01/04/2019	15/07/2019	60	4	100	A	N	Concluída

Créditos mínimos exigidos		Créditos obtidos
Para exame de qualificação	Para depósito de tese	
Disciplinas:	0	20
Estágios:		28
Total:	0	20

Créditos Atribuídos à Tese: 172

Conceito a partir de 02/01/1997:

A - Excelente, com direito a crédito; B - Bom, com direito a crédito; C - Regular, com direito a crédito; R - Reprovado; T - Transferência.

Um(1) crédito equivale a 15 horas de atividade programada.

Última ocorrência: Matrícula de Acompanhamento em 19/07/2021

Impresso em: 15/09/2021 07:51:28



XVII SIMPÓSIO
DE BIOSSEGURANÇA
E SEGURANÇA QUÍMICA E BIOLÓGICA
EM INSTITUIÇÕES DE ENSINO E PESQUISA

26 de outubro de 2018



Certificamos que o(a) Sr(a). *Eduardo Krebs Kleingesinds*,
participou do XVII SIMPÓSIO DE BIOSSEGURANÇA E SEGURANÇA QUÍMICA E BIOLÓGICA EM
INSTITUIÇÕES DE ENSINO E PESQUISA, realizado no dia 26 de outubro de 2018, no Auditório do
Centro de Difusão Internacional da Universidade de São Paulo, São Paulo-S.P., com carga horária
de 8hs.


Prof. Dr. João Carlos Monteiro de Carvalho
Presidente da Comissão Interna de Biossegurança da FCF/USP


Prof. Dr. Ricardo Pinheiro de Souza Oliveira
Presidente da Comissão Interna de Segurança
Química e Biológica da FCF/USP


Profa. Dra. Primavera Borelli
Diretora da Faculdade de Ciências Farmacéuticas da USP








Indicação de vídeo para Prêmio Vídeo Pós-Graduação USP 2019

Ao MSc Eduardo Krebs Kleingesinds

Venho por meio desta agradecer sua contribuição e certificar que seu vídeo foi indicado para representar o Programa de Pós-Graduação em Tecnologia Bioquímico-Farmacêutica, da FCF/USP no ano de 2019 na referida premiação, correspondente ao edital PRPG 14/2019.

PROFA. DRA. GISELE MONTEIRO

**COORDENADORA DO PROGRAMA DE PÓS-GRADUAÇÃO
EM TECNOLOGIA BIOQUÍMICO-FARMACÊUTICA - USP**

Attendance certificate at the induction regard the use and the management of animals in the laboratory



Capacitação no Uso e Manejo de Animais de Laboratório

Declaration

We declare that

Eduardo Krebs Kleingesinds

has successfully completed and was approved in the course "Capacitação no Uso e Manejo de Animais de Laboratório" (Capacitation in the use and handling of laboratory animals) in distance learning mode that was coordinated by the Institute of Biomedical Sciences and the School of Veterinary Medicine and Animal Science from University of Sao Paulo (Sao Paulo, Brazil) with the support of REBIOTERIO - CNPq.

São Paulo, 17 de abril de 2020

Central de Bioterismo
ICB USP



Instituto de Ciências Biomédicas | USP
Av. Prof. Lineu Prestes, 2415 • Cidade Universitária "Armando Salles Oliveira" • Butantã – São Paulo – SP • CEP 05508-900

Poster Presentation Certificate at the 10th Conference on Recombinant Protein Production, Crete, Greece, 2019.



The EFB Section on Microbial Physiology
and
The European Federation of Biotechnology
Certify that

Eduardo Kleingesinds

has participated and presented a poster in
the 10th Conference on Recombinant
Protein Production held in Crete, Greece
24 – 27 April 2019

A handwritten signature in blue ink, which appears to read 'Diethard Mattanovich', is positioned above a horizontal line.

Prof. Diethard Mattanovich
Conference co-Chair
Vice President of the EFB

A handwritten signature in blue ink, which appears to read 'Colin Robinson', is positioned above a horizontal line.

Prof. Colin Robinson
Conference co-Chair



Attendance certificate at the teaching internship in the Food Technology course,
University of São Paulo, Brazil, 2018.



PROGRAMA DE APERFEIÇOAMENTO DE ENSINO

ATESTADO

A Comissão Central do Programa de Aperfeiçoamento de Ensino atesta que o(a) Sr(a). EDUARDO KREBS KLEINGESINDS aluno(a) de pós-graduação, nível Doutorado, na área Tecnologia de Fermentações, do(a) Faculdade de Ciências Farmacêuticas, foi estagiário(a) do Programa de Aperfeiçoamento de Ensino, com carga horária total de 120 horas-atividade, de Fevereiro à Junho de 2018, tendo desenvolvido atividades didáticas junto à disciplina FBT0201 - Tecnologia de Alimentos do(a) Faculdade de Ciências Farmacêuticas, aos alunos de graduação, sob supervisão do(a) Prof(a). Susana Marta Isay Saad.

Este é um documento eletrônico dispensa carimbo e assinatura. Sua autenticidade pode ser comprovada fornecendo-se o código de controle na seguinte página da Universidade de São Paulo:
<http://uspdigital.usp.br/webdoc>



Documento emitido às 15:45:40 horas do dia 17/12/2018 (hora de Brasília).
Código de controle: 9Z5I-J8P4-GLER-LPYH

Attendance certificate at the teaching internship in the Pharmaceutical Biotechnology course, University of São Paulo, Brazil, 2018.



PROGRAMA DE APERFEIÇOAMENTO DE ENSINO

ATESTADO

A Comissão Central do Programa de Aperfeiçoamento de Ensino atesta que o(a) Sr(a). EDUARDO KREBS KLEINGESINDS aluno(a) de pós-graduação, nível Doutorado, na área Tecnologia de Fermentações, do(a) Faculdade de Ciências Farmacêuticas, foi estagiário(a) do Programa de Aperfeiçoamento de Ensino, com carga horária total de 120 horas-atividade, de Julho a Novembro de 2018, tendo desenvolvido atividades didáticas junto à disciplina FBT0535 - Biotecnologia Farmacêutica do(a) Faculdade de Ciências Farmacêuticas, aos alunos de graduação, sob supervisão do(a) Prof(a). Gisele Monteiro.

Este é um documento eletrônico dispensa carimbo e assinatura. Sua autenticidade pode ser comprovada fornecendo-se o código de controle na seguinte página da Universidade de São Paulo: <http://uspdigital.usp.br/webdoc>.



Documento emitido às 20:46:15 horas do dia 07/09/2019 (hora de Brasília).
Código de controle: MVJY-7NEK-DQLK-7PDV

Attendance certificate as instructor of the MSc Biopharmaceuticals Discovery course,
King's College London, United Kingdom, 2019.

**Faculty of Life
Sciences and
Medicine**

Institute of Pharmaceutical
Science

Paul F. Long
BSc MSc PhD
Professor of Marine Biotechnology &
Therapeutics

Room 3.10 Franklin-Wilkins Building
King's College London
150 Stamford Street
London SE1 9NH
Tel/Fax: +44(0)20 7 848 4842
paul.long@kcl.ac.uk



27th February 2019

To whom it may concern

I confirm that Mr Eduardo Krebs visited my laboratory from January 28th to February 23rd, 2019.

Whilst in my lab, Eduardo took part as an instructor for a 5 days laboratory class for the MSc in Biopharmaceuticals Discovery course code 7BBPM013.

Eduardo also performed proteomics analysis on his recombinant yeast cells to examine the effects of inducing recombinant protein expression on the physiology of the heterologous host. This experiment has never been reported in the literature and so the results will provide for a very unique chapter in his PhD thesis and a subsequent high impact publication.

Please contact me if you have any questions.

A handwritten signature in blue ink, appearing to read 'Paul F. Long'.

Paul F. Long

